UNIVERSITY OF CALIFORNIA, SAN DIEGO
SAN DIEGO STATE UNIVERSITY

Metabolic Role of Thioredoxin-Interacting Protein in Facilitating the Fasting Response

A dissertation submitted in partial satisfaction of the
requirements for the degree Doctor of Philosophy
in
Biology
by
Allen Mariano Andres

Committee in Charge:

University of California, San Diego
- Professor Stephen M. Hedrick
- Professor Immo E. Scheffler

San Diego State University
- Professor Roberta A. Gottlieb, Chair
- Professor Terrance G. Frey
- Professor Simon T.Y. Hui
- Professor Peter van der Geer

2009

The dissertation of Allen Mariano Andres is approved, and it is acceptable in quality and form for publication on microfilm and electronically:

_____

_____

_____

_____

_____

_____
Chair

University of California, San Diego 2009

San Diego State University 2009

DEDICATION

This work is dedicated first and foremost to my Almighty Father who has given me the opportunity to know Him, and to explore and understand a little part of the great design we know of as life. Through this journey thus far I have become enlightened to know that the more I understand the less I realize I know. I have come to accept that our being is limited in our ability to understand all things, and that our purpose should not solely be on the things that are seen, but to those things which are unseen.

I dedicate this work also to my mother Nobleza; for her unconditional love and support of me in all that I do. This work is also dedicated to my younger brother Don who has and always will serve as an inspiration to me to continue strive to set a good example in what it is to be the prototype. And finally, I dedicate this work to the rest of family and friends who have been a positive influence in my life towards inspiring me to complete this dissertation.

TABLE OF CONTENTS

LIST OF FIGURES AND TABLES

ACKNOWLEDGEMENTS

In memory, I would like to thank my previous mentor, and former chair of my dissertation committee, the late Dr. Roger A. Davis who has taught me that working in the field of Science is a privilege to enjoy. I am thankful for his enthusiastic support and guidance of me during the past five years in his lab prior to his passing.

I thank my current mentor and chair of my dissertation committee, Dr. Roberta A. Gottlieb for her willingness to take me under her care. Her advice and assistance in helping me to finish this work is very much appreciated.

I extend my thanks to my committee members: Dr. Immo E. Scheffler, and Dr. Stephen M. Hedrick of UCSD, and Dr. Terrence G. Frey, Dr. Peter van der Geer, and Dr. Simon T. Y. Hui of SDSU. I thank them for their advice, constructive criticism, support and time while serving on my committee.

I thank my good buddies in the SDSU Biology Department Patti Swinford and Sandra Talley for their unfaltering support in helping me get through one of the most delicate nasties in life: academic department paper work. Thank you both for always taking extra time to wait in case the other twin also wants to say “Hi!”

I also thank the former members of my lab under Dr. Davis for their stimulating company and for dealing with my spastic nature throughout the years. Thank you Doris Grotkopp for teaching me the art of mouse handling;

for before I generally feared mice, and now that will forever remain reversed. Thank you to Alejandra Gutierrez for bringing forth Spaz; I have learned to use my other personality for greater gain and amusement. Also I would like to thank Doug and Ron for their help and advice in lab, especially concerning dealing with the intriguing species from Venus. Thank you to the girls (Marlena, Amber, and Betty) for their assistance in many things, and for helping me to deal with Roger on numerous occasions! I would also like to thank Sowbarnika for her help with the many oxidation experiments, for putting up with some of my most cantankerous moments, and for extraneous services. I extend a very special thanks to my taller and quieter twin, partner in lab crime, bestest fishing buddy ever, and very good friend Eric P. Ratliff. Together we made getting by our tumultuous adventure through graduate school a much more manageable and memorable experience.

I acknowledge and thank the San Diego Chapter of ARCS for their generous support of me through the ARCS scholarship which I received for three years while a doctoral student. I also acknowledge the Rees-Stealy Foundation for two years of fellowship support.

Finally, I thank my family and friends who have either directly or indirectly helped me to endure and persevere during my course in completing this doctoral dissertation. To you I am forever grateful for inspiring me to become who I have become today.

Most importantly, I thank the Almighty who has blessed me with life and strength, and who has helped me through my darkest of days.

The text and figures presented in Chapter 2, in part, has been submitted for publication of the material as it may appear in Hui, Simon T. Y., Andres, Allen M., Miller, Amber K., Spann, Nathanael J., Potter, Douglas W., Post, Noah M., Chen, Amelia Z., Sachithanantham Sowbarnika, Jung, Dae Y., Kim, Jason K., and Davis, Roger A. (2008) Txnip balances metabolic and growth signaling via PTEN disulfide reduction. *Proceedings of the National Academy of Sciences*. Vol. 105, No. 10: 3921-3926. The dissertation author was the secondary investigator and author of this paper.

The text and figures presented in Chapter 3, in part, is currently being prepared for publication of the material. Andres, Allen M., Ratliff, Eric P., Sachithanantham, Sowbarnika, and Hui, Simon T.Y. The dissertation author was the primary investigator and author of this material.

VITA

2003	B.S. Biological Sciences University of California, Irvine Irvine, California
2004-2005	Master's Program in Molecular/Cell Biology San Diego State University San Diego, California
2005-2009	Joint Doctoral Program in Molecular and Cellular Biology University of California San Diego San Diego State University San Diego, California

PUBLICATIONS

Andres, A.M., Ratiff E.P., Sachithanantham S., and Hui, T.Y. (2009) Txnip modulates fasting response by maintaining high energy charge in oxidative muscle tissues. (Manuscript in progress/Title tentative).

Hui, T.Y., Andres, A.M., Miller, A.K., Spann, N.J., Potter, D.W., Post, N.M., Chen, A.Z., Sachithanantham S., Jung, D.Y., Kim, J.K., and Davis, R.A. (2008). Txnip balances metabolic and growth signaling via PTEN disulfide reduction. PNAS. **105.** (10), 3921-3926.

Sakai, A.K., Weller, S.G., Culley, T.M., Campbell, D.R., Dunbar-Wallis, A.K., and Andres, A. (2008) Sexual dimorphism and the genetic potential for evolution of sex allocation in the gynodioecious plant, Schiedea salicaria. J Evol Biol. **21.** (1), 18-29.

Gutierrez, A., Ratliff, E.P., Andres, A.M., Huang, X., McKeenan, W.L., and Davis, R.A. (2006). Bile acids decrease hepatic paraoxonase 1 expression and plasma high-density lipoprotein levels via FXR-mediated signaling of FGFR4. Arterioscler. Thromb. Vasc. Biol. **26.** (2), 301-306.

PRESENTATIONS

Kern Lipid Conference
2007, Aspen, CO (poster presentation)
"Ablation of Thioredoxin Interacting Protein Enhances Glucose Utilization and Insulin Sensitivity"

AWARDS

Mabel Myers Memorial Scholarship
San Diego State University
2005-2006

Rees-Stealy Fellowship Award
San Diego State University
2006-2008

Achievement Rewards for College Scientists (ARCS) Scholarship
ARCS Foundation, San Diego Chapter
2007-2009

FIELDS OF STUDY

Major Field: Biochemistry, Molecular/Cellular Biology
Studies in Cell Signaling and Regulation of Metabolic Response
Professor Roger A. Davis (2004-2008),
and Professor Roberta A. Gottlieb (2009)

ABSTRACT OF THE DISSERTATION

Metabolic Role of Thioredoxin-Interacting Protein in Facilitating the Fasting Response

by

Allen Mariano Andres

Doctor of Philosophy in Biology

University of California, San Diego 2009

San Diego State University 2009

Professor Roberta A. Gottlieb, Chair

Thioredoxin-interacting protein (Txnip) is a ubiquitously expressed protein whose well established function is to bind to thioredoxin, effectively inhibiting its ability to facilitate redox-mediated functions. Txnip has been characterized as a potent tumor suppressor and (through its association with thioredoxin) is involved in various cellular homeostatic functions that regulate

cell growth, proliferation, and apoptosis. Recently, Txnip has emerged as an important player in metabolism.

Here, we demonstrate that Txnip is essential for integrating signals that allow for an appropriate metabolic response to survive a fasting challenge. Using a mouse model harboring genetic disruption of the *Txnip* gene, we attempted to elucidate the role of Txnip in facilitating the fasting response where the body normally elicits a set of metabolic reactions to maintain energy homeostasis necessary for survival. We establish that loss of Txnip alone is sufficient to induce fasting hypoglycemia, hyperketonemia and hypertriglyceridemia. Furthermore, we show that *Txnip* ablation leads to attenuated mitochondrial oxidative phosphorylation of all major fuel substrate types (glucose, ketone bodies, and fatty acids) and enhances the propensity to utilize glucose in muscle tissues. Moreover, we establish that Txnip exerts its metabolic role in the fasting response in great part through the heart and skeletal muscles, as the phenotype of global Txnip knockout mice is closely recapitulated in the heart and skeletal muscle-specific knockout mice.

Upon concentrating our efforts to understand the function of Txnip in the heart and skeletal muscle of fasting Txnip -/- mice, we observed hypoactivation of AMPK in the more oxidative muscle tissues (heart and soleus muscles) relative to their controls. We found that this phenomenon is a consequence of a low AMP:ATP ratio (high energy state) and is associated with increased muscle glycogen content. In this dissertation we demonstrate that Txnip is an essential player for facilitating the glucose-fatty acid cycle,

which is an essential part of the fasting response. Because of the critical and influential role it plays in cellular energetics and house keeping functions, Txnip may be a potentially good target for therapeutic research into treating many of the metabolic maladies man faces today that include heart disease, cancer, and diabetes.

Chapter 1

Literature Review

Introduction to thioredoxin-interacting protein

Thioredoxin-interacting protein (Txnip) was first identified as a gene that is highly upregulated by 1,25 hydroxyvitamin D3 in treated HL-60 cells [1]. Txnip, also known as VDUP-1 (vitamin D-3 upregulated protein 1) or TBP-2 (thioredoxin binding protein 2), is a 46kDa ubiquitously expressed protein that is intimately involved in the maintenance of the cellular redox rheostat through its disulfide interaction with thioredoxin [2, 3]. Once bound to Txnip, thioredoxin is effectively sequestered from participating in its redox and transcription regulatory functions. Through subcellular fractionation and western blot analysis of muscle tissues, we and others have found that Txnip protein can be found in the nucleus, cytosol, and mitochondrial fractions (unpublished lab data and [4]). In this dissertation, we attempt to further elucidate the functional role of Txnip at the physiological and biochemical level in a mouse system.

Redox regulation by the thioredoxin system

The thioredoxin system plays an important cellular housekeeping role of facilitating redox reactions necessary for proper cell function. The thioredoxin system is vital for maintaining the homeostatic redox poise of the cell and for

protecting the cell from redox damage through its participation in scavenging reactive oxygen species (ROS) [5, 6]. There are several members of the thioredoxin superfamily of proteins that play distinct and overlapping roles in the general maintenance of intracellular redox poise [7]. A comprehensive review of this system along with the glutaredoxin system (the other major redox regulation system found in cells) is available in Holmgren, A. 1985 [8], and Ashan, K. 2009 [7]. The importance of thioredoxin is underscored by the fact that embryonic lethality occurs when either thioredoxin-1 or thioredoxin-2 is ablated [9-11]. Here we shall briefly review the thioredoxin system with a special focus on its connection with metabolism and thioredoxin-1, which is the established member of the thioredoxin family that interacts with Txnip [2, 3, 12-14].

The mechanism by which the thioredoxin system interacts to reduce proteins is distinct from the glutathione system in that it utilizes a disulfide exchange system. The glutathione system is able to interact with a greater number of oxidized constructs due to its monosulfhydryl exchange capability which allows interaction with mixed disulfide proteins [7, 8]. Thioredoxin-1, first discovered in 1964 as a hydrogen donor to ribonucleotide reductase, is a 12 kDa thiol oxidoreductase that is mainly found in the cytosol [7, 8, 15]. Thioredoxin-1 contains two redox active cysteine residues in its active site (Cys32-Gly-Pro-Cys35) [7, 8]. The basic mechanism of the thioredoxin-mediated reduction involves the interaction of reduced (active) thioredoxin (SH HS) with oxidized proteins in which two cysteines of close spatial proximity

have been oxidized (S-S). Through disulfide exchange, thioredoxin donates a proton to reduce an oxidized protein thus rendering itself in an oxidized (inactive) state (S-S). Oxidized thioredoxin is restored by the action of thioredoxin reductase, which uses NADPH as the cofactor to donate H^+ to reduce (reactivate) thioredoxin [5, 7, 8]. Txnip regulates this redox circuit by binding to thioredoxin and preventing its participation in the process. A schematic is shown to illustrate this mechanism (Figure 1).

Thioredoxin and Txnip: Regulation of cell growth and proliferation

Beyond its role in direct redox regulation, the thioredoxin system, which can be regulated by Txnip, extends its importance to signal transduction, cell growth and apoptosis [7, 8, 16]. Thioredoxins are known to inhibit programmed cell death by interfering with the Ras/Ref/ERK pathway [17, 18]. Additionally, the mitogen-activated protein kinase kinase kinase (MAPKKK), apoptosis signal regulating kinase 1 (ASK-1) is, under normal conditions, bound to thioredoxin-1 in the cytosol and thioredoxin-2 in the mitochondria preventing apoptosis [19]. When dissociated from thioredoxin-1 or thioredoxin-2, as could be the case in increased oxidative stress, ASK-1 is then free to interact with TNF-receptor associated factors (TRAFs) leading to activation of c-Jun N-terminal kinase (JNK) and p38 MAPK, which both initiate the apoptotic cascade [20-22]. In one report, thioredoxin-1 may also facilitate the ubiquitination of ASK-1 leading to its degradation [23]. Thioredoxin-2 also plays an important role in the regulation of programmed cell death by

preventing the release of cytochrome *c* and maintaining the mitochondrial membrane potential [24, 25].

Under certain conditions, such as an increase in oxidative stress, thioredoxin-1 may translocate into the nucleus to facilitate certain functions involving the regulation of transcriptional activity or may be exported out of the cell [26, 27]. Thioredoxin may also interact with and modify transcription factors in the cytosol, thus influencing their action. Thioredoxin-1 is associated with the regulation of a plethora of transcription factors that include, but are not limited to, AP-1, NF-κB, HIF-1α, Sp1, and p53 [28-34]. Cytosolic activation of Ref-1 by thioredoxin leads to the reductive activation of AP-1 to increase its DNA binding capacity, which enhances the transcription of many genes that promote cell growth [30]. NF-κB has been shown to be directly activated by thioredoxin-mediated reduction of Cys62 of its p50 subunit [33]. This transcription factor has been shown to be associated with cell proliferation control and is involved in the inflammatory response [35-38]. HIF-1α plays an important role in promoting cell survival in a hypoxic environment and is thus critical for the ability of cancer cells to develop into a tumor mass [39-41]. The activation of HIF-1α to facilitate this effect is redox regulated; thioredoxin has been demonstrated to play an essential role in this process [42-45]. Sp1 is another thioredoxin regulated transcription factor that is important in the progression of cancer due to its function to promote lipid synthesis and to facilitate rapid cell growth and proliferation [28, 46, 47]. Thioredoxin is also capable of directly or indirectly, like AP-1 (through Ref-1 activation), enhancing

the DNA binding capacity of p53, which is another important level of control for regulating apoptosis [34, 46, 48].

Given the established characteristic of Txnip to bind and inhibit thioredoxin-1 activity, it should be no surprise to realize its potential connection to cell growth and proliferation. Txnip has been characterized as a tumor suppressor that controls cell growth, proliferation and apoptosis through its regulation of thioredoxin [49-52]. In one example, thioredoxin is known to promote smooth muscle cell growth and this action is countered by expression of Txnip [53]. Additionally, Txnip expression has been found to be essential for the development of natural killer cells providing evidence for its importance in the realm of immunology [54]. In the following section, we will discuss the importance of the thioredoxin system in various metabolic diseases and will discuss the influence of Txnip in these processes when appropriate.

Thioredoxin and Txnip: Involvement in metabolic diseases

Thioredoxin and Txnip are associated with various metabolic diseases that include cancer, heart disease, and diabetes. Thioredoxin expression has been found to be elevated in many instances of cancer including hepatic [55-57], pancreatic [58, 59], lung [60, 61], and colon cancer [62]. In parallel, Txnip has been found to be down-regulated in a variety of cancers that include hepatocellular carcinoma [63], gastrointestinal [64], B-cell lymphoma [65], breast [66, 67], prostate, bladder and colon cancers [66]. Furthermore, melanoma metastasis is suppressed by Txnip expression [68]. These findings

exemplify the yin and yang relationship between thioredoxin and Txnip as far as their influence on the progression of cancer. Although the tumor-suppressive nature of Txnip may be explained in part by its inhibitory interaction with thioredoxin-1, it is still a possibility that this protein may have thioredoxin-independent functions that are related to cell cycle control that have yet to be discovered.

Thioredoxin also plays an important role in ischemic heart disease. Chronic intermittent hypoxia, which induces thioredoxin-1 expression, leads to decreased ischemia-reperfusion induced damage to the myocardium. However, short-term intermittent hypoxia, where thioredoxin expression remains low, has been shown to increase damage to the myocardium under the same treatment [69]. This suggests that the presence of thioredoxin-1 is cardioprotective and that the tissue may raise levels of thioredoxin as a mechanism to prevent further damage caused by the ischemic insult. This finding is supported in another study that demonstrates the protective effect of thioredoxin expression in preventing ischemia-reperfusion injury [70]. In another case, the expression of thioredoxin-1 and thioredoxin related protein 32 was increased by treatment with the ROS scavenger euryale ferox which provided an increased cardioprotective effect against ischemia-reperfusion damage [71]. Txnip, on the other hand, has been shown to counter the cardio-protective effects of thioredoxin with regards to ischemia-reperfusion induced damage. Over-expression of Txnip in cardiomyocytes has been demonstrated to predispose cells to oxidative stress-mediated apoptosis through inhibition

of thioredoxin [13]. Furthermore, cardiac function and cardiomyocyte survival is enhanced in an animal model of myocardial ischemia where *Txnip* has been disrupted [72].

Patients suffering from diseases related to increased oxidative stress have been shown to exhibit increased levels of thioredoxin in their serum. For example, this phenomenon is observed in patients suffering from burns [73], rheumatoid arthritis [74], and hepatitis C virus infections [75]. Secreted thioredoxin has been implicated as functioning as a co-cytokine to stimulate cell proliferation in human tumor cell lines [76]. Moreover, thioredoxin in the plasma or serum has been reported to exhibit chemokine-like activity to recruit neutrophils, monocytes, and T-cells [77]. Increased plasma or serum levels of thioredoxin-1 have also been reported in patients suffering acute myocardial infarction or coronary spastic angina, thus making thioredoxin a good marker for these afflictions [78-80]. It would be interesting to see the level of control Txnip may exert on the process of secreting thioredoxin; even more intriguing would be to see if Txnip is secreted to control the activity of thioredoxin-1 released into blood.

The thioredoxin system is also involved in controlling cardiac hypertrophy. Expression of a dominant negative thioredoxin-1 harboring double mutation of its critical cysteine residues necessary for its reductive function (C32S and C35S) causes increased cardiac hypertrophy and oxidative stress [81]. In addition, the down-regulation of thioredoxin-1 in a mouse menopause model leads to an increase in cardiac hypertrophy and

Fibrosis, which is associated with upregulation of ASK1/caspase signaling [82]. This mechanism was elucidated in cardiomyocytes where ASK-1-induced cardiac apoptosis and hypertrophy was inhibited by direct binding of thioredoxin-1 and thioredoxin-2 with the N-terminal regulatory domain of ASK-1 [83]. Congestive heart failure is prevented by treatment with estrogen which upregulates thioredoxin-1 and thioredoxin reductase, again leading to the inhibition of ASK-1 [84]. Cardiac hypertrophy can also be controlled in a thioredoxin-dependent/ASK-1 independent manner. This mechanism involves enhanced regulation of protein expression of mitochondrial proteins such as PPARγ coactivator-1α (PGC-1α) and nuclear respiratory factors (NRFs), which improves mitochondrial oxidative function and is associated with preventing cardiac hypertrophy [85]. Suppression of Txnip in cardiomyocytes has been shown to prevent cardiac hypertrophy [53], most likely due to a release of its inhibition of thioredoxin-1. Clearly, cardiac hypertrophy is regulated by the opposing influence of thioredoxin action versus Txnip-mediated inhibition of thioredoxin.

Role of Txnip in glycemic control and the metabolic syndrome

Txnip has been implicated as an important element in the regulation of glucose homeostasis, and thus may play an important role in the etiology of diabetes mellitus. Many studies have established that Txnip is potently induced by increased concentrations of glucose [86-90]. Disruption of the Txnip gene lead to a metabolic profile that increases glucose tolerance

in both humans and mice [91, 92]. Muscle expression of Txnip was found to be consistently increased in humans with diminished glucose tolerance and diabetes versus those with normal glucose tolerance [92]. In parallel, increased Txnip expression is also observed in diabetic animal models. When treated with insulin, animals, human skeletal myocytes, adipocytes, and INS-1E β-cells exhibit downregulation of Txnip expression [92-94]. This down-regulation of Txnip expression by insulin is lost in insulin receptor ablated mice illustrating the importance of an intact insulin signaling pathway in this mechanism [92]. These findings bring to light the importance of Txnip in glucose homeostasis, underscore its importance in diabetes, and establish its reciprocal regulation by insulin and glucose. Figure 2 is a schematic depicting the metabolic involvement of Txnip in maintaining whole-body glucose homeostasis.

Glucose has been shown to be able to induce upregulation of Txnip in the pancreas, which may be critical for the control of insulin secretion [87]. However, high concentrations of circulating glucose have also been shown to cause β-cell mass loss [50]. Glucotoxicity of the pancreas, which leads to β-cell loss and dysfunction and impaired transcription of insulin, has been established in many studies [95-100]. Thus, there exists the possibility that Txnip expression may be a factor in linking pancreatic toxicity to increased glucose levels.

Some evidence for this possibility include the finding that increased expression of Txnip in many cell lines is associated with sensitization to oxidative stress that leads to increased apoptosis [101]. The anti-apoptotic properties of the anti-diabetic drug, exenatide, is mediated through Txnip reduction [102]. In the pancreas, loss of Txnip is associated with increased Akt/Bcl-xL signaling, increased β-cell mass, and resistance to streptozotocin-induced β-cell apoptosis [103]. These findings are complementary to the established characteristic of Txnip as tumor suppressor gene.

The development of obesity and insulin resistance are significant risk factors in the progression of type 2 diabetes mellitus [104-106]. In turn, diabetes is an established risk factor for the onset of various vascular maladies including coronary artery disease, atherosclerosis, peripheral artery disease, and stroke [94, 107-109]. This metabolic epidemic is of particular importance in the context of Western society's progressive tendency to consume food in severe excess of need, while concomitantly shifting towards a lifestyle of diminished activity. The associated hyperglycemia that usually follows then leads to glucotoxicity of the pancreas, which is facilitated by Txnip, thus exacerbating the loss of glycemic control. Therefore understanding the mechanistic role of Txnip in this process may be essential for stemming the onslaught of this devastating metabolic disease.

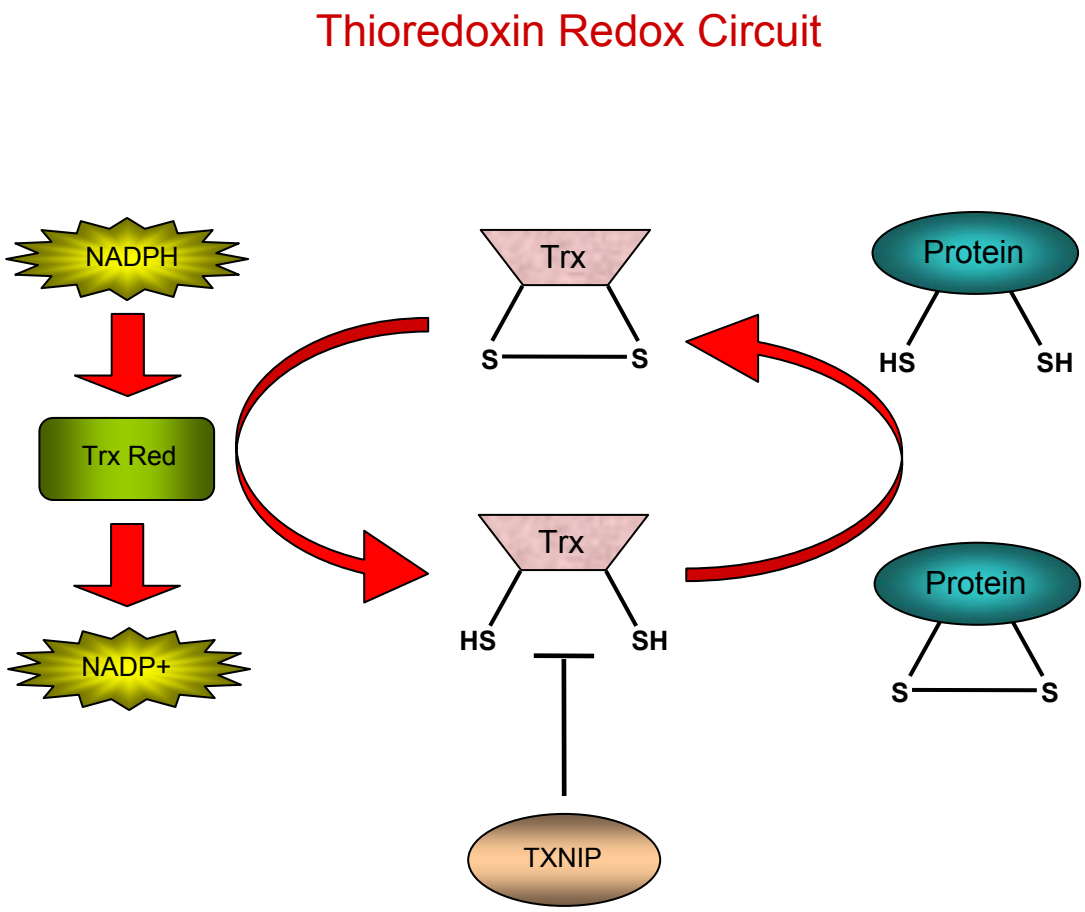

Figure 1: Schematic representation of the thioredoxin redox circuit. Reduced thioredoxin (Trx HS SH) is sequestered by Txnip which prevents it from participating in this circuit of reducing oxidized proteins. By the action of reducing other proteins, thioredoxin renders itself in its oxidized form that is no longer able to fulfill is reducing capacity (Trx S-S). Using NADPH, thioredoxin reductase restores Trx to its redox active form (Trx HS SH).

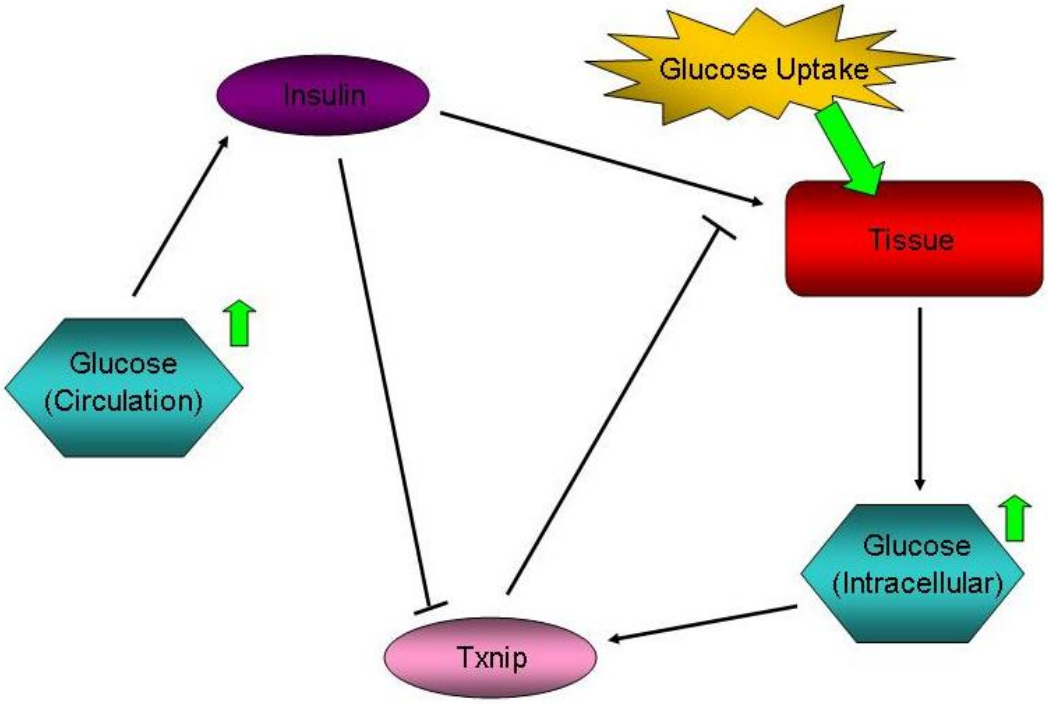

Figure 2: Involvement of Txnip in glucose homeostasis. Increased glucose concentrations in circulation leads to the secretion of insulin by the pancreatic β cells. Insulin then increases glucose uptake in insulin-sensitive tissues, such as skeletal muscle, consequently increasing their intracellular glucose concentration. High intracellular glucose levels triggers the increase of Txnip expression. Txnip then counters the action of insulin by attenuating glucose uptake in tissues. As another level of whole-body homeostatic control, insulin potently inhibits the transcription of Txnip.

Chapter 2

Role of Txnip in Metabolic Fasting Response

Recently, Txnip has emerged as an important metabolic regulator with regards to the physiological need to regulate fuel utilization in animals [91, 110, 111]. We previously demonstrated that Txnip is essential for mediating an appropriate metabolic response to fasting in the HcB-19 mouse strain [110], a recombinant congenic mouse model that expresses a truncated and non-functional Txnip protein [112]. When challenged with an overnight fast, these mice become hypoglycemic, hyperketotic, and hypertriglyceridemic [110]. The exact mechanism of this process remains poorly understood and stands as the basis of investigation for this dissertation.

In an effort to ascertain that the mutation in Txnip alone is the cause for these metabolic phenotypes, our lab generated whole-body and tissue-specific Txnip -/- mice on a C57Bl/6 background using the Cre-loxP-mediated gene recombination system [113]. Whole-body Txnip -/- mice were created by crossing $Txnip^{fl/fl}$ mice with mice expressing cre-recombinase under the control of the zp3 promoter [114]. As anticipated, whole-body Txnip -/- mice displayed hypoglycemia, hyperketonemia, and hypertriglyceridemia after an overnight fast (Figure 3), which was consistent with the phenotype of other Txnip-deficient mice [4, 110, 112]. We also found that the onset of hypoglycemia and hyperketonemia in Txnip -/- mice occurs almost

simultaneously within the course of 4 hours after food deprivation and through the dark period where mice are most active; hypertriglyceridemia occurs several hours later (Figure 4). Interestingly, the hypoglycemia that occurs in Txnip -/- mice seems to reach its metabolic set point after 4 hours upon removing their food. Mice that were provided food *ad libitum* do not exhibit these drastic plasma phenotypes. Global Txnip -/- mice (TKO), liver-specific Txnip -/- mice (LKO) and heart and skeletal-muscle specific Txnip -/- mice (MKO) did not exhibit abnormalities in morphology, viability, or reproductive capacity.

RESULTS

Ablation of Txnip enhances glucose utilization and tolerance in mice

To better understand the basis for the hypoglycemia observed we examined levels of circulating plasma insulin and glucagon in fasted mice. Insulin plays a critical role in glucose homeostasis by signaling to insulin-responsive tissues (such as heart, skeletal muscle and adipose) to take up glucose through the canonical Akt-mediated signaling pathway, that when activated leads to the translocation of glucose transporters (mainly Glut-4 in adipose and muscle tissues) to the plasma membrane [115-118]. Uptake of glucose into tissues is largely a passive process that is facilitated by glucose transporters. Glucagon antagonizes the effects of insulin and promotes the mobilization of glucose stores, namely glycogen in muscles and liver, and the

mobilization and release of fatty acids from adipose depots [119-121]. Interestingly we found no differences in the levels of both these hormones in the plasma of fasted wild-type and Txnip -/- mice (Figure 5). This finding suggested that ablation of Txnip may increase insulin sensitivity, decrease hepatic production of glucose and/or increase the uptake of glucose in tissues. It is important to note that insulin is known to exert its metabolic effects primarily during periods after an animal has consumed a meal. Therefore it seemed unlikely that the hypoglycemic phenotype would be connected with increased insulin sensitivity. After ingesting a bolus of food, plasma glucose levels tend to rise leading to insulin secretion by the pancreatic β cells to allow for the uptake and storage of glucose as glycogen in muscle tissues and liver and esterified fatty acids in adipose (all insulin-sensitive tissues).

We then performed an intraperitoneal glucose tolerance test to examine the capacity of mice to clear a given bolus of glucose in two hours. Mice lacking Txnip were able to clear this given bolus of glucose more efficiently in comparison to their wild-type littermates (Figure 6) demonstrating an increased tolerance and ability to utilize glucose. This finding was supported by our collaboration with Jason Kim at Pennsylvania State University, who performed hyperinsulinemic-euglycemic clamp experiments on these mice. From these studies we found that Txnip -/- mice exhibited increased glucose uptake in gastrocnemius muscle, increased glucose infusion (which became necessary to maintain euglycemia), increased glucose turnover, and increased

production of glucose by the liver (Figure 7). Given these findings, we were compelled to examine the basis of this increased propensity to utilize glucose and hypothesized that perhaps loss of Txnip leads to increased insulin sensitivity.

Loss of Txnip enhances glucose tolerance mainly through an insulin-independent pathway

In an effort to determine the remote possibility of increased insulin sensitivity we examined the activation state of Akt/PKB in several tissues. Phosphorylation of Akt at Thr 308 and Ser 473 increases the kinase activity of this protein which is involved in stimulating Glut-4 translocation to the plasma membrane to facilitate the uptake of glucose in muscles (Figure 8 – Akt signaling – Canonical pathway involved in Glut-4 recruitment to the plasma membrane) [122-124]. Initially, others in my lab reported a 3 to 4 fold increase of Akt activation in soleus muscle and hearts of overnight fasted Txnip -/- mice versus their controls (Figure 9) [91]. This result proved to be very controversial after publication as it could not be repeated despite numerous efforts by me and other colleagues. Instead we were able to reproduce consistently the finding that, after an overnight fast, there is no discernable difference between Txnip -/- mice and their respective controls in the activation state of Akt/PKB in tissues such as the heart and soleus muscles (Figure 10). This finding indicated that Txnip enhances glucose tolerance mainly through a insulin-independent manner. This result makes sense in the context that the

abnormal metabolic phenotype of Txnip ablated mice occurs after an energy insult such as fasting where insulin is not a dominant signaling hormone. Furthermore, more recent findings (concerning downstream targets of the insulin-sensitive pathway) from our lab and others strongly support this notion as will be clarified in the last two chapters of this dissertation. Although in our hands we conclude that the enhanced glucose tolerance conferred upon Txnip ablation is more likely due to an insulin-independent mechanism rather than an insulin-dependent one, the possibility that Txnip ablated mice may have some degree of increased insulin sensitivity cannot be discounted. For example, a study examining glucose tolerance and diabetes in a human study strongly suggests a positive correlation between increased insulin sensitivity and disruptions in Txnip [92].

Txnip ablation impairs mitochondrial oxidative phosphorylation and enhances glycolysis.

To gain insight of the mishandled fuel partitioning caused by Txnip ablation we examined the ability of these mice to utilize different fuel substrates. We began by investigating the basis for hyperketosis seen in fasted Txnip -/- mice. The increased level of circulating ketone bodies could be a result of several factors: 1) Increased hepatic production of ketones, 2) Impaired ability to clear ketones from the circulation via urine and/or 3) Impaired ability to utilize ketones by tissues (mainly the brain and muscle tissues). To examine the first possibility we examined the expression of HMG-

CoA synthase and HMG-CoA lyase in liver. The expression of these two enzymes is necessary for the ability of liver to produce ketone bodies (especially mitochondrial HMG-CoA synthase which is the rate limiting step in ketogenesis) [125, 126]. Real-time quantitative PCR revealed that both these enzymes were in fact increased in livers of Txnip -/- mice (Figure 11), an indication of increased hepatic production of ketone bodies. To examine the second possible scenario, our lab measured the amount of ketone bodies excreted in the urine of mice using a colorimetric kit, which revealed that levels of excreted 3-hydroxybutyrate was an astonishing ~30-fold higher in Txnip -/- mice [91]. Combined with the finding that hepatic ketone body production may be increased, these findings suggested that the increased levels of circulating ketone bodies in Txnip -/- mice may be due to both increased ketone production and an impaired ability to utilize ketones.

To investigate the possibility of impaired ability to utilize ketones we examined the dynamics of ketone body uptake in skeletal muscle by injecting intravenously a bolus saline containing cold 3-hydroxybutyrate and tracer [1^{14}C]-D,L-3-hydroxybutyrate. Mice were then sacrificed and perfused with phosphate buffered saline 30 minutes post tracer injection. Hind limb muscles were harvested and uptake of ketone was estimated by determining radioactivity per gram tissue. We found that there was no difference between wild-type and Txnip -/- mice in the incorporation of [1^{14}C]-D,L-3-hydroxybutyrate in skeletal muscle (hind limb) (Figure 12). We then examined the ability of Txnip -/ mice to oxidize [1^{14}C]-D,L-3-hydroxybutyrate by

performing an *ex vivo* experiment to examine the ability of soleus muscle to oxidize 3-hydroxybutyrate; the major ketone body synthesized by the liver that can be converted reversibly to acetoacetate [126]. We found that oxidation of 3-hydroxybutyrate was decreased by ~60% in soleus muscles of Txnip -/- mice, as compared to wild-type samples (Figure 13A).

Upon discovering that oxidation of 3-hydroxybutyrate through the oxidative phosphorylation pathway was impaired, we were prompted to examine the oxidation of fatty acids and glucose as well. To examine the ability to oxidize fatty acids through the mitochondria we used [1^{14}C] oleic acid as a substrate, which showed that oxidation of this fuel was diminished by ~48% in Txnip -/- mice (Figure 13B). We then examined the oxidation of glucose and were surprised to find that oxidation of this fuel was diminished by ~43% (Figure 13C). Overall, we found that Txnip ablation diminishes mitochondrial oxidation of all major fuels including glucose, ketone bodies and fatty acids.

Given that we observed increased ability to clear a bolus glucose it was quite surprising to find that oxidation of glucose through the mitochondria was decreased in Txnip -/- mice. This suggested that glycolysis may be increased in these mice. To ascertain this possibility we examined levels of circulating plasma lactate, as an indicator of increased glycolytic rate [127]. Increased glycolysis in tissues leads to an accumulation of lactate in cells, which is subsequently released into the blood and is thus an indicator of glycolytic rate. We found that plasma levels of lactate were indeed elevated in fasting

Txnip -/- mice (Figure 14). This finding was revealing in that it demonstrated that Txnip ablated mice undergo a metabolic shift towards relying more on glycolysis for energy and away from mitochondrial oxidative phosphorylation.

Oxidation of PTEN is increased by ablation of Txnip

Based on the initial finding that Akt signaling may be increased in oxidative muscle tissues we investigated the major phosphatase responsible for attenuating this signaling pathway, PTEN (Phosphatase and tensin homolog deleted on chromosome 10) [128, 129]. PTEN contains a catalytic site consisting of two cysteine residues that must be in a reduced state in order to maintain phosphatase activity. Thioredoxin has be shown to be the major factor in keeping PTEN in a reduced and active state [129-131]. We hypothesized that somehow Txnip ablation may affect the thioredoxin system in such a way as to prevent the reactivation of PTEN, thus leading to increased Akt signaling. As mentioned earlier, the initial finding that Txnip ablation leads to increased Akt activation was not reproducible, hence there is no need to discuss the importance of Txnip ablation in this context. However, the plausibility of increased oxidation of proteins in Txnip -/- tissues remains an interesting avenue to investigate. PTEN will serve as the example protein for the remainder of this portion discussing the importance of Txnip and the thioredoxin system in the cellular environment. High rates of glycolysis may divert glucose from entering the predominant pathway for NADPH generation (the pentose phosphate shunt). NADPH is necessary to maintain a functional

thioredoxin circuit and the risk of its depletion in skeletal muscle and heart tissues is increased in these tissues because of their reduced capacity to regenerate this metabolite [132]. Typically, growth factor signaling activates tyrosine kinases leading to an oxidative burst (ROS production) and subsequent inactivation of phosphatases like PTEN by forming a disulfide bond in the catalytic domain of the protein [130, 131, 133]. PTEN is then reactivated by thioredoxin–NADP(H) dependent reduction of the cysteine residues important for its activity. NADH has been shown to inhibit thioredoxin-NADP(H) dependent reactivation of PTEN in a dose dependent manner [134]. Thus, one avenue to examine not investigated in this work is to see if changes in NADH/NADPH ratio correlate with PTEN activation.

To examine if PTEN oxidation state was somehow increased in Txnip -/- mice, we performed western blot analysis showing that soleus muscle extracts from Txnip -/- mice displayed a ~50% decrease in detectable PTEN under non-reducing conditions (i.e. not recognized by a polyclonal PTEN antibody without prior disulfide reduction by DTT) whereas no differences in PTEN were observed under reducing conditions (Figure 15). Likely due to conformational changes as a result of disulfide oxidation, this result demonstrates that Txnip -/- soleus muscle extracts contain more masked epitope sites that are unable to be recognized by the polyclonal anti-PTEN antibody used suggesting that PTEN and perhaps many other proteins, are in a more oxidized state in the soleus muscles of Txnip -/- mice versus their wild-type littermates.

Examining the role of Txnip in the liver

Due to the dominant role the liver plays in the regulation of circulating fuels such as glucose, fats and ketone bodies [135] and because studies of the HcB-19 mouse strain reported an increase of VLDL secretion by the liver [136], we hypothesized that Txnip may contribute greatly to the observed fasting phenotype mainly through its effects in the liver. To this effect, we first generated liver-specific Txnip -/- mice (designated LKO mice) to examine the contribution of Txnip ablation in the liver to the fasting phenotype observed. LKO mice were generated by crossing $Txnip^{fl/fl}$ mice to mice expressing cre recombinase under the control of the albumin promoter [137]. The generated LKO mice were backcrossed to C57Bl/6 mice at least four times before performing experiments. Surprisingly, LKO mice did not exhibit any notable difference from their wild-type littermates with regards to their fasting plasma metabolite profile (Figure 16). This finding strongly suggested that Txnip exerts its metabolic influence, in the context of fasting response, mainly through extra-hepatic tissues.

Determining the expression pattern of Txnip

Before proceeding to generate other tissue-specific Txnip ablated strains our lab decided to first examine the expression of Txnip in different tissues under non-fasting and fasting conditions. To this end, C57Bl/6 mice were sacrificed to provide samples of liver, pancreas, white adipose tissue, spleen, heart, lung, kidney, brain and skeletal muscle. After processing these

samples for quantitative real-time PCR, we found that Txnip mRNA expression was highest in white adipose, heart, kidney, and skeletal muscle, and that in general its expression is increased during fasting (Figure 17).

Examining the role of Txnip in heart and skeletal muscle

Because of the importance of skeletal muscle tissue and heart in total body glucose disposal [138-141], and the role these tissues play in facilitating the glucose-fatty acid cycle [142-145], we hypothesized that Txnip may exert its metabolic influence mainly through these tissues. Skeletal muscle and heart-specific Txnip -/- mice (designated MKO mice) were generated by crossing $Txnip^{fl/fl}$ mice to mice expressing Cre-recombinase under the control of the muscle creatine kinase promoter [146]. This targeted deletion of Txnip generated mice that, when fasted, exhibit a plasma phenotype that was similar to, albeit less drastic, than the global Txnip knockout mice. The similar phenotype also extends to their ability to oxidize fuel substrates through the mitochondria, that is attenuated like global Txnip -/- mice [91]. This finding strongly suggested that the function of Txnip in heart and skeletal muscle tissue is critical for the ability of mice to properly respond to a fasting challenge.

EXPERIMENTAL PROCEDURES

Animal Studies

Txnip knockout mice and their wild-type (C57BL/6 background) littermates were housed in a temperature controlled room (25±1^{o}C) under a 12 hour light and 12 hour dark system (6PM-6AM dark). Mice were allowed free access to water and standard mouse chow (Lab Diet 5001, Purina Mills). For fasting experiments, mice were moved into a new cage without chow at 4PM and sacrificed after ~18 hours (overnight fasting). All experimental procedures were approved by the Institutional Animal Care and Use Committee at San Diego State University.

Plasma Metabolite Assays

Whole blood was collected retro-oribitally using heparinized capillary tubes. The blood was then spun down at 10,000 x g for 5 minutes at 4^{o}C to separate plasma that was then assayed immediately or frozen in aliquots and stored at -20^{o}C. Colorimetric kits were used to measure glucose and triglycerides (Wako Chemicals), 3-hydroxybutyrate (Stanbio Labs), and lactate levels (Eton Bioscience) according to manufacturer's instructions. Insulin and glucagon levels were assayed using radioimmunoassay (RIA) kits (Linco) and performed according to manufacturer's instructions.

Glucose Tolerance Test

Overnight fasted mice (~18 hours) were subject to intraperitoneal injection with a solution of glucose carried in saline (2g/kg body weight). Control mice were treated only with saline. Over a two hour time course, blood was drawn from a small tail clip and glucose levels were determined with a glucometer (Becton Dickinson).

Hyperinsulinemic-Euglycemic Clamp Experiment

After an overnight fast (~18 hours), a 2 hour hyperinsulinemic-euglycemic clamp was administered in awake Txnip -/- and wild-type mice. Treatment conditions included a dose of 150milliunits/kg body weight insulin followed by 2.5milliunits/kg per minute insulin infusion [147]. Basal and insulin-stimulated whole-body glucose turnover was estimated while administering a continuous infusion of [3-^{3}H] glucose before and during the clamp experiment. Insulin-stimulated glucose uptake in skeletal muscle was determined by administering an intravenous bolus of 2-deoxy-D-[1^{14}C] glucose (Perkin Elmer). Rates of basal hepatic glucose production and insulin-stimulated whole-body glucose and skeletal muscle glucose uptake were measured using an established method [147]. These procedures were approved by the Pennsylvania State University Animal Care and Use Committee, and performed at the Pennsylvania State University Mouse Metabolic Phenotyping Center.

Western Blotting

Details for the western blotting procedure done in Figure 8 are described in Hui, S.T.Y., et. al. 2008. [91]. For the Akt blots performed here, we used several buffer systems including that detailed in reference 91, and other buffers listed here in attempts to recapitulate the data reproduced previously which were unsuccessful. Below describes the additional western blotting procedures used for Figure 9 results:

Tissues were homogenized in ice-cold buffer containing 50mM Tris pH 8, 150mM NaCl, 2mM EGTA, 1mM EDTA, 1% NP-40, 0.5% Sodium Deoxycholate, 0.1% SDS, 20mM NaF, 1mM $NaVO_4$, 1mM PMSF, 10ug/mL aprotinin, 10ug/mL leupeptin and 10ug/mL pepstatin (Standard radio-immunoprecipitation buffer RIPA). For other batches, tissues were homogenized in ice-cold buffer containing 120mM Tris pH 7.4, 2mM EDTA, 150mM NaCl, 1% Triton-X 100, 20mM NaF, 1mM $NaVO_4$, 20ug/mL aprotinin, 20ug/mL leupeptin (TETN buffer). Proteins were fractionated by SDS-PAGE using tris glycine gels (Invitrogen) and then electroblotted onto polyvinylidene difluoride membranes (PVDF). Blots were blocked using 5% non-fat dried milk in tris buffered saline with 1% tween-20. The following primary antibodies used were: phosphoAkt Thr 308, phosphoAkt Ser 473, and totalAkt all from Cell Signaling Technology. After incubation in peroxidase-conjugated secondary antibodies (KPL), blots were visualized using Super Signal West Dura Extended Duration Substrate (Thermo Scientific).

Extraction of Total RNA and Quantitative Real-Time PCR

Frozen tissue samples were processed using a Total RNA Tissue isolation kit (Versagene) according to the manufacturer's instructions. Total RNA was converted to cDNA using iScript (BioRad) according to the manufacturer's instructions. Quantitative Real-Time PCR was performed using the BioRad iCycler system (BioRad). The primers used to determine mitochondrial HMG-CoA synthase mRNA expression were 5' - GTTGGAGTGTTCTCTTACGGTTCTG - 3' (forward) and 5'- CGATCCGAGGGCCTCACTA -3' (reverse) [148]. The primers used for HMG-CoA lyase were 5'- CTGGGCTTAACGGGTCCTC -3' (forward) and 5'- TGGCAGTGGACAGCCAATGC -3' (reverse) [149]. The primers used for PEPCK were 5'- CCACAGCTGCTGCAGAACA -3' (forward) and 5'- GAAGGGTCGCATGGCAAA -3' (reverse). The house-keeping gene Ribosomal 18S, 5' – AGTCCCTGCCCTTTGTACACA – 3' (forward) and 5' – CGATCCGAGGGCCTCACTA – 3' (reverse) was used as control. Primers without an attached reference were designed using Primer 3 software. Results are displayed as change relative to control wild-type mice.

Ex Vivo Fuel Oxidation Experiments

Oxidation of fuel substrates by isolated soleus muscles were performed following a previously described procedure with slight modifications [150]. Overnight fasted mice (~18 hours) were sacrificed and soleus muscles were carefully extracted and immediately placed into a stoppered 25mL e-flask

containing 3mLs of pre-oxygenated (bubbled 95% oxygen: 5%CO_2 mixture for at least 1 minute) pH 7.4 Krebs Ringer solution (10mM Glucose, 1.2mM $MgSO_4$•$7H_2O$, 1.2mM KH_2PO_4, 25mM $NaHCO_3$, 5mM KCl, 125mM NaCl and 2.5mM $CaCl_2$•H_2O) at 37^oC in a shaking water bath for 20mins (preincubation step). Tissues were then moved into a new flask with the same buffer and conditions supplemented with either ^{14}C-Glucose (0.5µCi/mL), 16mM D,L 3-hydroxybutyrate (0.5µCi/mL), or 4% BSA and 0.5mM oleate (0.5µCi/mL). The atmospheric air of the flasks were then re-equilibrated with 95% oxygen: 5% CO_2 mixture and a new stopper with a holding well containing a piece of filter paper was used to seal the flasks. Tissues were then left to incubate in the 37^oC shaking water bath for 1hour. After this time, 350µl of 1M hyamine hydroxide (Perkin Elmer) was injected through the stopper into the center well, and the oxidation reaction was stopped by injecting 400µl 1M sulfuric acid directly into the media. CO_2 was allowed to collect overnight, and the filter papers were then transferred to vials for liquid scintillation counting.

Assessing PTEN Oxidation State

Soleus muscle from overnight fasted mice (~18 hours) were homogenized in buffer containing (50mM Na_2HPO_4 (pH 7.0), 1mM EDTA, 10mM N-ethylmaleimide, 10mM iodoacetic acid, 5mM NaF, 50µg/ml aprotinin, 50µg/ml leupeptin, and 1% Triton-X 100. Under reducing or non-reducing buffer, 20ug of sample homogenates were resolved by SDS/PAGE and then transferred unto PVDF membranes. Blots were probed with polyclonal rabbit

antibodies against PTEN (Cell Signaling Technology) and then stripped to re-probe with antibodies against tubulin (Sigma) as a loading control.

Statistical Methods

All data are reported as the average ± S.D. The two-tailed Student's *t* test was used to analyze data. Results having p-values less than 0.05 were considered significant

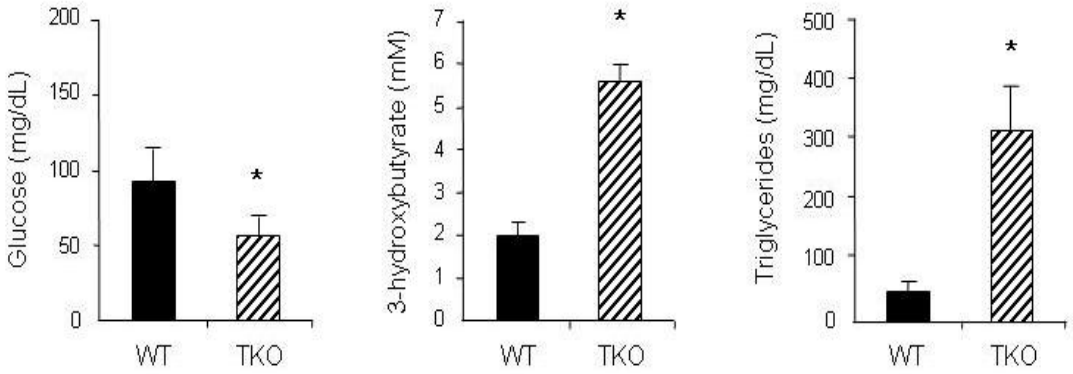

Figure 3: Fasting Plasma Metabolite Profile. Plasma levels of glucose, 3-hydroxybutyrate and triglycerides were assessed after an overnight fast using a standard calorimetric commercial kit. N=9 mice per group. WT=wild-type, TKO=Txnip -/-. Results are presented as mean ± S.D. * Denotes significant statistical difference, $p<0.01$.

Figure 4: Plasma metabolite profile of Txnip -/- mice over a time course. Plasma levels of (A) glucose, (B) 3-hydroxybutyrate and (C) triglycerides were assessed in Txnip -/- mice during the onset of a fasting challenge. Mice were fasted at 4PM prior to 6PM (the onset of dark for the mice). Plasma was obtained by retro-orbital means at 4PM, 8PM, 10PM, 12AM and 2AM. No plasma was taken at 6PM for analysis. N=3 mice per group. Results are presented as mean ± S.D.

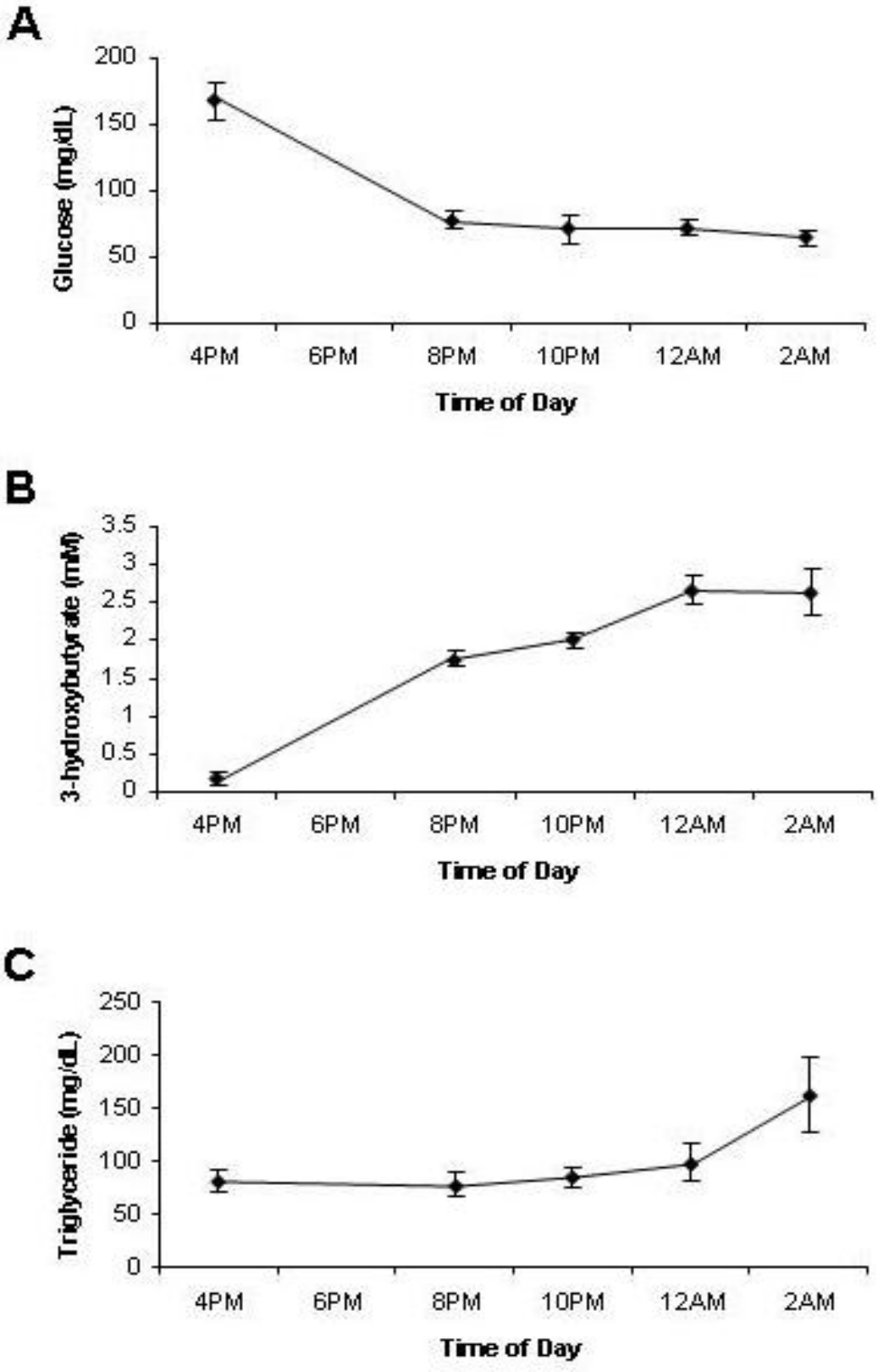
A
Glucose (mg/dL)
200
150
100
50
0
4PM
6PM
8PM
10PM
12AM
2AM
Time of Day
B
3-hydroxybutyrate (mM)
3.5
3
2.5
2
1.5
1
0.5
0
4PM
6PM
8PM
10PM
12AM
2AM
Time of Day
C
Triglyceride (mg/dL)
250
200
150
100
50
0
4PM
6PM
8PM
10PM
12AM
2AM
Time of Day

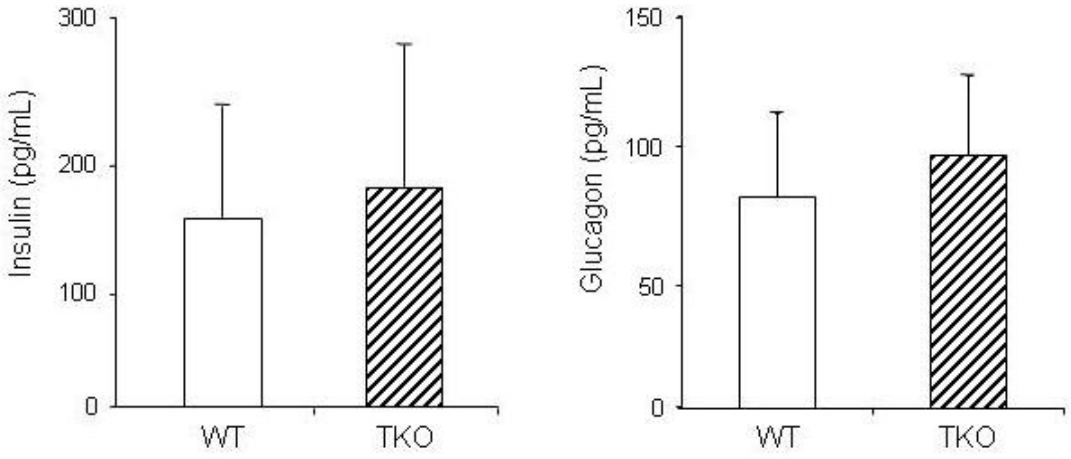

Figure 5: Plasma insulin and glucagon levels. Circulating levels of plasma insulin and glucagon were assessed from overnight fasted mice (~18 hours) using radio-immunosorbent (RIA) assay kits. N=10 mice per group. WT=wild-type, TKO=Txnip -/-. No statistical difference was observed between the two groups.

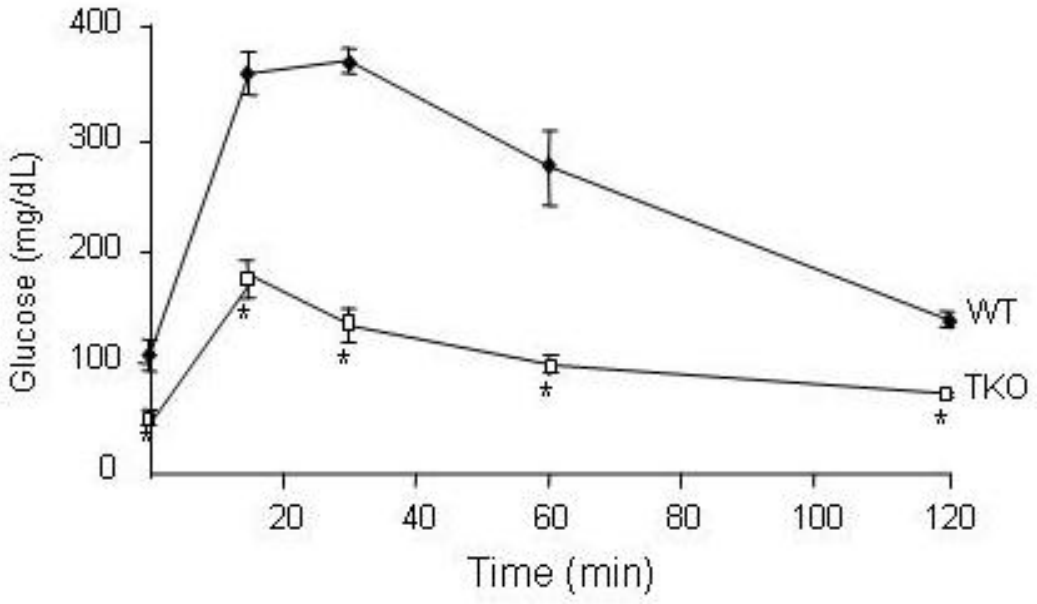

Figure 6: Glucose tolerance test. Overnight fasted mice were injected intraperitoneally with a bolus of glucose carried in saline and normalized to their body weight (2g glucose/kg mouse). Plasma levels of glucose were monitored from WT mice (filled diamonds) and TKO mice (open squares) by glucometer over a time course of 2 hours. N=4 mice per group. WT=wild-type, TKO=Txnip -/-. Results are presented as mean ± S.D. * Denotes significant statistical difference, $p<0.01$.

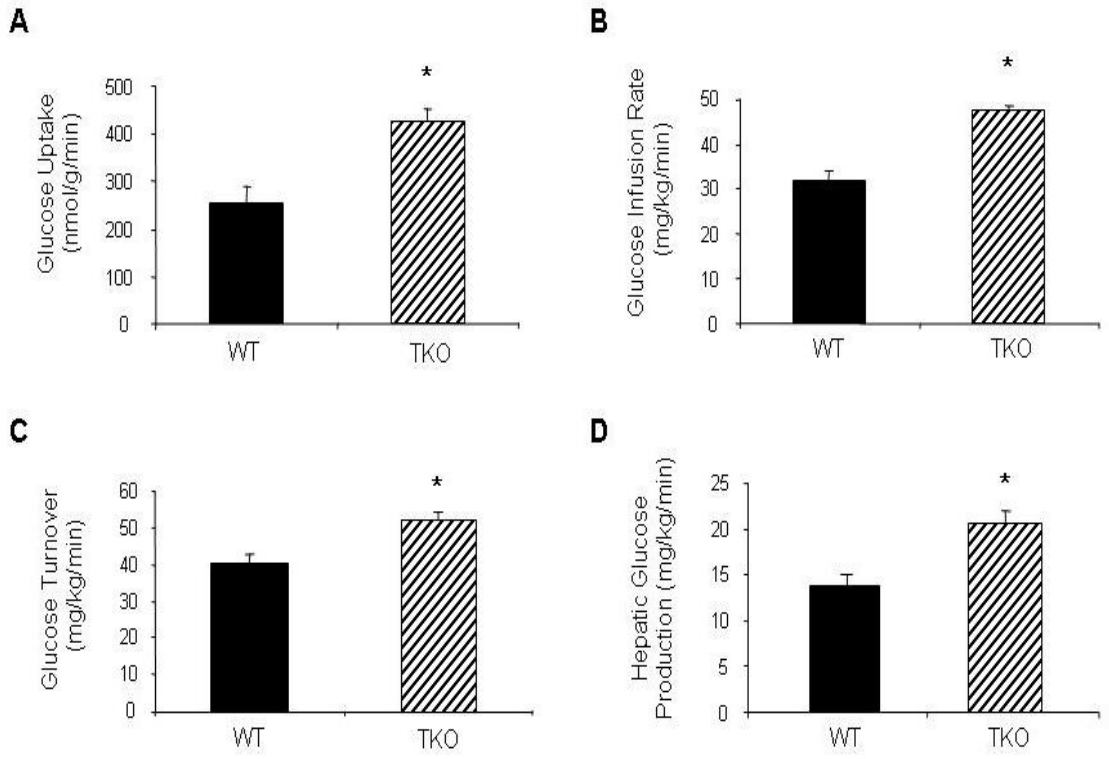

Figure 7: Hyperinsulinemic-euglycemic clamp experiments. Awake overnight fasted mice were subject to hyperinsulinemic-euglycemic clamp studies. (A) Insulin-stimulated glucose uptake in gastrocnemius muscle. (B) Steady-state glucose infusion rate during 80-120 minutes of clamps. (C) Insulin-stimulated whole-body glucose turnover. (D) Basal hepatic glucose production rate. N=8 mice per group. WT=wild-type, TKO=Txnip -/-. Results are presented as mean ± S.D. * Denotes significant statistical difference, $p<0.01$.

Figure 8: Akt signaling – Canonical pathway involved in Glut-4 recruitment to the plasma membrane. Growth factor stimulation of surface receptors (in this case insulin and the insulin-receptor) leads to autophosphorylation event of the receptor leading to the recruitment and activation of insulin-receptor substrates (IRS) that a consequently activates phosphoinositide 3-kinase (PI3K). This kinase phosphorylates plasma membrane anchored phosphotidylinositol (3,4) –bisphosphate (PIP_2) converting it into phosphotidylinositol (3,4,5) –trisphosphate (PIP_3) that acts as a docking site for recruiting and activating phosphoinositide dependent kinase 1 (PDK1) and the mammalian target of rapamycin (mTOR)/Rictor complex. Together PDK1 and the mTOR/Rictor complex phosphorylate and activate Akt at Thr 308 and Ser 473 respectively. Activated Akt then proceeds to perform its positive influence in promoting/regulating survival, growth and proliferation and metabolism. An important aspect of Akt activation is its action of promoting Glut-4 carrying intracellular membranes to translocate to the plasma membrane to allow the glucose transporters to increase glucose uptake. Phosphatase and Tensin Homolog Deleted on Chromosome Ten (PTEN) is the major phosphatase that attenuates this pathway at the level of the PIPs. Txnip, through its relation with thioredoxin is associated to PTEN's action thus connecting Txnip to Akt signaling although the exact mechanism of action is still uncertain.

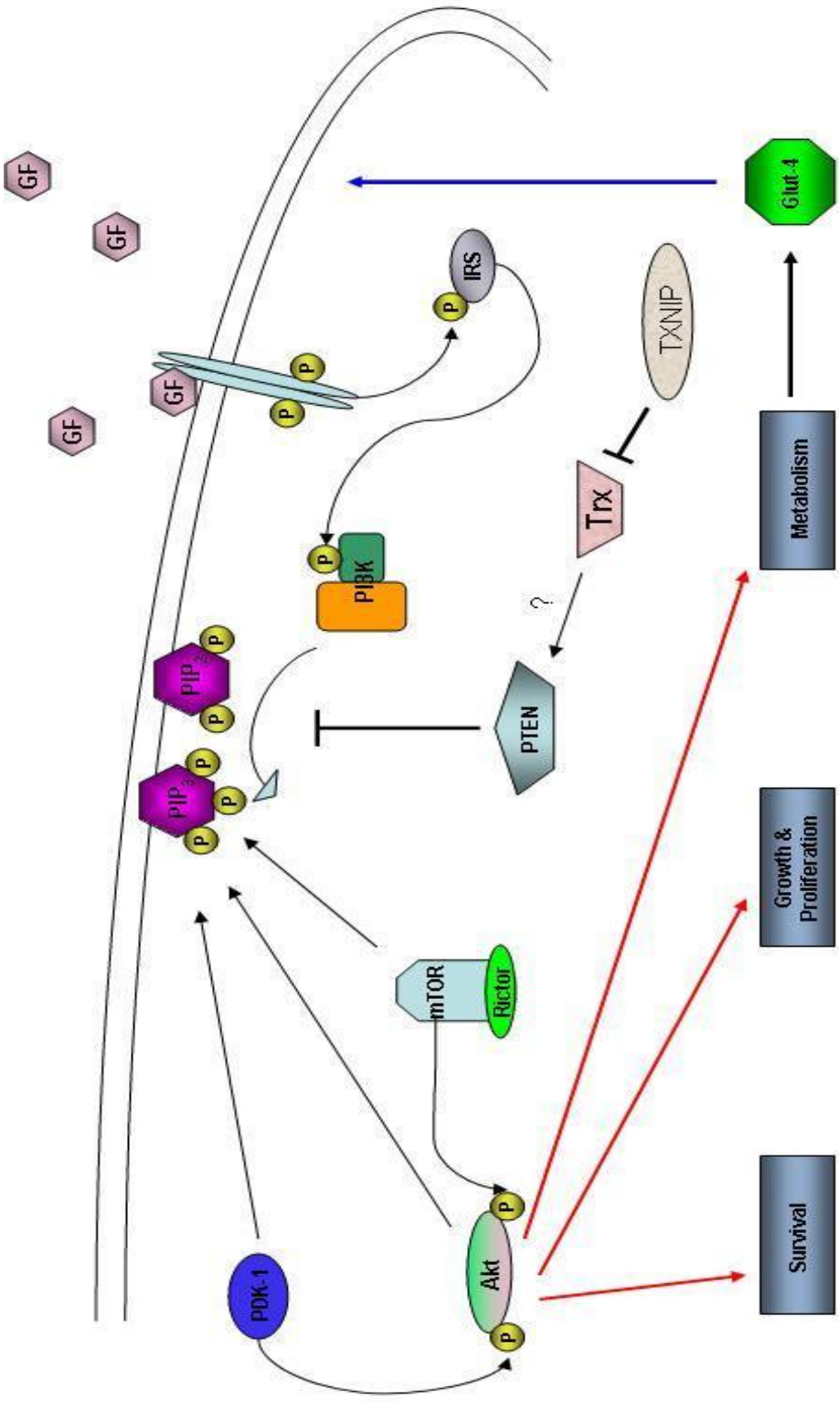
GF
GF
GF
GF
IRS
P
P
P
PIBK
PIP2
PIP3
PTEN
?
Trx
TXNIP
Glut-4
Metabolism
Growth &
Proliferation
Survival
mTOR
Rictor
PDK-1
Akt

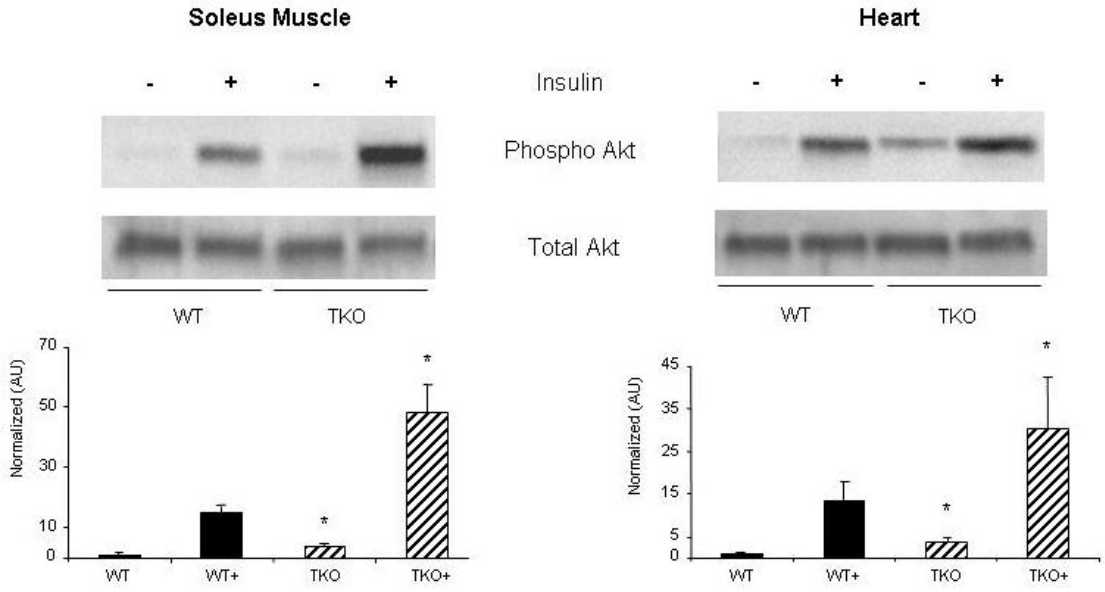

Figure 9: Initial finding of Akt activation state in Txnip -/- mice. Insulin-stimulated and basal Akt phosphorylation in soleus muscle and hearts of overnight fasted mice. WT=wild-type, TKO=Txnip -/-. * Denotes significant statistical significance, $p<0.05$. A full description of the generation of this figure can be found in Hui, *et. al.* 2008 [91]. The author of this dissertation is second author on that manuscript, did not participate in the generation of this figure, and has voiced his concern over the reproducibility of this finding.

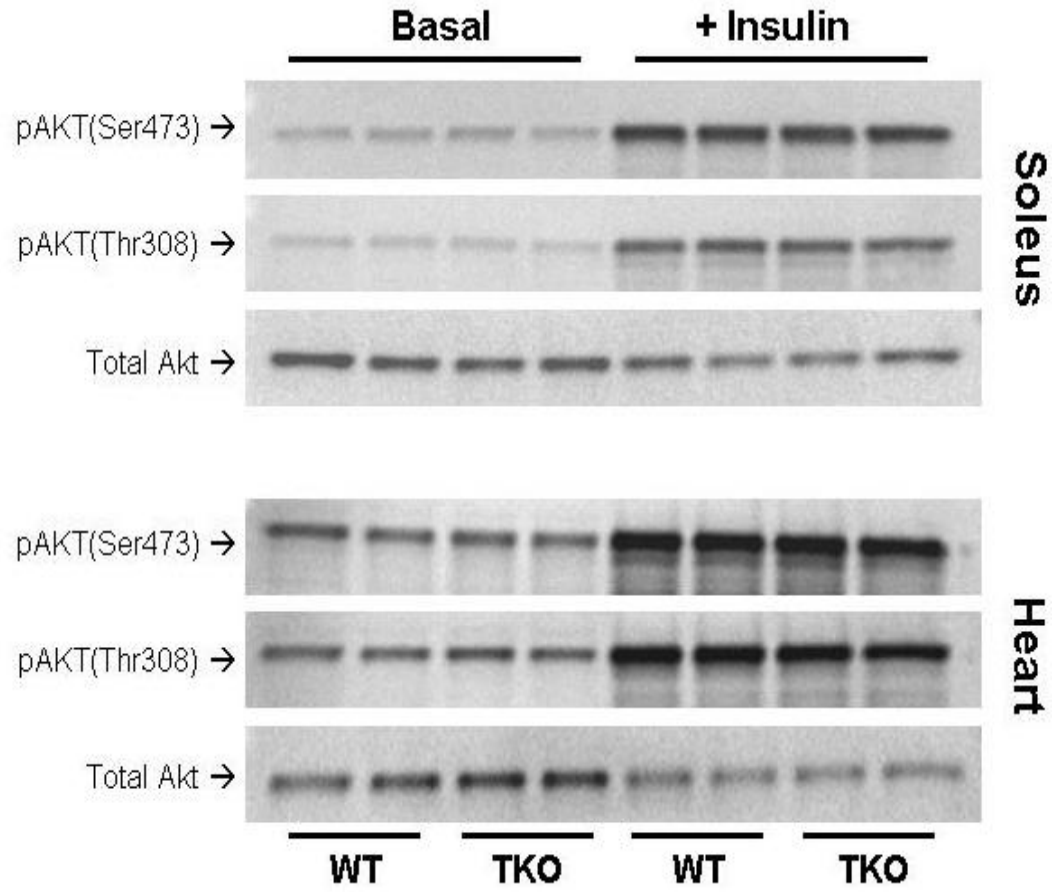

Figure 10: Reproducible finding of Akt activation state in Txnip -/- mice. Representative blots are presented to show all relevant conditions illustrating Akt activation at the basal state in soleus muscle and hearts of mice fasted overnight, and when stimulated with an intraperitoneal injection of insulin as described [91]. After insulin treatment mice were sacrificed after 8 minutes to harvest tissues that were immediately snap-frozen in liquid nitrogen before preparation for western analysis. These experiments were done with at least three batches of mice. N=3 to 4 mice per group for each batch used.

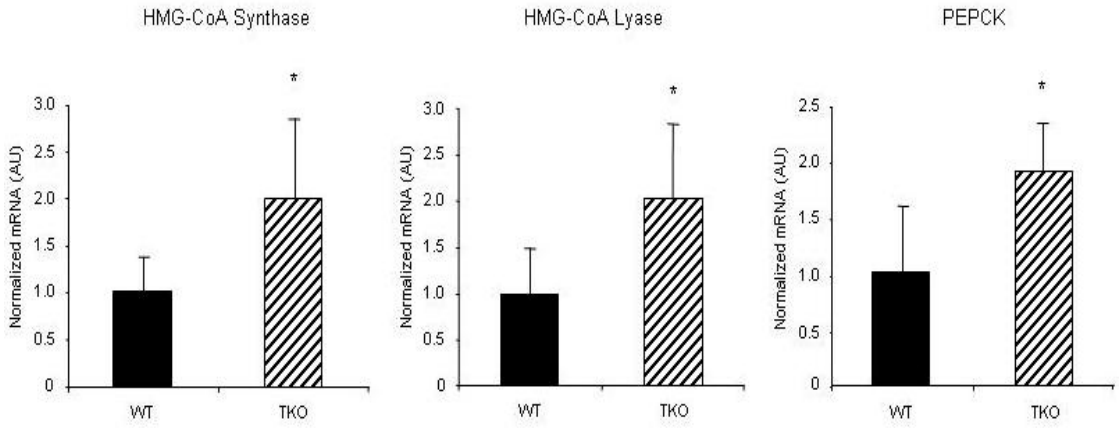

Figure 11: Hepatic expression of ketogenic and gluconeogenic enzymes. Total RNA was isolated from the livers of overnight fasted mice. mRNA levels of mitochondrial HMG-CoA synthase, HMG-CoA lyase and PEPCK were determined by quantitative real-time PCR normalized to 18S RNA. N=5 mice per group. Results are presented as mean ± S.D. WT=wild-type, TKO=Txnip -/-. * Denotes significant statistical significance, $p<0.05$.

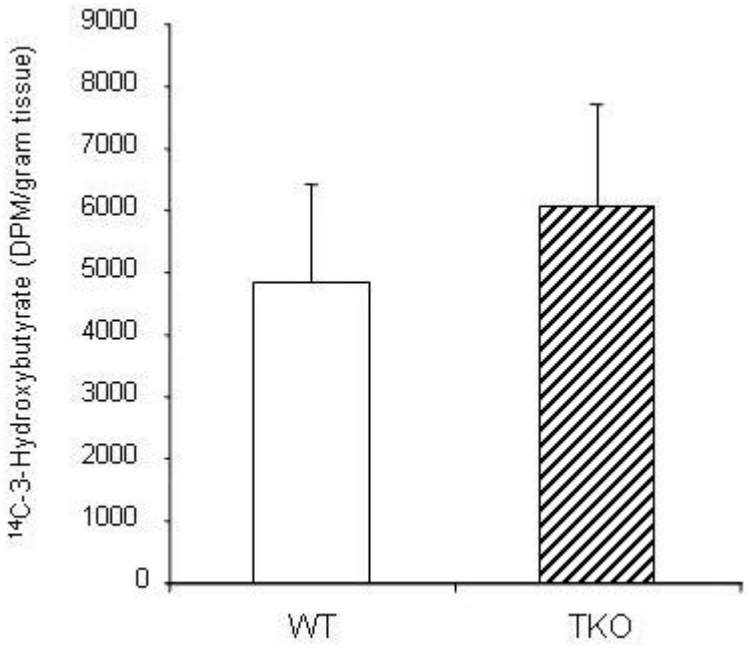

Figure 12: Incorporation of ^{14}C 3-hydroxybutyrate in muscle tissues. Overnight fasted mice were injected intravenously with 0.05μCi of [1-^{14}C]-3-hydroxybutyrate. After 30 minutes skeletal muscle from hind limbs were taken for determination of 3-hydroxybutyrate incorporation. N=5 mice per group. WT=wild-type, TKO=Txnip -/-. No statistical difference was seen between the two groups.

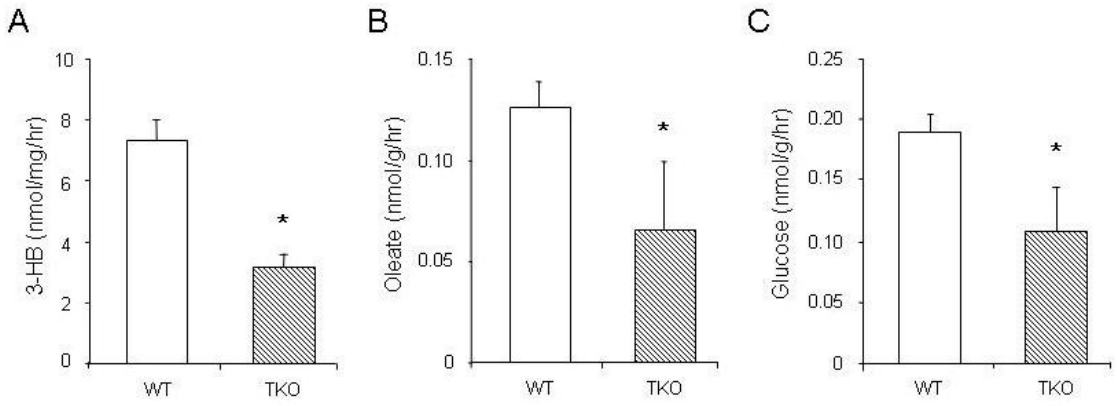

Figure 13: Mitochondrial *ex vivo* fuel substrate oxidation experiments. Soleus muscle from overnight fasting mice were incubated, for 1 hour at 30^{o}C, with (A) [1-^{14}C]-3-hydroxybutyrate(0.5 µCi/mL). (B) [1-^{14}C]-oleate (0.5 µCi/mL), and (C) [U-^{14}C]-glucose. N=5 mice per group, for each fuel substrate experiment. The amount of $^{14}CO_2$ generated was quantified by scintillation counting. Results are presented as mean ± S.D. WT=wild-type, TKO=Txnip -/-. * Denotes statistical significance, $p<0.05$ for (A) and (C) and $p<0.01$ for (B).

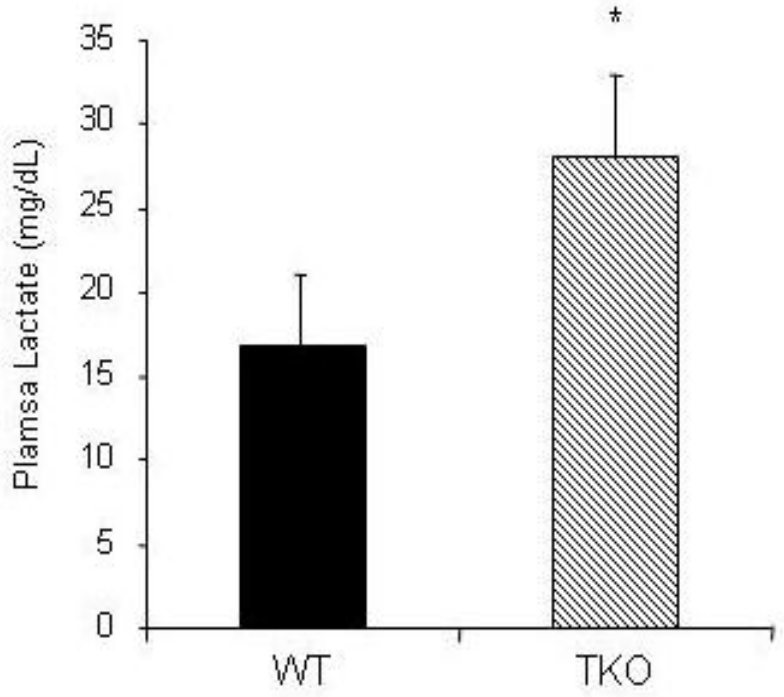

Figure 14: Plasma lactate concentrations. Plasma lactate levels of overnight fasted mice (18 hours) were assessed by a standard colorimetric kit. N=6 mice per group. WT=wild-type, TKO=Txnip -/-. Results are presented as mean ± S.D. * Denotes significant statistical significance, $p<0.05$.

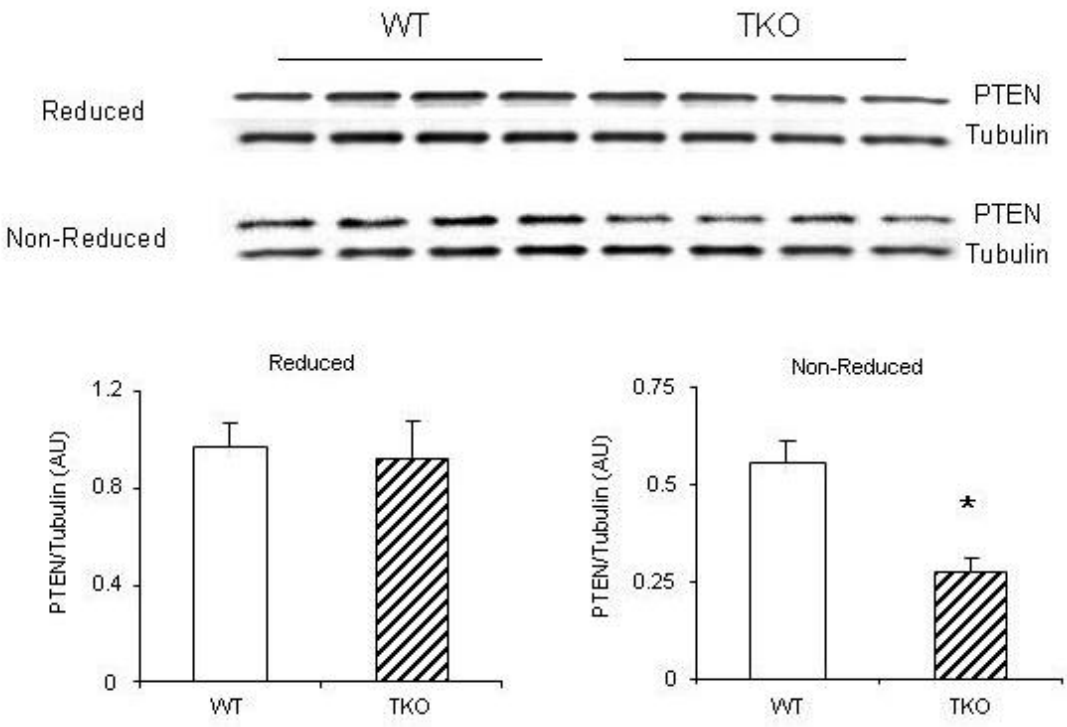

Figure 15: PTEN oxidation state. Protein extracts of soleus muscles from overnight fasted mice were prepared in homogenization buffer containing 10mM N-ethylmaleimide and 10mM iodoacetate. 20ug of protein were then added to reducing sample buffer of non-reducing buffers and fractions on Tris-glycine gels and electroblotted onto PVDF membranes. Blots were then probed with antibodies against PTEN and tubulin. N=4 mice per group. WT=wild-type, TKO=Txnip -/-. Results are presented as mean ± S.D. * Denotes significant statistical significance, $p<0.05$.

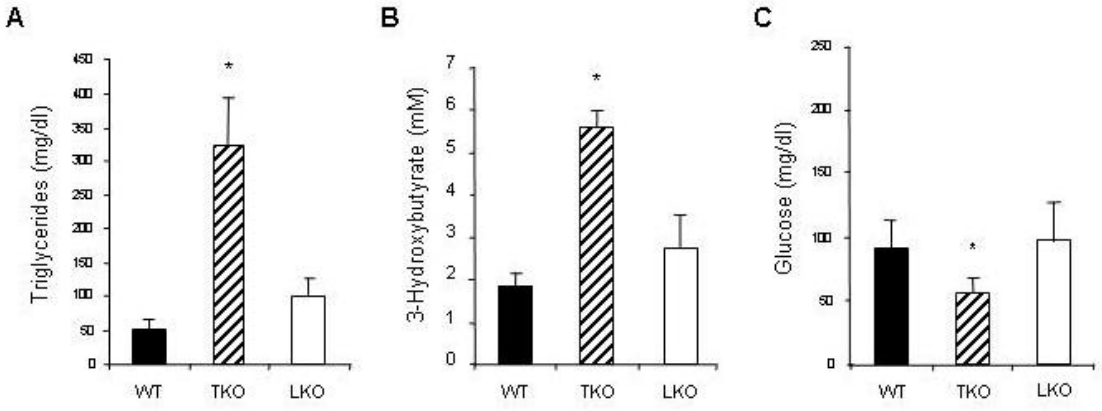

Figure 16: Plasma metabolite profile of liver-specific Txnip -/- mice (LKO) compared to global Txnip -/- (TKO), and control wild-type mice (WT). Plasma levels of triglycerides, 3-hydroxybutyrate and glucose were assessed after overnight fast using standard calorimetric commercial kits. N=8 to10 mice per group. Results are presented as mean ± S.D. * Denotes significant statistical significance, $p<0.01$.

Figure 17: Txnip mRNA expression in wild-type mice under non-fasting and fasting conditions. Total RNA was prepared from various tissues harvested from non-fasted and overnight fasted wild-type mice. Levels of Txnip mRNA expression were determined by quantitative real-time PCR normalized to 18S RNA. N=8 to 10 mice per group. White bars represent non-fasted mice, and black bars represent overnight fasted mice. Results are presented as mean ± S.D. * Denotes significant statistical significance, $p<0.05$.

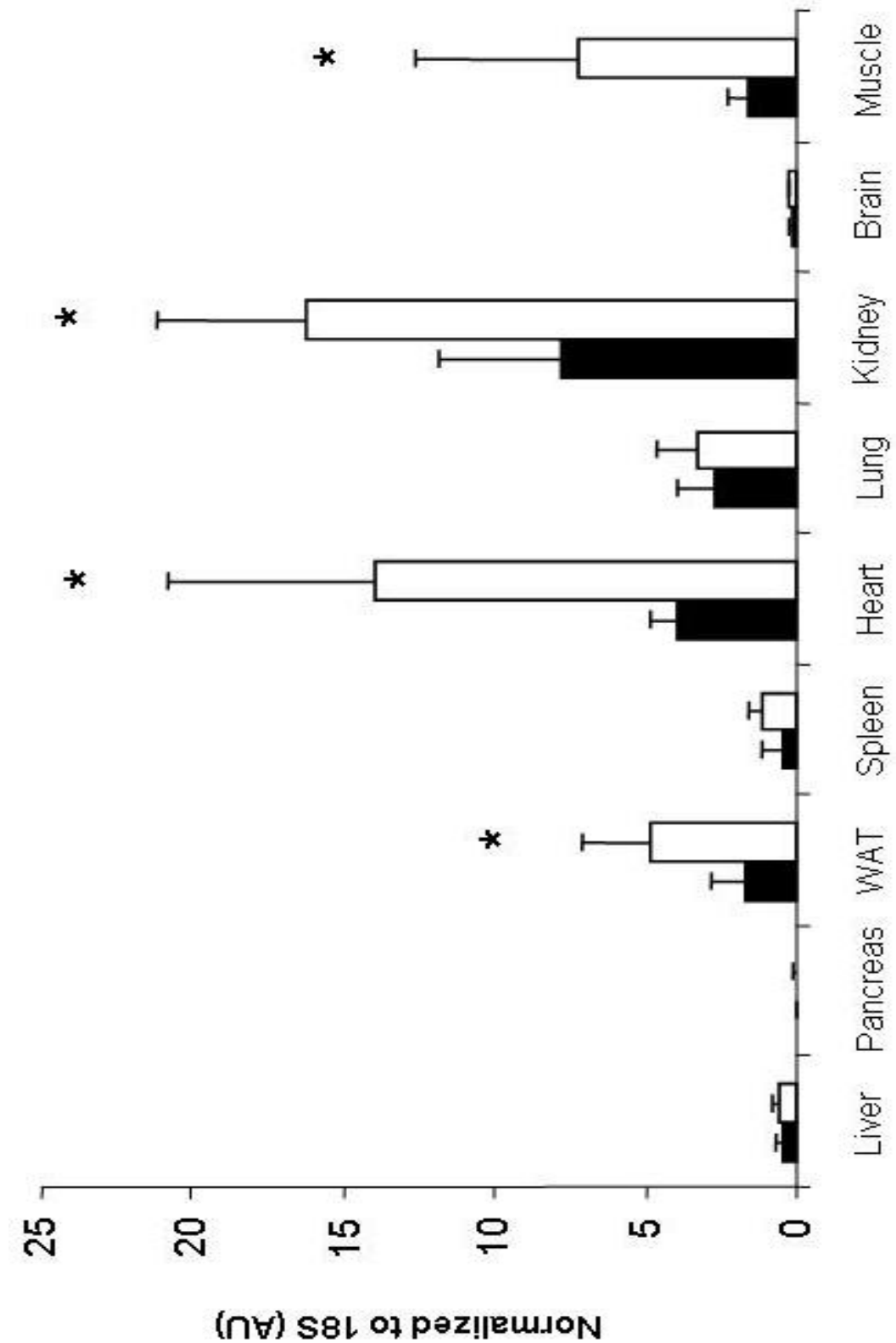
Normalized to 18S (AU)
25
20
15
10
5
0
Liver
Pancreas
WAT
Spleen
Heart
Lung
Kidney
Brain
Muscle
*
*
*
*

The text and figures presented in Chapter 2, in part, has been submitted for publication of the material as it may appear in Hui, Simon T. Y., Andres, Allen M., Miller, Amber K., Spann, Nathanael J., Potter, Douglas W., Post, Noah M., Chen, Amelia Z., Sachithanantham Sowbarnika, Jung, Dae Y., Kim, Jason K., and Davis, Roger A. (2008) Txnip balances metabolic and growth signaling via PTEN disulfide reduction. *Proceedings of the National Academy of Sciences*. Vol. 105, No. 10: 3921-3926. The dissertation author was the secondary investigator and author of this paper.

Chapter 3

Importance of Txnip in Energy Homeostasis of Muscle Tissues

In response to a fasting challenge, we and others have found that Txnip expression becomes highly induced in heart and skeletal muscle [4, 91]. Previously we have shown that Txnip ablation in heart and skeletal muscle alone is sufficient to elicit the abnormal fasting phenotype displayed in global knockout mice that is characterized by hypoglycemia, hyperketosis and hypertriglyceridemia [91]. Thus we sought to further investigate Txnip's role in the regulation of energy homeostasis specifically in muscle tissues.

AMP-activated protein kinase (AMPK) is a well conserved sensor of energy status and is important in the ability of muscle tissue to regulate its energy needs [151, 152]. Under conditions of low cellular energy levels (high AMP:ATP ratio), the α-subunit of AMPK becomes activated through phosphorylation at the Thr 127 site [151, 153-155]. The major kinases involved in the activation of AMPK are LKB1, Ca^{2+}-calmodulin-dependent kinase kinase, and transforming growth factor-β-activated protein kinase 1 (TAK1) [155]. LKB1 has been proposed to act as the primary kinase involved in AMPK activation in skeletal muscles during energy stress conditions [155, 156]. Animals subject to an energy stress challenge such as fasting activate AMPK leading to a cascade of downstream events ultimately increasing energy generating (catabolic - fatty acid oxidation, glycogen breakdown and glucose

uptake) processes and attenuating energy consuming (anabolic – glycogen, fatty acid and lipid synthesis) ones (see Figure 18) [153, 157, 158].

Heart and skeletal muscle tissues play a key role in facilitating an appropriate metabolic response to fasting due to their ability to switch fuel consumption towards fat-derived sources by increasing oxidative phosphorylation to meet their energy needs. This ability to switch substrate utilization in an effort to conserve glucose was first described as the glucose-fatty acid cycle by Sir Philip Randle [144]. To date, it is accepted that there is a reciprocal relationship between the utilization of fat-derived fuels (fatty acids and ketone bodies) and the use of glucose where the use of one substrate negatively affects the selection of the other as an energy substrate [143, 145, 159, 160]. The phenomenon of fuel switching has been validated over the years by many laboratories and yet the complexity of this process remains immense and there are still many unknowns despite the level of understanding we possess so far.

We have observed in previous studies (Chapter 2) that deletion of Txnip leads to a shift towards increased glycolysis and diminished use of the mitochondrial oxidative machinery as a source for generating ATP in soleus muscle of mice [91]. We hypothesize that loss of Txnip in muscle renders these tissues unable to initiate the glucose-fatty acid cycle, which consequently leads to an improper metabolic response to a fasting challenge. Given the striking influence muscle-specific Txnip ablation has with regards to disrupting the normal metabolic response to fasting, and the importance of

AMPK in muscle tissue energy homeostasis, we were compelled to investigate the possible association of Txnip to AMPK signaling. Here we have attempted to shed light into this possible association to further elucidate the mechanism of Txnip action with regards to metabolism.

RESULTS

Activation of AMPK is reduced in oxidative muscle tissues of fasting Txnip -/- mice

Our previous characterization of muscle-specific Txnip -/- mice clearly demonstrated that loss of Txnip in muscle tissue is sufficient to cause the anomalous metabolic fasting response seen in global Txnip -/- mice which leads to plasma hypoglycemia, hyperketonemia and hypertriglyceridemia, increased glycolysis, and diminished oxidation of fuel substrates through the mitochondria [91]. To investigate if Txnip ablation affects AMPK signaling in muscle tissue, samples from overnight fasted mice were subject to western blot analysis. We found that the activation of AMPK was markedly diminished in oxidative muscle tissues such as soleus muscle and heart, but interestingly no difference was observed in gastrocnemius muscle (Figure 19). As expected, the phosphorylation of a downstream AMPK target, acetyl-CoA carboxylase (ACC), was decreased in both soleus and hearts of Txnip -/- versus their controls (Figure 20). Previously we reported that Akt signaling may be increased in fasting Txnip -/- mice, and this may influence the activation of AMPK. AMPK may be phosphorylated by Akt at Ser 485/491

(AMPKα/β); sites that when phosphorlyated may inhibit the phosphorylation of AMPK at its well known target site at threonine 172 (AMPKα). To see if Akt signaling may be affecting the AMPK pathway directly in this manner, we compared the phosphorylation level of AMPK at Ser 485/491 and found that there is no difference between Txnip -/- mice and their wild-type littermates (Figure 21).

Ablation of Txnip leads to decreased fasting basal levels of AMP:ATP in oxidative muscle tissues

To gain some insight into the mechanism underlying the diminished activation of AMPK observed in oxidative muscle tissues of fasting Txnip -/- mice, we first examined the possibility that ablation of Txnip may affect the function of LKB1, the major upstream kinase known to activate AMPK in an energy stress-dependent manner [154]. To determine if LKB1 was functioning normally in Txnip -/- mice, we examined total levels of LKB1 in whole tissue homogenates, the nucleus, and in the cytosol. LKB1 is normally localized in the nucleus due to a nuclear localization sequence and must translocate to the cytosol in order to interact and activate AMPK (Figure 22) [161-163]. No differences were found in total levels of LKB1, its abundance in the nucleus, and its abundance in the cytosol (Figure 23) of fasted muscle tissues. To confirm that LKB1 is functioning properly we examined the phosphorylation status of an alternate downstream target, MARK1. There was no difference found in the LKB1 phosphorylation site of MARK1 between Txnip -/- mice and

their wild-type controls (Figure 24). This result strongly indicated that the hypoactivation of AMPK observed in fasting Txnip -/- mice is not due to a functional defect in LKB1, and may instead be due to a lower AMP:ATP ratio.

To directly examine this possibility, we quantified tissue nucleotide levels by LC/MS processed through the Yale Mouse Metabolic Phenotyping Center. We found that indeed AMP:ATP ratios were lower in oxidative muscle tissues including soleus and hearts of Txnip -/- mice, and surprisingly also in the more glycolytic gastrocnemius muscle in which we did not detect a significant difference in AMPK phosphorylation at Thr172 (although we have seen trends to show decreased AMPK activation through repetitions of the experiment) (Table 1). Interestingly, we did not detect a significant decrease in concentration of AMP in gastrocnemius muscle of Txnip -/- mice compared to wild-type which may be the ultimate reason why we could not see a statistically significant and visual decrease in the phosphorylation of AMPK in this tissue as AMP has been shown to have a higher affinity for binding to AMPK than ATP [164, 165] thus changes in its concentration are most important in regulating AMPK activity.

To eliminate the possibility that Txnip ablation may affect another kinase linked to AMPK activation (such as CaMKK or TAK1) and to ascertain that AMP:ATP ratio is the underlying cause for hypoactivation of AMPK, we examined the effects of acute AICAR treatment on the activation of AMPK in soleus muscle *in vivo*. AICAR is an AMP analog that becomes metabolized to AICAR monophosphate (ZMP) once inside a cell and mimics the effects of

AMP on inducing the activation of AMPK at Thr 172 [166]. Txnip -/- mice subcutaneously injected with AICAR displayed a similar maximal activation level of AMPK at the given treatment (0.5mg/g mouse for 1hr) when compared to wild-type mice (Figure 25). The robust activation of AMPK by acute AICAR treatment seen in Txnip -/- mice demonstrates that the hyopactivation of AMPK is not due to deficiencies in upstream kinase function or the capability of AMPK to become activated, but rather a consequence of having a decreased basal fasting AMP:ATP ratio, and more importantly low AMP concentrations.

Glucose transporter expression is not associated with increased glucose uptake and glycolysis in muscle tissues of Txnip -/- mice

We previously found that Txnip -/- mice have an increased propensity to utilize glucose and decrease their use of mitochondrial oxidation during fasting [91]. To determine if ablation of Txnip leads to this phenomenon by increasing expression of glucose transporters, we examined the expression of Glut-1 and Glut-4, the glucose transporters most highly expressed in muscle tissues [167]. To assess the contribution of Glut-1 to the increased utilization of glucose in Txnip -/- mice we first looked at gene expression by quantitative real-time PCR. Glut-1, which is expressed in many tissues [168], is responsible for the basal uptake of glucose in muscle tissues [169] and its functional expression is regulated at the level of transcription [170, 171]. Glut-1 is mainly regulated at the transcriptional level and anchors to the plasma

membrane upon synthesis of the protein [172]. We found that Glut-1 mRNA expression was diminished in soleus, heart and gastrocnemius muscles (Figure 26A) and this correlates well with its protein expression (Figure 26B). Glut-4 expression was examined as its abundance on the plasma membrane. Glut-4 is normally stored in intracellular membranes that are induced to translocate to the plasma membrane by signaling pathways such as Akt or AMPK activation [115, 173-175]. After plasma membrane enrichment of heart, soleus and gastrocnemius muscles we found that there is no difference in Glut-4 expression in these tissues between Txnip -/- mice and wild-type mice (Figure 27). This finding along with the fact that there is an obvious decrease in AMP:ATP ratio and attenuation of mitochondrial oxidative phosphorylation strongly indicates that it is the increased glucose uptake and glycolysis associated with Txnip ablation that leads to the high energy state of these tissues (*i.e.* low AMP:ATP ratio).

Txnip ablation induces inhibition of the mitochondrial pyruvate dehydrogenase complex and is associated with increased tissue glycogen content

A high energy state (low AMP:ATP ratio) is known to potently activate pyruvate dehydrogenase kinases (PDKs), which in turn phosphorylate and inhibit the mitochondrial pyruvate dehydrogenase complex (PDC) (reviewed in [176] and Figure 28). To determine if this was occurring in the tissues of fasting Txnip -/- mice we examined the state of inhibition of the PDC by

examining thephosphorylation state of its pyruvate dehydrogenase E1α subunit. We found a markedly increased phosphorylation of the pyruvate dehydrogenase E1α subunit of the PDC (Figure 29), which would be consistent with the decreased fuel flux through the mitochondria we had earlier observed when performing *ex vivo* substrate oxidation experiments on soleus muscles of fasted mice [91].

Under various circumstances AMPK activity has been linked to the regulation of glycogen content in tissues as it has been found to have glycogen binding domains [177, 178]. Disruptions in the ability of AMPK to become activated has been associated with increased cardiac and skeletal muscle glycogen accumulation [179, 180]. Because we found that AMPK activation is decreased in heart and soleus muscle of fasting Txnip -/- mice, we hypothesized that these mice may also exhibit, to some extent, some form of glycogen storage abnormality. To test this hypothesis, we measured muscle tissue levels of glycogen in muscle tissues. Surprisingly tissues of overnight fasted Txnip ablated mice displayed increased glycogen content in soleus and heart muscle, but not in gastrocnemius muscle (Figure 30). For a brief review of the regulation of glycogen content in tissue see Figure 31. In line with the findings of others mentioned above, we found that the hypoactivation of AMPK in heart and soleus muscle correlates with increased glycogen content in these tissues. Likewise, glycogen content in gastrocnemius muscle and AMPK activation display no differences when comparing Txnip -/- tissues to their wild-type counterparts. Although we did not investigate the state of AMPK or

nucleotide level in liver tissue we did find significantly increased levels of glycogen in the liver of fasting Txnip -/- mice versus their controls.

To examine a proximal reason for why Txnip -/- mice have increased glycogen content in their heart and soleus muscles, we examined the activity state of glycogen synthase kinase 3β (GSK-3β), which regulates glycogen storage in an insulin-dependent manner and is inhibited by Akt phosphorylation at Ser 9 [181, 182]. As its name implies, GSK-3β phosphorylates glycogen synthase (GS) at multiple sites to inhibit its ability to promote glycogen storage (with Ser 640 as the most potent inhibition site) [183-185]. We found that there was no difference in the phosphorylation (inhibition) state between Txnip -/- mice and wild-type of GSK-3β at Ser 9. This is consistent with our more recent finding that Txnip ablation does not affect Akt activation in heart and soleus muscle during fasting. Surprisingly, we found that phosphorylation of GS at Ser 640 is about 75% greater in Txnip -/- soleus tissues compared to controls (Figure 32). This indicates that factors other than GSK-3β are affecting this enzyme and, due to its increased inhibition by phosphorylation at Ser 640, suggests that the increased glycogen content in these tissues may be due to inhibition of glycogen break-down rather than synthesis. We cannot fully exclude increased glycogen storage though because GS is also controlled via allosteric activation by glucose-6-phosphate (G6P) [186, 187], which may likely be increased in these muscle tissues due to the increased glucose uptake and glycolysis we have observed. On the other hand, glycogen phosphorylase (GP – which breaks down

glycogen) is activated by AMP and inhibited by G6P and ATP [188]. Our data of high energy metabolite content and the possibility of increase G6P in these tissues strongly suggests that glycogen phosphorylase should be in a more inhibited state in Txnip -/- mice. Clearly a more thorough investigation into the activity states of glycogen synthase and phosphorylase and overall flux of glucose into and out of glycogen stores in these muscle tissues would be an interesting area to investigate to get a more concrete answer. Unfortunately, given our financial situation and other academically related events, we were constrained to end our research at this point.

EXPERIMENTAL PROCEDURES

Animal Studies

Txnip knockout mice and their wild-type (C57BL/6 background) littermates were housed in a temperature controlled room (25±1^{o}C) under a 12 hour light and 12 hour dark system (6PM-6AM dark). Mice were allowed free access to water and standard mouse chow (Lab Diet 5001, Purina Mills). For fasting experiments, mice were moved into a new cage without chow at 4PM and sacrificed after ~18 hours. All experimental procedures were approved by the Institutional Animal Care and Use Committee at San Diego State University.

Extraction of Total RNA and Quantitative Real-Time PCR

Frozen tissue samples were processed using an RNA isolation kit from 5-Prime according to the manufacturer's instructions. Total RNA was converted to cDNA using iScript (BioRad) according to the manufacturer's instructions. Quantitative Real-Time PCR was performed using the BioRad iCycler system (BioRad). The primers used for Glut-1 mRNA expression were 5'-GGTGTGCAGCAGCCTGTGTA - 3' (forward) and 5'-ACAAACAGCGACACCACAGT - 3' (reverse). The house-keeping gene Cyclophilin, 5' – TGGAGAGCACCAAGACAGACA – 3' (forward) and 5' – TGCCGGAGTCGACAATGAT – 3' (reverse) was used as control. Primers were designed using Primer 3 software. Results are displayed as percent change relative to control mice.

Western Blotting

Tissues were homogenized in ice-cold buffer containing 50mM Tris pH 8, 150mM NaCl, 2mM EGTA, 1mM EDTA, 1% NP-40, 0.5% Sodium Deoxycholate, 0.1% SDS, 20mM NaF, 1mM $NaVO_4$, 1mM PMSF, 10ug/mL aprotinin, 10ug/mL leupeptin and 10ug/mL pepstatin. Proteins were fractionated by SDS-PAGE using tris glycine gels (Invitrogen) and then electroblotted onto polyvinylidene difluoride membranes. Blots were blocked using 5% non-fat dried milk in tris buffered saline with 1% tween-20. The following primary antibodies were used: phosphoAMPK Thr 172, phosphoAMPK Ser 485/491, AMPK, phosphoACC Ser 79, ACC, Integrin β1,

phosphoGlycogen Synthase Ser 640, phosphoGlycogen Synthase Kinase 3β (Ser 9), and phosphoMARK1 (activation loop) were from Cell Signaling Technology. Anti-Tubulin antibody was obtained from Sigma. Anti-phosphoPDH-E1α (Ser 293) was obtained from Calbiochem. Antibodies for LKB1, Glut-1 and Glut-4 were obtained from Santa Cruz Biotechnology. After incubation in peroxidase-conjugated secondary antibodies (KPL), blots were visualized using Super Signal West Dura Extended Duration Substrate (Thermo Scientific).

AICAR Treatment Experiment

Mice were fasted over night prior to subcutaneous injection of AICAR (Toronto Research Chemicals) (0.5mg/g mouse) in saline or just saline. After 1hr mice were sacrificed and soleus muscles were prepared for western blot analysis.

Quantification of Tissue High Energy Metabolites

Snap-frozen tissues from overnight fasted mice (~18 hours) were sent to the Mouse Metabolic Phenotyping Center at the Yale University School of Medicine for quantification of nucleotide levels by LC/MS.

Tissue Glycogen Content

Frozen tissues (~20-50mg) were dissolved in 1N KOH in a shaking water bath for 20mins at 65^{o}C. Samples were vortexed occasionally. A portion of the resulting mixture was then treated with activated amyloglucosidase (Sigma) in an acidic buffer overnight at room temperature to allow for the breakdown of glycogen into free glycosyl units. Samples were neutralized with 1N NaOH and assayed using a standard glucose kit (Wako). Tissue glycogen content is expressed as the amount free glycosyl units (µmol)/gram tissue.

Subcellular Fractionation

Soleus, heart and gastrocnemius samples from overnight fasted mice were processed for plasma membrane preparations as described in [189] with minor modifications. Upon extraction tissues were immediately minced and homogenized in ice-cold buffer containing 20mM HEPES, 250mM sucrose, 1mM EDTA, 10ug/mL aprotinin, 10ug/mL leupeptin, and 10ug/mL pepstatin, pH 7.4 (Buffer 1). Large debris was discarded after a 2,000 g spin for 10min at 4^{o}C. A portion of the resulting mixture was saved as the whole homogenate to assess levels of Glut-1 protein. The remaining mixture was then centrifuged at 9,000 g for 20min at 4^{o}C. The pellet was set aside as P1. The resulting supernatant was then centrifuged at 180,000 g for 1.5hrs at 4^{o}C to yield the cytosolic fraction and new pellet containing the plasma and intracellular membranes. The pellet was then resuspended in 20mM Hepes, 30% sucrose, 1mM EDTA, 10ug/mL aprotinin, 10ug/mL leupeptin, and 10ug/mL pepstatin,

pH 7.4 (Buffer 2) and subject to a 216,000 g centrifugation step for 1hr at 4^{o}C to separate the intracellular membranes (supernatant) from the plasma membranes (pellet, P2). P1 and P2 were combined and resuspended in buffer 1 for assessing the levels of Glut-4 found on the plasma membrane.

Statistical Methods

All data are reported as the average ± S.D. The two-tailed Student's *t* test was used to analyze data. Results having p-values less than 0.05 were considered significant.

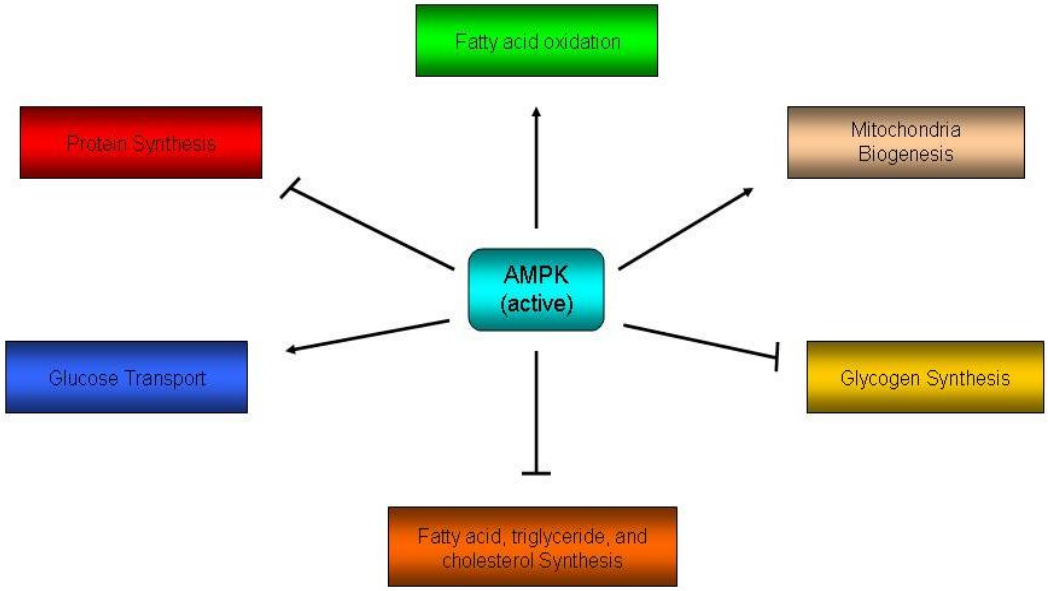

Figure 18: Actions of activated AMPK. Active AMPK promotes energy generating catabolic pathways such as increasing glucose transport, fatty acid oxidation, and mitochondrial biogenesis. Simultaneously, active AMPK inhibits energy consuming anabolic pathways such as protein synthesis, glycogen synthesis and the synthesis of fatty acids, triglycerides and cholesterol.

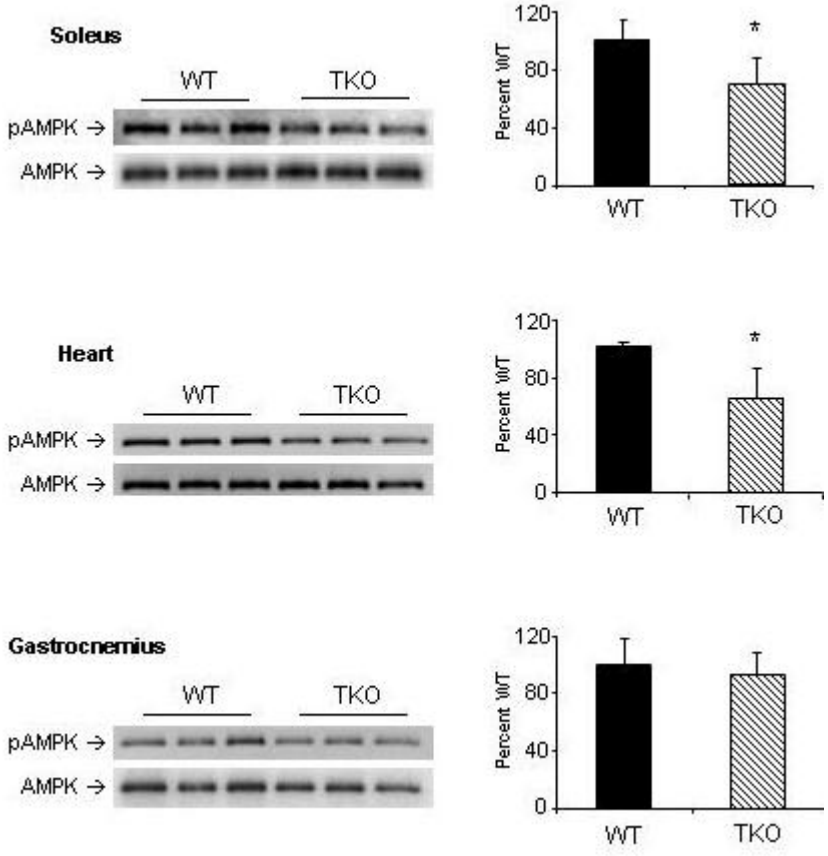

Figure 19: Fasting activation state of AMPK. 20ug of protein from soleus, heart, and gastrocnemius muscles of overnight fasted mice (~18 hours) were fractionated on Tris-glycine gels and electroblotted onto PVDF membranes. Blots were then probed with antibodies against phosphoAMPK (Thr 172). After stripping, blot was then probed for total AMPK as a loading control. N=3 mice per group. WT=wild-type, TKO=Txnip -/-. Results are presented as mean ± S.D. * Denotes significant statistical significance, $p<0.05$.

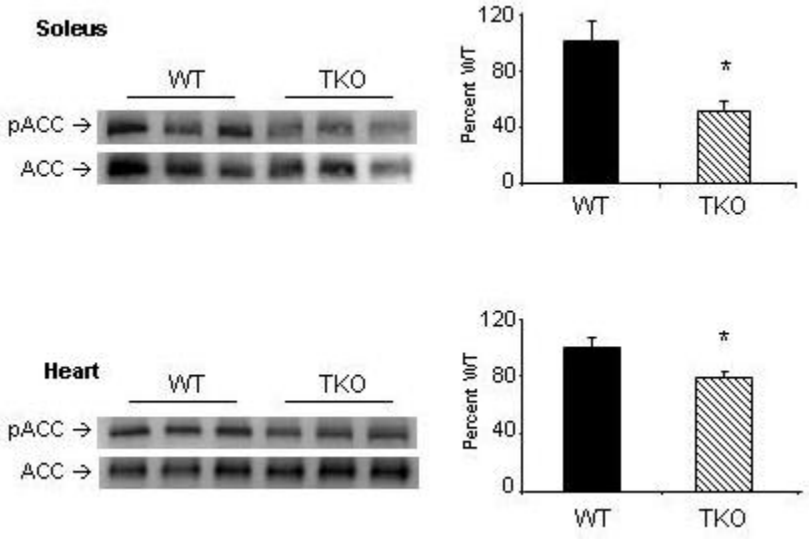

Figure 20: Fasting inhibition state of ACC. 20ug of protein from soleus muscle, and heart of overnight fasted mice (~18 hours) were fractionated on Tris-glycine gels and electroblotted onto PVDF membranes. Blots were then probed with antibodies against phosphoACC (Ser 79). After stripping, blot was then probed for total ACC as a loading control. N=3 mice per group. WT=wild-type, TKO=Txnip -/-. Results are presented as mean ± S.D. * Denotes significant statistical significance, $p<0.05$.

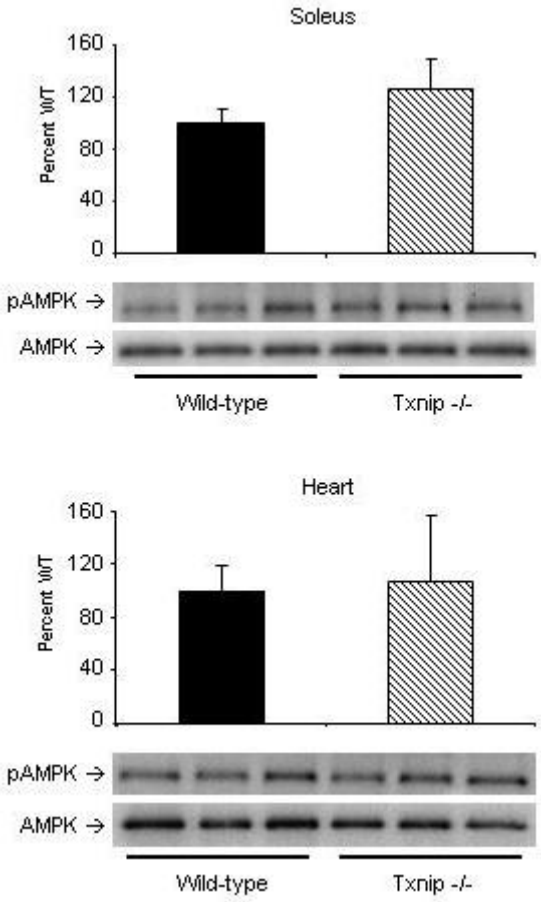

Figure 21: pAMPK (Ser 485/491) – Akt target site phosphorylation. 20ug of protein from soleus muscle, and heart of overnight fasted mice (~18 hours) were fractionated on Tris-glycine gels and electroblotted onto PVDF membranes. Blots were then probed with antibodies against phosphoAMPK (Ser 485/491). After stripping, blot was then probed for total AMPK as a loading control. N=3 mice per group. WT=wild-type, TKO=Txnip -/-. Results are presented as mean ± S.D. No statistical difference was seen between the two groups for both soleus and heart tissues.

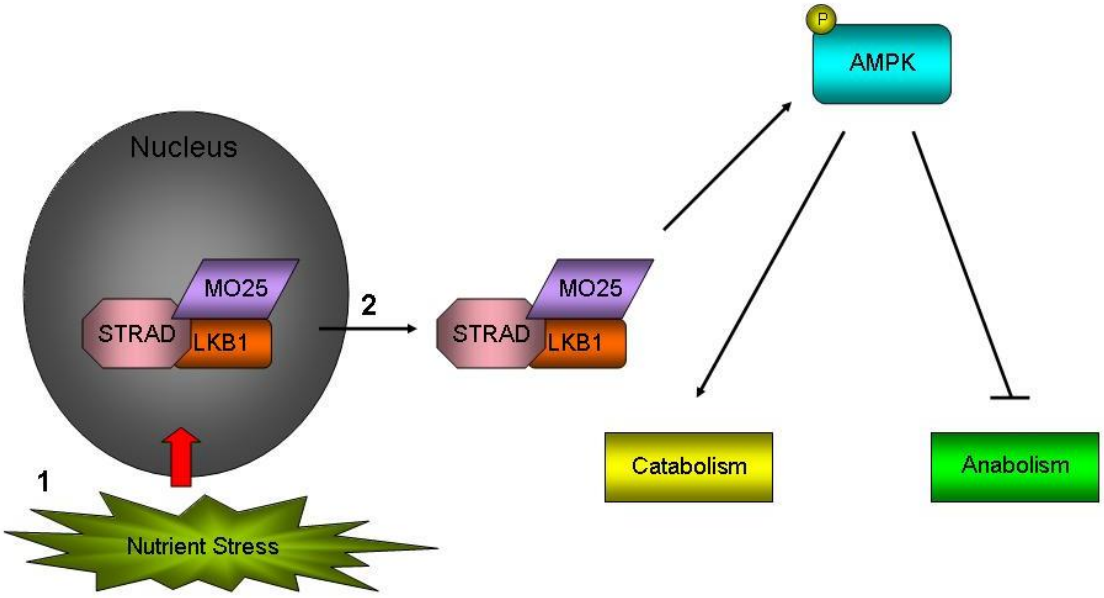

Figure 22: LKB1 activation of AMPK. LKB1 is normally sequestered in the nucleus and is considered to be a constitutively active kinase. Under conditions of nutrient stress (such as fasting) (**1**) LKB1 complexes with mouse protein 25 (MO25) and Ste20-related adaptor protein (STRAD) which allows the complex to (**2**) translocate into the cytosol where LKB1 can then interact and activate AMPK. Active AMPK then promotes catabolism, and inhibits anabolism in general.

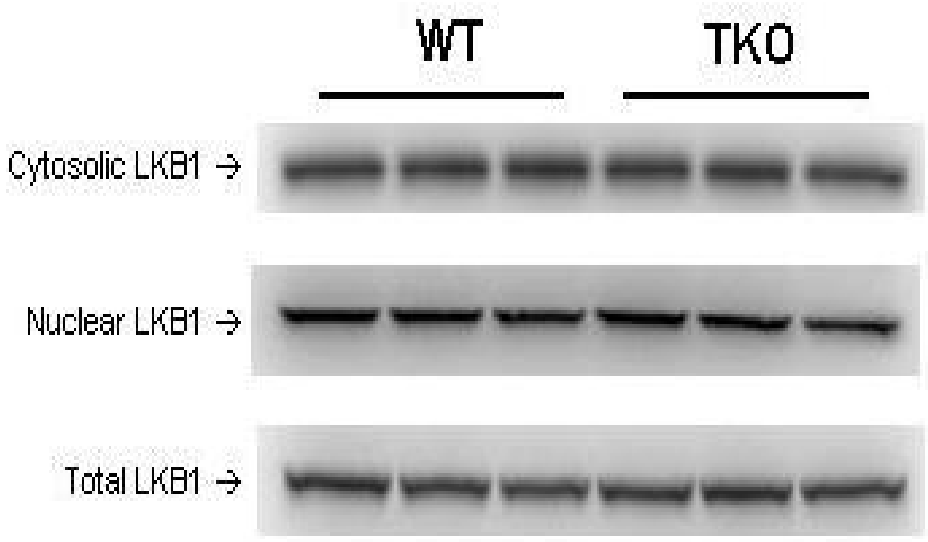

Figure 23: LKB1 subcellular localization. Soleus muscles from overnight fasted mice (~18 hours) were subject to subcellular fractionation to obtain cytosolic and nuclear fractions. 10ug of protein from cytosol, nuclear fractions and saved whole homogenate of soleus muscle were then fractionated on Tris-glycine gels and electroblotted onto PVDF membranes. Blots were then probed with antibodies against LKB1. N=3 mice per group. WT=wild-type, TKO=Txnip -/-.

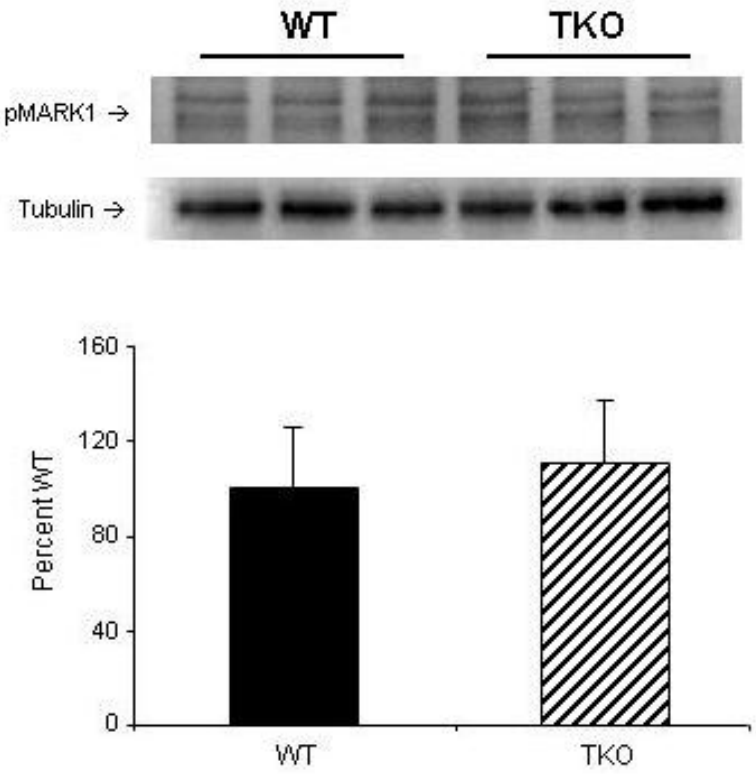

Figure 24: pMARK1 (activation loop) – Alternate LKB1 target. 50ug of protein from whole homogenate of soleus muscle was fractionated on a Tris-glycine gel and electroblotted onto a PVDF membrane. Blot was then probed with antibodies against phosphoMARK1 (activation loop). After stripping, blot was then probed for tubulin as a loading control. N=3 mice per group. WT=wild-type, TKO=Txnip -/-. Results are presented as mean ± S.D. No statistical difference was seen between the two groups.

Table 1: High energy metabolite concentrations in muscle tissues.
ATP, ADP, AMP and AMP/ATP ratios from soleus, heart and gastrocnemius muscles were analyzed by the Mouse Metabolic Phenotyping Center at the Yale University School of Medicine by LC/MS. Concentrations are expressed as nmole/mg tissue. N=8 to 10 mice per group. WT=wild-type, TKO=Txnip -/-. Results are presented as mean ± S.D. * Denotes significant statistical significance from control WT group, $p<0.05$. ** Denotes significant statistical significance from control WT group, $p<0.01$.

	Soleus		Heart		Gastrocnemius	
	WT	TKO	WT	TKO	WT	TKO
ATP	9.27 ± 1.08	10.64 ± 1.32*	7.07 ± 0.39	6.38 ± 0.34**	7.16 ± 0.76	8.72 ± 0.33**
ADP	0.62 ± 0.09	0.59 ± 0.05	0.65 ± 0.10	0.63 ± 0.05	0.47 ± 0.04	0.56 ± 0.04**
AMP	0.25 ± 0.07	0.09 ± 0.02**	6.53 ± 1.73	4.44 ± 1.11**	0.21 ± 0.02	0.20 ± 0.04
AMP/ATP	0.027 ± 0.007	0.009 ± 0.002**	0.93 ± 0.27	0.70 ± 0.20*	0.029 ± 0.004	0.023 ± 0.004**

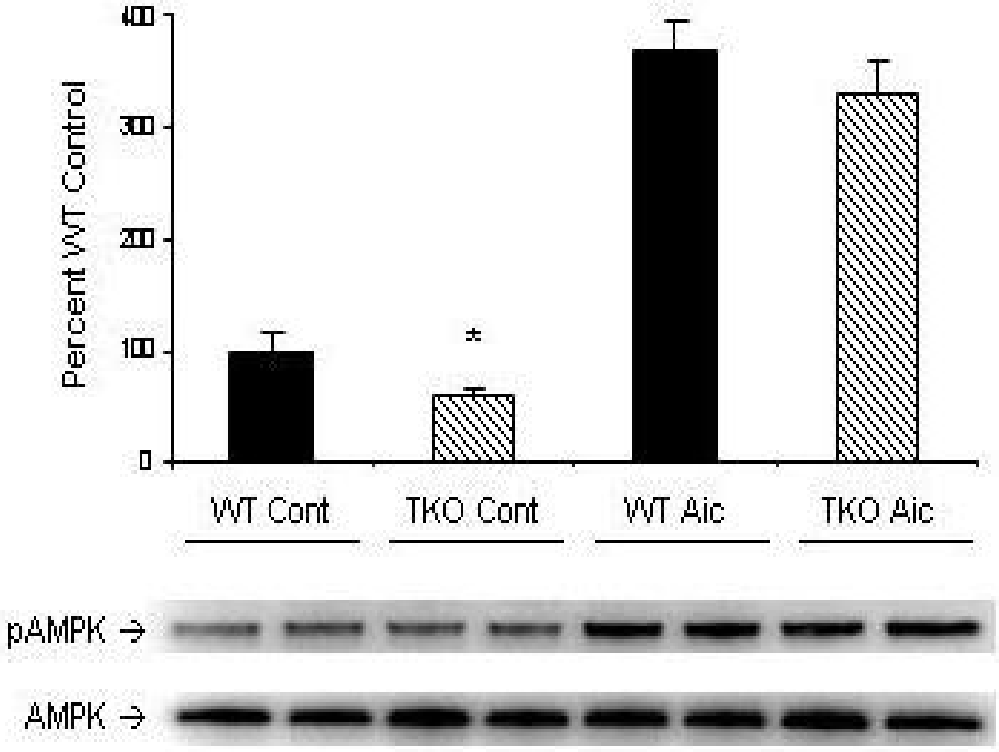

Figure 25: Effects of AICAR treatment on activation of AMPK. Overnight fasted mice (~18 hours) were given a subcutaneous injection of saline or AICAR carried in saline. After 1 hour mice were sacrificed and soleus muscle was prepared for western analysis. 20ug of protein for each condition was then fractionated on Tris-glycine gels and electroblotted onto PVDF membranes. Blots were then probed with antibodies against phosphoAMPK (Thr 172). After stripping, blot was then probed for total AMPK as a loading control. N=3 mice per group. A representative blot is shown above to display all sample categories. WT=wild-type, TKO=Txnip -/-. Cont=treated with saline only, Aic=given AICAR carried in saline (0.5mg/g mouse). Results are presented as mean ± S.D. * Denotes significant statistical difference between WT mice given the same treatment, $p<0.05$.

Figure 26: Glut-1 mRNA and protein expression. (A) Total RNA was prepared from soleus, heart and gastrocnemius muscles harvested from overnight fasted mice (~18 hours). Glut-1 mRNA expression was determined by quantitative real-time PCR normalized to Cyclophilin RNA. N=5 mice per group. Results are presented as mean ± S.D. * Denotes significant statistical significance, $p<0.01$. (B) 20ug of protein from soleus, heart, and gastrocnemius muscles of overnight fasted mice (~18 hours) were fractionated on Tris-glycine gels and electroblotted onto PVDF membranes. Blots were then probed with antibodies against Glut-1. After stripping, blot was then probed for total tubulin as a loading control. N=4 mice per group. WT=wild-type, TKO=Txnip -/-. Results are presented as mean ± S.D. * Denotes significant statistical significance, $p<0.05$.

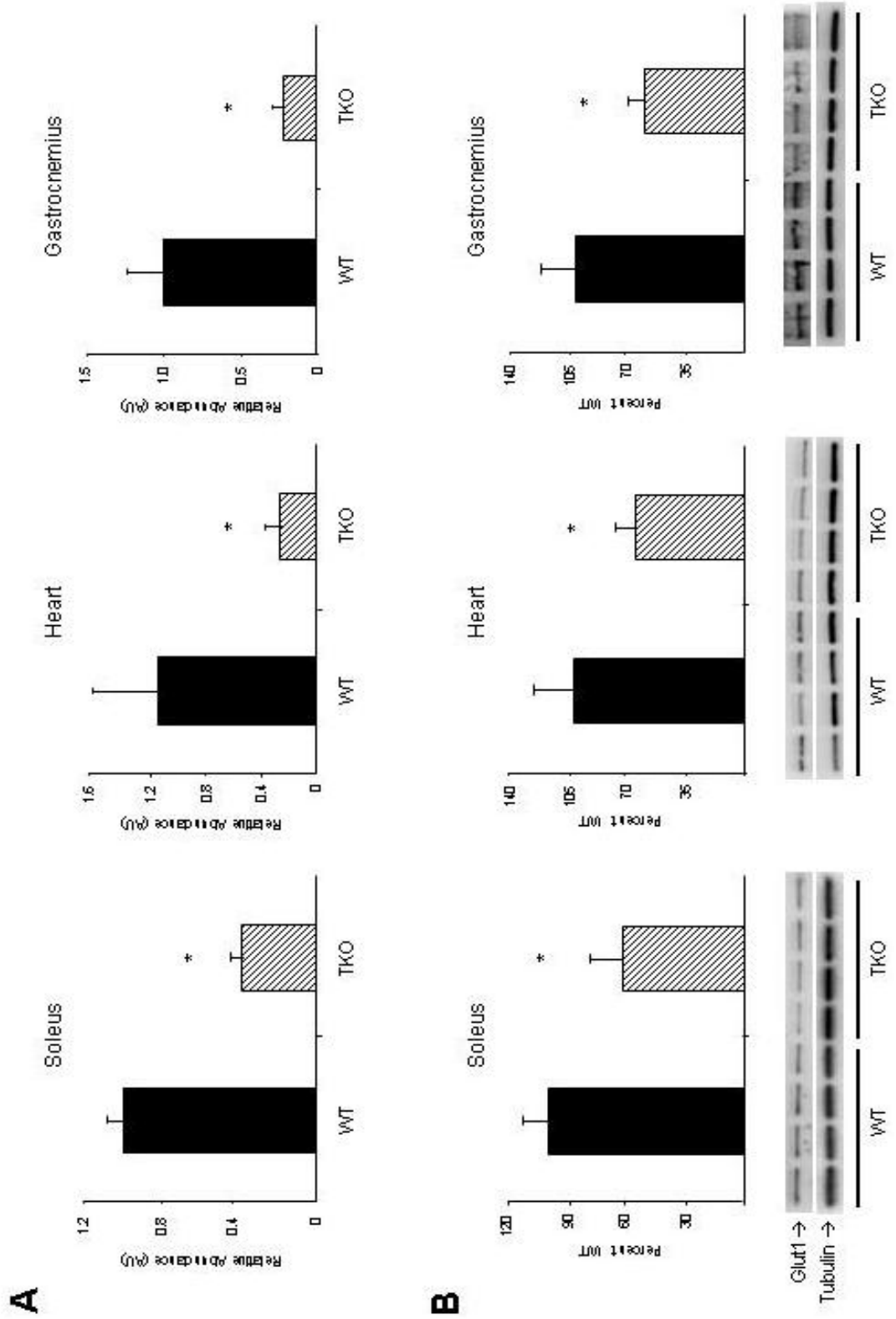
A
Soleus
Heart
Gastrocnemius
Relative Abundance (AU)
WT
TKO
*
B
Soleus
Heart
Gastrocnemius
Percent WT
WT
TKO
*
Glut1 →
Tubulin →

Figure 27: Glut-4 plasma membrane expression. Subcellular fractionation was performed on heart, soleus and gastrocnemius muscles of overnight (~18 hours) fasted mice to obtain enriched plasma membrane (PM) fractions. 10ug of protein from the PM enriched fractions of (A) heart, (B) soleus, and gastrocnemius muscles were fractionated on Tris-glycine gels and electroblotted onto PVDF membranes. Blots were then probed with antibodies against Glut-4. From those same samples, 40ug of protein were fractionated on Tris-glycine gels and electroblotted onto PVDF membranes. Blots were then probed with antibodies against integrin (A) as a loading control. Attempts to probe for integrin in the soleus and gastrocnemius samples were unsuccessful after many attempts. N=3 mice per group. WT=wild-type, TKO=Txnip -/-. Results are presented as mean ± S.D. No significant statistical differences were observed between the groups for (A) and no difference was visually apparent for (B). (C) Assay control blot using overnight fasted mice. All lanes were loaded with 30ug of protein from their respective samples as indicated: (Lanes 1-6 are all plasma membrane fractions) Lane: 1=soleus of WT, 2=soleus of WT treated with AICAR (0.5mg/g mouse) for 1 hour, 3=soleus of TKO,4=heart of WT, 5=heart of WT treated with AICAR (0.5mg/g mouse) for 1 hour, 6=heart of TKO, 7=WT heart cytosolic fraction, 8=WT heart intermembrane vesicle fraction, and 9=WT heart whole homogenate. Blot was first probed for integrin, was stripped, and then probed for Glut-4.

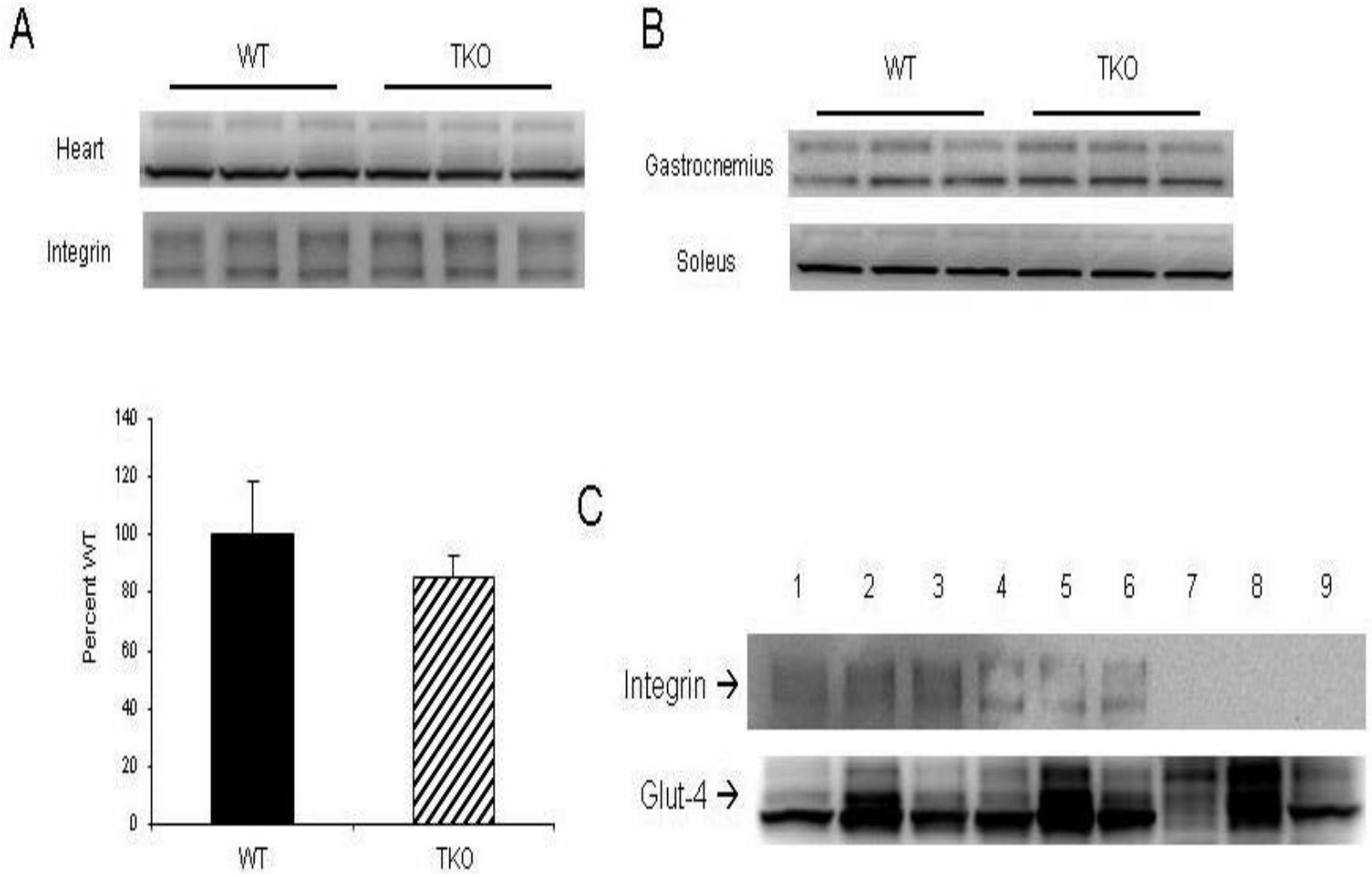
A
WT
TKO
Heart
Integrin
B
WT
TKO
Gastrocnemius
Soleus
Percent WT
140
120
100
80
60
40
20
0
WT
TKO
C
1
2
3
4
5
6
7
8
9
Integrin →
Glut-4 →

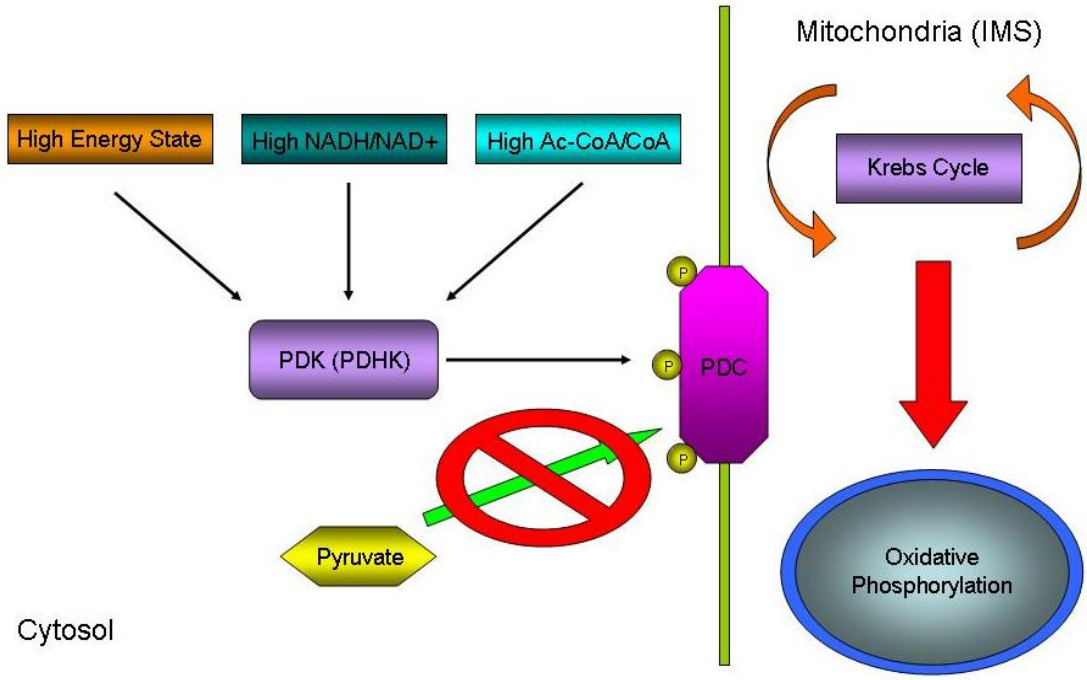

Figure 28: Inhibition of the pyruvate dehydrogenase complex. Under conditions of high energy, high NADH/NAD+, and/or high Acetyl-CoA/CoA the activity of pyruvate dehydrogenase kinases (PDK (PDHK)) is increased markedly. This leads to increased phosphorylation of the pyruvate dehydrogenase complex (PDC) which inhibits the entry of pyruvate into the mitochondria to undergo β-oxidation, thus preventing oxidation of glucose through the mitochondria. Because pyruvate entry into the mitochondria is essential to replenish elements in the Krebs Cycle (anaplerosis), inhibition of pyruvate entry into the mitochondria can slow the flux of all fuels into the mitochondria leading to diminished mitochondrial oxidative phosphorylation.

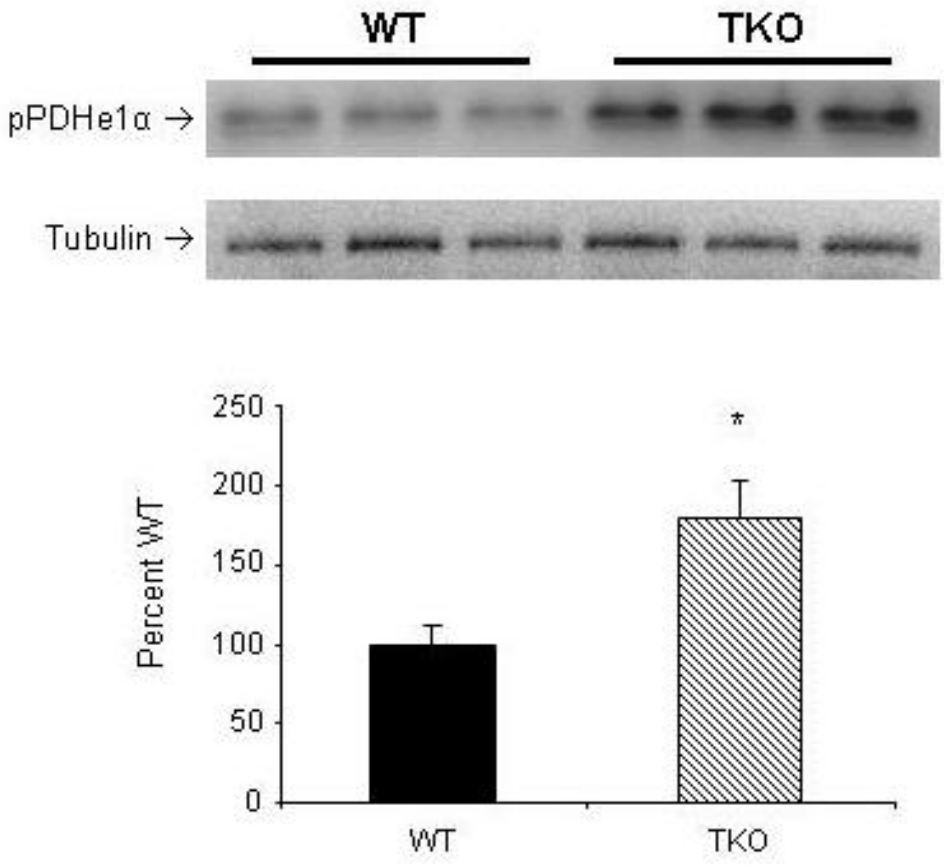

Figure 29: Inhibitory phosphorylation state of mitochondrial pyruvate dehydrogenase E1α subunit. 20ug of protein from whole homogenate of soleus muscle from overnight fasted mice (~18 hours) was fractionated on a Tris-glycine gel and electroblotted onto a PVDF membrane. Blot was then probed with antibodies against phosphoPDH E1α (Ser 293). Another blot was run using the same samples and 20ug of protein as well. The finished blot was probed for tubulin as a loading control. N=3 mice per group. WT=wild-type, TKO=Txnip -/-. Results are presented as mean ± S.D. * Denotes significant statistical difference, $p<0.05$.

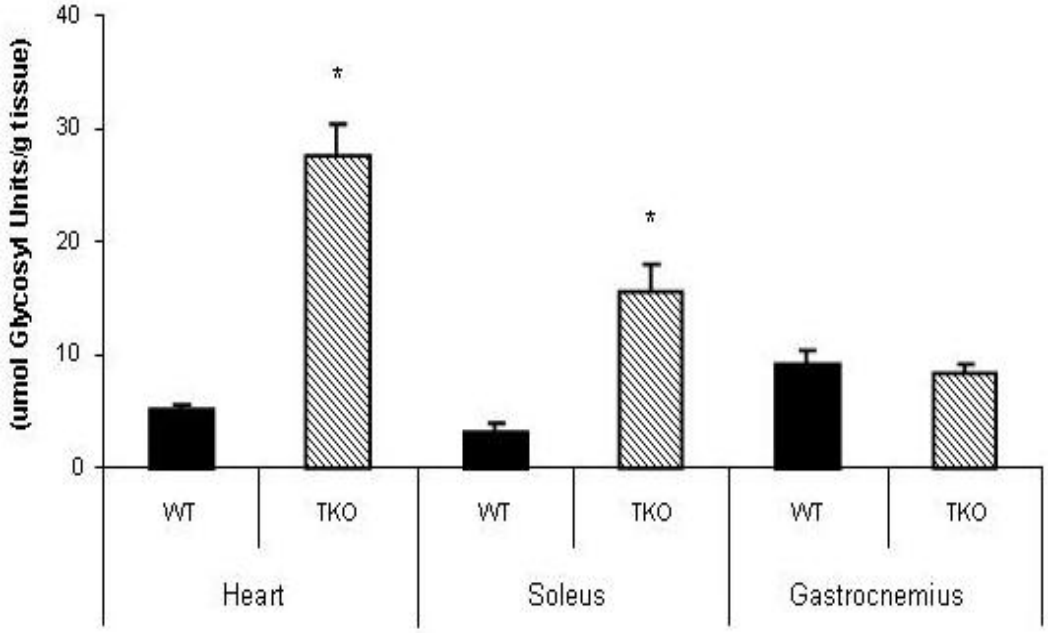

Figure 30: Tissue glycogen content. Heart, soleus and gastrocnemius muscle from overnight fasted mice (~18 hours) were processed to liberate glycosyl units from tissues as described. Glycosyl concentration was then assessed by a standard glucose colorimetric kit. Results are normalized to tissue weight. N=4 mice per group. WT=wild-type, and TKO=Txnip -/-. Results are presented as mean ± S.D. * Denotes significant statistical difference, $p<0.05$.

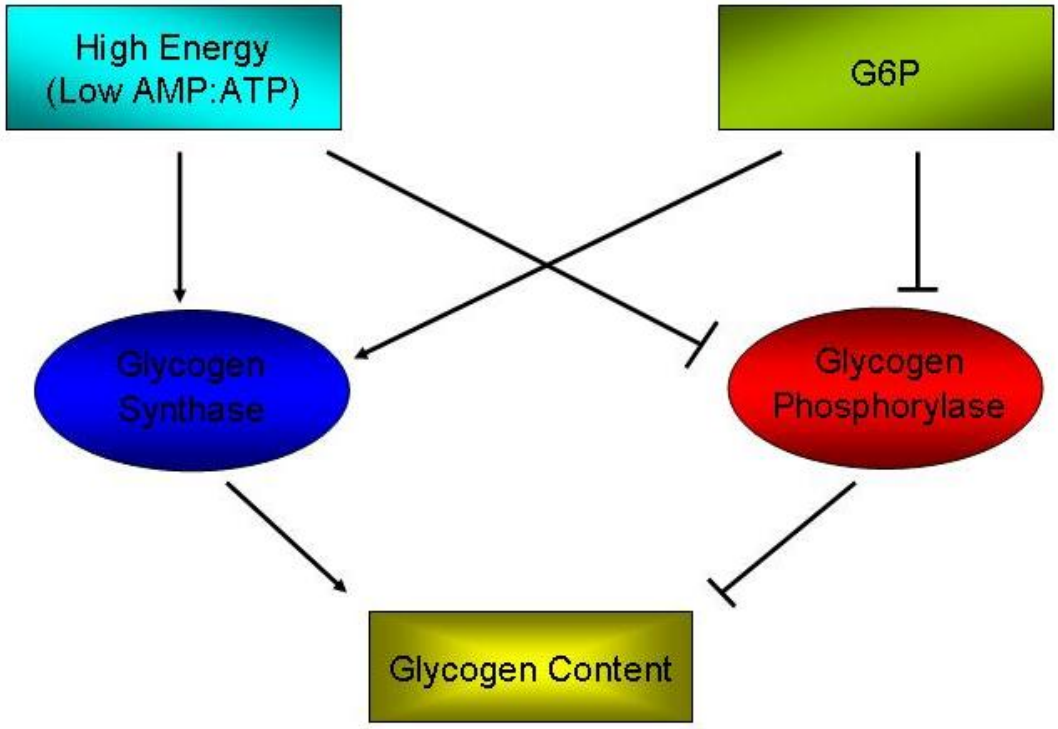

Figure 31: Regulation of tissue glycogen content. Tissue glycogen content is determined by the net action of glycogen synthase (GS) and glycogen phosphorylase (GP). A high intracellular energy state and/or increased G6P levels activate GS which promotes the build-up of glycogen. In contrast, the above mentioned conditions inhibit glycogen phosphorylase which is necessary for accessing glycogen stores.

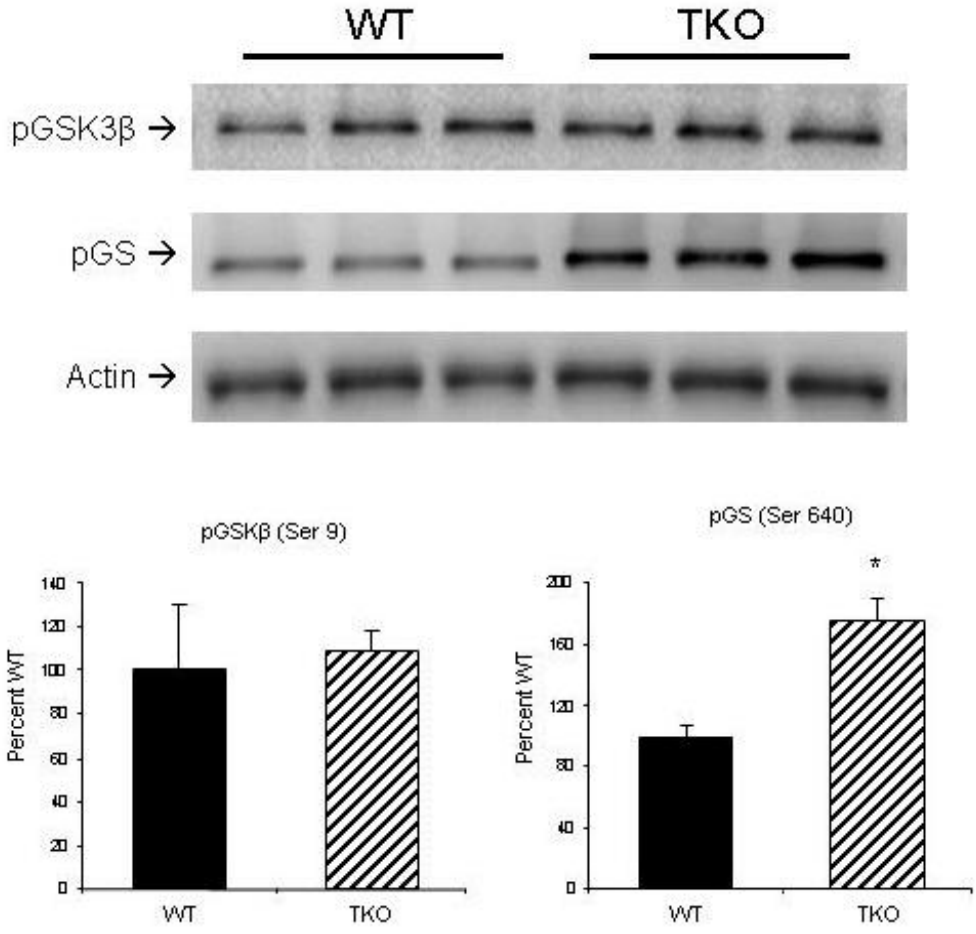

Figure 32: Phoshporylation state of key enzymes that regulate glycogen. 20ug of protein from whole homogenate of soleus muscle from overnight fasted mice (~18 hours) was fractionated on a Tris-glycine gel and electroblotted onto a PVDF membrane. Blot was then probed with antibodies against phosphoGSKβ (Ser 9). Another blot was run using the same samples (20ug) to probe for phosphoGS (Ser 640). This blot was then stripped and probed for actin as a loading control. N=3 mice per group. WT=wild-type, TKO=Txnip -/-. Results are presented as mean ± S.D. * Denotes significant statistical difference, $p<0.05$.

The text and figures presented in Chapter 3, in part, is currently being prepared for publication of the material. Andres, Allen M., Ratliff, Eric P., Sachithanantham, Sowbarnika, and Hui, Simon T.Y. The dissertation author was the primary investigator and author of this material.

Chapter 4

Discussion and Future Directions

Txnip's importance to the fasting response

In a normal metabolic response, Txnip is upregulated in many tissues of a fasting wild-type mouse to maintain whole-body energy homeostasis. As evidenced in this work, genetic ablation of Txnip alone is sufficient to disrupt this process, thus establishing Txnip as a keystone modulator of metabolic response. As a consequence, when fasted, mice lacking Txnip become characteristically hypoglycemic, hyperketotic and hypertriglyceridemic. The exact mechanistic role Txnip plays in allowing for a coordinated set of responses required for an appropriate metabolic response to fasting is poorly understood to date. In this dissertation we have attempted to elucidate this mechanism by examining in detail the phenotypic consequences that arise during fasting because of Txnip ablation.

In this work we have shown that Txnip ablation is associated with improved glucose tolerance. This is achieved by the increased propensity of muscle tissues to increase glucose uptake and glycolysis which is accompanied by attenuated mitochondrial oxidation of all major fuel types including glucose, 3-hydroxybutyrate (ketone) and fatty acids. The increased glucose tolerance is not due to altered circulating insulin or glucagon levels and is not associated with increased insulin-sensitivity in the periphery.

Rather, Txnip loss in muscle tissues leads to increased intracellular utilization of promotes increased glucose tolerance.

The reasons for the hypertriglyceridemic phenotype exhibited by overnight fasted Txnip -/- mice was not examined in detail in this dissertation as it will be covered in detail in the dissertation of my colleague E.P Ratliff (to be completed shortly after this dissertation's submission). Our examination into the reason for the build-up of plasma triglycerides in fasting Txnip -/- mice demonstrated that these mice have an impaired ability to clear triglycerides (intralipid clearance test). No differences were observed in the production of triglycerides between Txnip -/- mice and wild-type as determined by monitoring the build-up of plasma triglycerides over a time course after administration of a lipoprotein lipase inhibiting drug. Finally, we determined that the impaired ability to clear a bolus of intralipid is ultimately due to diminished lipoprotein lipase activity in muscle tissues and heart.

From our studies using mice with liver-specific ablation of Txnip, we found no noticeable fasting metabolic aberrancies, which suggested that Txnip exerts its metabolic importance in energy homeostasis in extra-hepatic tissues. Later, our group found that Txnip loss in the heart and skeletal muscles alone is sufficient to elicit the majority of the characteristic fasting metabolic phenotypes exhibited by whole-body Txnip -/- mice [91]. The importance of muscle tissues with regards to the economics of fuel partitioning was highlighted in 1963 by Sir Philip Randle who coined the term glucose-fatty acid cycle to describe the events that occur in these tissues to allow an animal

to survive an energy challenge [144]. Through the years Randle eventually found that the use of glucose and fat-derived fuels is reciprocal in nature such that that increased use of glucose inhibits fatty acid oxidation and conversely fatty acid oxidation can attenuate glucose oxidation [143, 145, 190, 191]. As we have seen, loss of Txnip in these tissues disrupts this metabolic process and leads to the various phenotypic abnormalities exhibited by Txnip -/- mice and thus we focused our attention into characterizing Txnip action in these tissues.

Association of Txnip ablation with Akt and glycemic control

The cause for the fasting hypoglycemia associated with Txnip disruption was first attributed to increased insulin production based on previous work by our lab examining the Hcb-19 mouse strain that expresses a truncated non-functional Txnip protein [110]. In that study, circulating levels of plasma insulin were significantly increased in fasting HcB-19 mice versus their controls. Moreover, gluconeogenesis in the liver appeared to be unchanged as mRNA expression of a rate-limiting factor in this process, phosphoenol pyruvate carboxy kinase (PEPCK) was decreased in the liver. Liver is an insulin responsive tissue in which transcription of PEPCK is potently down-regulated by insulin [192, 193]. Therefore, it was concluded that Txnip ablation may cause selective insulin resistance in the liver. The increased insulin levels, which decrease gluconeogenesis, could then be the underlying factor in the hypoglycemia observed mediated through extra-hepatic tissues.

Surprisingly, we did not see any difference in circulating insulin concentrations between our Txnip -/- whole-body knockout mice versus their control wild-type littermates. However Txnip -/- mice still exhibited the characteristic hypoglycemia in a fasted state. The findings in our previous strain using HcB-19 mice could then be attributed to other genetic factors in that strain in addition to Txnip disruption. We then revised our hypothesis concerning the hypoglycemia that arises in Txnip -/- mice: the loss of Txnip may lead to increased insulin sensitivity. This notion was initially supported in our lab upon the report of two previous members in our lab showing that there was a drastic increase in Akt activation in heart and soleus muscles. Akt is a well characterized downstream target of insulin signaling and its activation is linked to increased glucose utilization [194-196].

One hypothesis at the time was based on the theory that lack of Txnip would increase the chance for thioredoxin to bind to and inhibit PTEN, the major attenuator of PI3K/Akt activation cascade. Inhibitition of PTEN would then lead to increased Akt activation [128, 197, 198]. The possibility is controversial in that thioredoxin was shown to bind to an inhibit PTEN in only one study reported in a relatively obscure journal [199]. More accepted today is the concept that many phosphatases, including PTEN, are rendered inactive by increased oxidative stress, which leads to the oxidization of an intermolecular disulfide bond located in their phosphatase domain thus rendering it inactive [200-202]. In fact it has been recently demonstrated that thioredoxin is the most important activator of PTEN through its action of

reducing the key disulfide in its phosphatase domain to reactivate this phosphatase [130].

Another hypothesis was that lack of Txnip may lead to a paradoxical attenuation of the thioredoxin-NADPH circuit. The thought was that in non-lipogenic oxidative tissues such as the heart and soleus muscles, which have a reduced capacity to produce NADPH [132], the ablation of Txnip allows thioredoxin activity to go unabated during a critical period occurring at the onset of fasting, which depletes NADPH effectively inhibiting thioredoxin-NADPH-dependent reactions. As a collateral consequence, NADH/NADPH ratios would rise adding another level of negative regulation of PTEN; increasing NADH concentrations *in vitro* is able to inhibit the reductive reactivation of PTEN [134].

After painstaking attempts to recapitulate the previous finding concerning Akt activation, I and others in our lab could not repeat these findings, but consistently observed no difference in the activation of Akt in heart and soleus muscles between fasted Txnip -/- mice and their wild-type controls. Additionally, Txnip -/- mice and their wild-type littermates do not exhibit any difference in insulin-stimulated Akt activation. Meticulous work has shown that given a fair number of fasted mice to examine, Akt phosphorylation levels of residues Thr 308 or Ser 473 in muscle tissues of Txnip -/- or wild-type exhibit no differences under basal fasting conditions, or when insulin-stimulated. Another thing to note, as mentioned earlier in Chapter 2, is that insulin is really not a dominant hormone during the fasting state, which should

have been a red flag to the senior members of our lab to be cautious about publishing that Txnip ablation increases insulin sensitivity.

Many additional findings in our lab support the conclusion that there is no real difference in Akt activation state in soleus and/or heart muscle tissue between Txnip -/- mice and controls. Some of these that are found in this dissertation which contradict our lab's initial finding about Akt activation include: 1) No differences seen in the Akt phosphorylation site of AMPK at Ser 485/491 (Figure 19), 2) Glut-1 mRNA expression is decreased in Txnip -/- mice (Figure 23), and 3) no differences in phosphorylation of glycogen synthase kinase 3β (GSK-3β) at Ser 9, which is a downstream target phosphorylation site of Akt (Figure 27). Akt has been shown to phosphorylate residue Ser 485/491 of AMPK in the heart which prevents further phosphorylation of its activation site at Thr 172 [203, 204]. Aside from its well know function to increase Glut-4 translocation to the plasma membrane, Akt can affect glucose uptake by increasing Glut-1 expression indirectly through its action on mTOR signaling and HIF-1α [205-207]. We found that Glut-1 expression in Txnip -/- mice is diminished at both the transcription and translation levels which conflicts with the former finding that Akt is markedly upregulated. Finally, Akt is known to phosphorylate and inhibit GSK-3β by phosphorylating residue Ser 9 [181, 182], however we observe no noticeable difference between Txnip -/- mice and wild-type. With all these downstream targets not reflecting an increased activation of Akt, it is difficult to believe that Txnip -/- mice have increased Akt activation in the fasting state that is

physiologically meaningful, yet alone a ~3 to 4 fold increase in its phosphorylation state to increase its activity as previously reported [91]. With a building evidence of data against the previous finding that Akt activity is increased, pursuit of dissecting a pathway linking Txnip ablation to increased PI3K/Akt signaling in muscle tissues of fasted mice was eventually halted.

Txnip mediates cellular energy balance between glycolysis and mitochondrial oxidative phosphorylation

Since there is support suggesting that Txnip ablation can both contribute to insulin-dependent and/or insulin-independent regulation of glucose homeostasis [92], we can only wait to see other works in the future that may clarify this current ambiguity. However, what is clear in the realm of Txnip is that lack of expression of this protein during fasting increases utilization of glucose through the glycolytic pathway while concomitantly attenuating mitochondrial oxidative phosphorylation. In this aspect, Txnip takes center stage as a molecular switch that links and balances the reciprocal nature of these two modes of energy generation.

Although Txnip is linked to the yin and yang relationship between glucose utilization and mitochondrial oxidative phosphorylation, there remains an uncertainty concerning the cause and effect relationship that exists here. An important question to ponder, at the cellular level, is whether or not Txnip ablation first leads to increased glucose utilization as fasting develops, which in turn leads to the attenuation of mitochondrial oxidation of fuels, or vice-

versa. The metabolic phenomenon of increased glucose utilization that then leads to diminished mitochondrial oxidation of fuels, termed the Warburg Effect, was first described by Otto Warburg in 1956 and has since been a topic of great interest to many as it describes the metabolism exhibited by most cancers [208-212] . In fact, so well established is the propensity for cancer cells to shift their metabolism away from mitochondrial oxidation and towards glycolysis that this property has been exploited as a means to detect tumors using positron emission tomography (PET) scans [213-216]. Though we cannot know for certain until the functionality of mitochondria is directly addressed, based on our findings it appears as though loss of Txnip leads to the classical Warburg Effect phenotype specifically in muscle tissues. Because of the important role muscle tissues play in whole-body partitioning of fuels, the effects of Txnip ablation at the cellular level in muscle tissues then extends to affecting whole-body energy homeostasis. Given that the hallmark of many cancer cell lines is the tendency to have an increased dependency on glycolysis, the hypothesis that Txnip loss leads to the Warburg phenotype complements very well the established role of Txnip as a tumor suppressor.

Because non-fasted Txnip mice show no observable metabolic phenotype changes [91, 110], it appears that basal mitochondrial function remains intact in these mice until they are challenged with fasting. Understanding the molecular and biochemical events leading to the attenuated function of mitochondria and the concomitant shift towards increased glycolysis in muscle tissues of Txnip -/- mice should now be the

focus of future studies of this topic. One possibility is that Txnip upregulation during fasting could be a necessary step in maintaining mitochondrial quantity and/or quality. Thus, without Txnip expression during the critical moments of the onset of energy crisis brought about by fasting, mitochondria function fails to meet energy requirements which then triggers an increase in glycolysis as a measure to meet this demand. Characterizing mitochondrial oxidative capacity and quality over the fasting period could be revealing in this aspect to see if Txnip loss may negatively affect mitochondrial function in a more direct manner.

In Txnip -/- mice, it is possible that the high rates of glycolysis in muscle tissues leads to the reduction of mitochondrial oxidation through cellular signaling mechanisms. In support of this hypothesis we found that the pyruvate dehydrogenase complex (PDC), which serves as the gate-keeper for pyruvate entry into the mitochondria, is in a more inhibited state in Txnip -/- soleus muscle through increased phosphorylation of the pyruvate dehydrogenase E1α subunit (Figure 25). Sequential phosphorylation of three key serine residues in the E1 α-subunit of pyruvate dehydrogenase increasingly renders the complex unable to facilitate oxidation of pyruvate through the mitochondria [142, 176, 217]. Phosphorylation of pyruvate dehydrogenase by pyruvate dehydrogenase kinases is a reversible process that is balanced by pyruvate dehydrogenase phosphatases [99, 218]. Together the combined influence of pyruvate dehydrogenase kinases and

pyruvate dehydrogenase phosphatases determine the activity state of the pyruvate dehydrogenase complex.

High rates of glycolysis generate NADH which increase the intracellular concentration of NADH/NAD+ in the cell. A high NADH/NAD+ ratio is known to robustly activate the pyruvate dehydrogenase kinases, which subsequently inactivate the PDC through multi-site phosphorylation of its pyruvate dehydrogenase component [219-222]. Phosphorylation of the pyruvate dehydrogenase E1α subunit of the PDC is known prevent the entry of pyruvate into the Krebs cycle, thus reducing overall flow of all fuels through the mitochondria [223-225]. Decreased pyruvate entry into the mitochondria then would result in reduced anaplerosis to replenish citric acid cycle intermediates thus slowing down the entire mitochondrial oxidative pathway [40, 41]. As high rates of glycolysis continue in fasting Txnip -/- fasting mice and the PDC complex continues to be relatively inhibited, pyruvate which is built up in the muscle tissue is eventually exported into circulation as lactate. Lactate can then beused by the liver as a substrate for gluconeogenesis (Cori cycle) [226, 227] to try to meet the increased demand for glucose exhibited by these mice. Indeed our hyperinsulenimic-euglycemic clamp experiments reveal that hepatic glucose production is increased, which complements our findings of increased concentrations of plasma lactate that can provide the liver substrates for facilitating gluconeogenesis.

In lieu of our findings in this dissertation, it is clear that in order to further elucidate Txnip’s metabolic role in the fasting response, more

emphasis needs to be placed in clarifying the cause and effect relationship between glycolysis and mitochondrial oxidative phosphorylation in the context of Txnip ablation. One major avenue to consider is to inhibit glycolysis in a Txnip -/- model to see if mitochondrial oxidative capacity is able to be increased to sustain energy homeostasis. If this were the case, then it would be made clear that glycolysis is an event that is upstream of the attenuated mitochondrial oxidative phosphorylation. Emphasis then should be placed on examining factors that Txnip may affect in the glycolytic pathway. On the other hand, a thorough characterization of mitochondrial quantity and quality could be made to assess whether or not Txnip ablation has a more direct and physical influence on attenuating mitochondrial function. If this were the case, it is still plausible that glycolysis is then increased to compensate for the inability of the mitochondria to sustain energy homeostasis.

Txnip is linked to fasting-induced AMPK activation in oxidative muscle tissues

Given our findings that Txnip elicits its metabolic influence mainly through heart and skeletal muscle tissues, and the importance of these tissues in the glucose-fatty acid cycle and glucose disposal, we decided to explore the possibility that AMP-activate protein kinase (AMPK – the master regulator of energy homeostasis) may be affected by Txnip ablation in these tissues. Interestingly we found that in response to fasting, mice lacking Txnip display a markedly lower activation state of AMPK in soleus and heart tissues;

surprisingly no differences in AMPK activation were observed in gastrocnemius muscle of Txnip -/- mice versus their wild-type controls.

The hypoactivation of AMPK in heart and soleus muscle, and not in the gastrocnemius muscle, provides a clue to the importance of Txnip within tissue fiber types of muscles. The heart and soleus muscles are known to be highly oxidative, while the gastrocnemius is mainly glycolytic. The hypothesis arises then that perhaps Txnip more specifically exerts its role through oxidative muscle tissues (with the added emphasis on its importance in the glucose-fatty acid cycle). Oxidative tissues such as the heart and soleus muscle are mitochondria rich tissues that have the unique ability to switch their fuel substrate dependency towards more fat-derived substrates such as ketone bodies and fatty acids in response to energy crisis such as fasting. This allows for the sparing of glucose for other tissues such as the brain that cannot efficiently use fats to meet their energy requirements especially during times of energy crisis.

Txnip regulates AMPK activity through modulation of high energy metabolites

Interestingly we have found that soleus and heart tissues, but not gastrocnemius, of mice lacking Txnip display a low AMP:ATP ratio (high energy state) despite enduring an overnight fast, which is consistent with the observed activation state of AMPK. Although we did not find noticeable changes in AMPK activation in a highly glycolytic tissue such as the

gastrocnemius muscle, it would be naive to completely ignore the role of Txnip in more glycolytic skeletal muscle tissue types like the gastrocnemius. Recall that in our hyperinsulinemic-euglycemic clamp experiments we found that glucose uptake is increased in gastrocnemius muscle when compared to control mice. Additionally, ATP levels were statistically higher in this tissue which lead to a significant difference in AMP:ATP ratios in this tissue despite the lack of difference seen in AMP concentrations (Table 1). This demonstrates that while Txnip ablation may affect AMPK signaling in oxidative muscle tissues, there still are metabolic effects on the predominantly glycolytic fiber type muscle tissues that appear to be AMPK-independent, but still alters the levels of high energy metabolites. Given these findings, elucidating the fiber type specific role of Txnip in muscle tissues may be a fruitful avenue to investigate.

The paradoxical finding that oxidative muscle tissues of Txnip deficient mice are in a higher energy state than their wild-type controls provides a rationalization in part for why these mice do not respond normally to fasting. Moreover, this finding eliminates to a great degree the potential contribution of functional deficiencies in kinases upstream of AMPK. This is further supported by the robust activation of AMPK after AICAR treatment in Txnip -/- mice (Figure 22). Despite a prolonged fast, oxidative muscle tissues lacking Txnip are not experiencing an energy deprived state at the biochemical level. Therefore it is compelling to conclude that this state of muscle energy homeostasis may be the primary factor that leads to the attenuation of

mitochondrial oxidative phosphorylation. Aside from increased NADH/NAD+ levels as discussed earlier, low AMP/ADP:ATP levels and high acetyl-CoA:CoA ratios have been shown to greatly induce the activity of pyruvate dehydrogenase kinases [219-222], again providing another factor that could lead to blocking the PDC.

Hypoactivation of AMPK during the fasting state may contribute to the attenuation of substrate oxidation through the mitochondria

Finally, another level of control that may add to the observed fasting-induced attenuation of oxidation of fuel substrates through mitochondrial oxidative phosphorylation is the influence of diminished AMPK activity in Txnip -/- mice. AMPK protects against energy deprivation brought about by energetic challenge such as fasting or exercise by increasing glucose uptake through facilitating Glut-4 translocation to the plasma membrane [174, 175, 228-230], and by increasing fatty acid oxidation through inhibition of acetyl coA carboxylase (ACC) [175, 231, 232]. Inhibition of ACC prevents the generation of malonyl-CoA, which relieves inhibition of carnitine palmitoyltransferase I (CPT1) thereby allowing entry of long chain fatty acids into the mitochondria to undergo β-oxidation and ultimately oxidative phosphorylation [135, 233, 234]. The hypoactivated AMPK in fasting Txnip -/- mice would allow for the increased generation of malonyl-CoA to reduce fatty acid oxidation when compared to wild-type mice.

Additionally, there is a possibility that Txnip -/- mice may experience chronic cycles of decreased AMPK activity (even when provided food *ad libitum*) as the natural cycle of hunger eventually would affect these mice daily. AMPK activation has been implicated as an important element in maintaining mitochondrial quality/function in many contexts through its association with inducing PGC-1α gene expression which controls mitochondrial biogenesis [235-238]. Therefore, ablation of Txnip may attenuate the over all contribution of mitochondria in maintaining energy homeostasis in a fasting mouse by virtue of its negative influence on AMPK activation during energy crisis, thus creating a necessity for increased glucose utilization to meet energy needs.

Increased glycolysis is not associated with increased glucose transporter expression

In lieu of our findings, it became imperative to shed light on the mechanism by which Txnip ablation increases the uptake and utilization of glucose to sustain glycolysis. To this end we examined the expression of the primary glucose transporters found in heart and skeletal muscle tissue: mainly Glut-1 and Glut-4 [167]. Surprisingly we found no obvious difference in the amount of Glut-1 expressed, nor in the abundance of Glut-4 found on the plasma membranes. With these findings, and given the facilitative nature of these glucose transporters, it is reasonable to conclude that the increased glucose uptake and glycolysis observed is a consequence of Txnip loss that shifts cellular metabolism towards increased glucose metabolism which

increases glucose flux through these tissues. Coupled to this is then the attenuation of mitochondrial oxidative phosphorylation.

Txnip's role in glucose homeostasis may be independent of thioredoxin

The possibility that Txnip may exert a metabolic role independent of thioredoxin has been a lingering and untested possibility until recently. A seminal paper just released by Patwari *et. al.* 2009 demonstrates that Txnip can function as a metabolic regulator of glucose homeostasis independent of its ability to bind to thioredoxin [239]. This article highlights Txnip as a member of the alpha arrestin family of proteins whose properties may be what provide Txnip its characteristic property of regulating glucose homeostasis independent of its ability to bind to an inhibit thioredoxin. Arrestins are generally known to mediate receptor signaling events as scaffolds that aid in the recruitment of other elements of cell signaling [240]. Using adipocytes and primary skin fibroblasts, they demonstrate that a mutated Txnip (C247S) rendered unable to interact with thioredoxin still inhibits glucose uptake and lactate output in these cells. Moreover, one arrestin family member Arrdc4 exhibits this same property. If these findings hold true, investigating the thioredoxin-independent role of Txnip as an arrestin controlling glucose homeostasis at the cellular level may be the path to fully unlocking Txnip's role in glucose homeostasis and the metabolic fasting response at the whole body level.

References

1. Chen, K.S. and H.F. DeLuca, *Isolation and characterization of a novel cDNA from HL-60 cells treated with 1,25-dihydroxyvitamin D-3.* Biochim Biophys Acta, 1994. **1219**(1): p. 26-32.

2. Nishiyama, A., et al., *Identification of thioredoxin-binding protein-2/vitamin D(3) up-regulated protein 1 as a negative regulator of thioredoxin function and expression.* J Biol Chem, 1999. **274**(31): p. 21645-50.

3. Patwari, P., et al., *The interaction of thioredoxin with Txnip. Evidence for formation of a mixed disulfide by disulfide exchange.* J Biol Chem, 2006. **281**(31): p. 21884-91.

4. Oka, S., et al., *Impaired fatty acid utilization in thioredoxin binding protein-2 (TBP-2)-deficient mice: a unique animal model of Reye syndrome.* Faseb J, 2006. **20**(1): p. 121-3.

5. Chae, H.Z., S.J. Chung, and S.G. Rhee, *Thioredoxin-dependent peroxide reductase from yeast.* J Biol Chem, 1994. **269**(44): p. 27670-8.

6. Kang, S.W., et al., *Mammalian peroxiredoxin isoforms can reduce hydrogen peroxide generated in response to growth factors and tumor necrosis factor-alpha.* J Biol Chem, 1998. **273**(11): p. 6297-302.

7. Ahsan, K., et. al., *Redox regulation of cell survival by thioredoxin super-family: An implication of redox gene therapy in the heart.* Antioxidants and Redox Signaling, 2009.

8. Holmgren, A., *Thioredoxin.* Annu Rev Biochem, 1985. **54**: p. 237-71.

9. Matsui, M., et al., *Early embryonic lethality caused by targeted disruption of the mouse thioredoxin gene.* Dev Biol, 1996. **178**(1): p. 179-85.

10. Nonn, L., et al., *The absence of mitochondrial thioredoxin 2 causes massive apoptosis, exencephaly, and early embryonic lethality in homozygous mice.* Mol Cell Biol, 2003. **23**(3): p. 916-22.

11. Yamawaki, H., J. Haendeler, and B.C. Berk, *Thioredoxin: a key regulator of cardiovascular homeostasis.* Circ Res, 2003. **93**(11): p. 1029-33.

12. Schulze, P.C., et al., *Vitamin D3-upregulated protein-1 (VDUP-1) regulates redox-dependent vascular smooth muscle cell proliferation through interaction with thioredoxin.* Circ Res, 2002. **91**(8): p. 689-95.

13. Wang, Y., G.W. De Keulenaer, and R.T. Lee, *Vitamin D(3)-up-regulated protein-1 is a stress-responsive gene that regulates cardiomyocyte viability through interaction with thioredoxin.* J Biol Chem, 2002. **277**(29): p. 26496-500.

14. Yamanaka, H., et al., *A possible interaction of thioredoxin with VDUP1 in HeLa cells detected in a yeast two-hybrid system.* Biochem Biophys Res Commun, 2000. **271**(3): p. 796-800.

15. Laurent, T.C., E.C. Moore, and P. Reichard, *Enzymatic Synthesis of Deoxyribonucleotides. Iv. Isolation and Characterization of Thioredoxin, the Hydrogen Donor from Escherichia Coli B.* J Biol Chem, 1964. **239**: p. 3436-44.

16. Nakamura, H., K. Nakamura, and J. Yodoi, *Redox regulation of cellular activation.* Annu Rev Immunol, 1997. **15**: p. 351-69.

17. Kuster, G.M., et al., *Alpha-adrenergic receptor-stimulated hypertrophy in adult rat ventricular myocytes is mediated via thioredoxin-1-sensitive oxidative modification of thiols on Ras.* Circulation, 2005. **111**(9): p. 1192-8.

18. Kuster, G.M., et al., *Role of reversible, thioredoxin-sensitive oxidative protein modifications in cardiac myocytes.* Antioxid Redox Signal, 2006. **8**(11-12): p. 2153-9.

19. Saitoh, M., et al., *Mammalian thioredoxin is a direct inhibitor of apoptosis signal-regulating kinase (ASK) 1.* Embo J, 1998. **17**(9): p. 2596-606.

20. Fujino, G., et al., *Thioredoxin and TRAF family proteins regulate reactive oxygen species-dependent activation of ASK1 through reciprocal modulation of the N-terminal homophilic interaction of ASK1.* Mol Cell Biol, 2007. **27**(23): p. 8152-63.

21. Sun, H.Y., et al., *Postconditioning attenuates cardiomyocyte apoptosis via inhibition of JNK and p38 mitogen-activated protein kinase signaling pathways.* Apoptosis, 2006. **11**(9): p. 1583-93.

22. Zhang, R., et al., *Thioredoxin-2 inhibits mitochondria-located ASK1-mediated apoptosis in a JNK-independent manner.* Circ Res, 2004. **94**(11): p. 1483-91.

23. Liu, Y. and W. Min, *Thioredoxin promotes ASK1 ubiquitination and degradation to inhibit ASK1-mediated apoptosis in a redox activity-independent manner.* Circ Res, 2002. **90**(12): p. 1259-66.

24. Damdimopoulos, A.E., et al., *Human mitochondrial thioredoxin. Involvement in mitochondrial membrane potential and cell death.* J Biol Chem, 2002. **277**(36): p. 33249-57.

25. Tanaka, T., et al., *Thioredoxin-2 (TRX-2) is an essential gene regulating mitochondria-dependent apoptosis.* Embo J, 2002. **21**(7): p. 1695-703.

26. Masutani, H., et al., *Transactivation of an inducible anti-oxidative stress protein, human thioredoxin by HTLV-I Tax.* Immunol Lett, 1996. **54**(2-3): p. 67-71.

27. Rubartelli, A., et al., *Secretion of thioredoxin by normal and neoplastic cells through a leaderless secretory pathway.* J Biol Chem, 1992. **267**(34): p. 24161-4.

28. Bloomfield, K.L., et al., *Thioredoxin-mediated redox control of the transcription factor Sp1 and regulation of the thioredoxin gene promoter.* Gene, 2003. **319**: p. 107-16.

29. Ema, M., et al., *Molecular mechanisms of transcription activation by HLF and HIF1alpha in response to hypoxia: their stabilization and redox signal-induced interaction with CBP/p300.* Embo J, 1999. **18**(7): p. 1905-14.

30. Hirota, K., et al., *AP-1 transcriptional activity is regulated by a direct association between thioredoxin and Ref-1.* Proc Natl Acad Sci U S A, 1997. **94**(8): p. 3633-8.

31. Hirota, K., et al., *Nucleoredoxin, glutaredoxin, and thioredoxin differentially regulate NF-kappaB, AP-1, and CREB activation in HEK293 cells.* Biochem Biophys Res Commun, 2000. **274**(1): p. 177-82.

32. Hirota, K., et al., *Distinct roles of thioredoxin in the cytoplasm and in the nucleus. A two-step mechanism of redox regulation of transcription factor NF-kappaB.* J Biol Chem, 1999. **274**(39): p. 27891-7.

33. Matthews, J.R., et al., *Thioredoxin regulates the DNA binding activity of NF-kappa B by reduction of a disulphide bond involving cysteine 62.* Nucleic Acids Res, 1992. **20**(15): p. 3821-30.

34. Ueno, M., et al., *Thioredoxin-dependent redox regulation of p53-mediated p21 activation.* J Biol Chem, 1999. **274**(50): p. 35809-15.

35. Chen, F., V. Castranova, and X. Shi, *New insights into the role of nuclear factor-kappaB in cell growth regulation.* Am J Pathol, 2001. **159**(2): p. 387-97.

36. Chen, F., et al., *New insights into the role of nuclear factor-kappaB, a ubiquitous transcription factor in the initiation of diseases.* Clin Chem, 1999. **45**(1): p. 7-17.

37. Gilmore, T.D., *The Re1/NF-kappa B/I kappa B signal transduction pathway and cancer.* Cancer Treat Res, 2003. **115**: p. 241-65.

38. Karin, M., et al., *NF-kappaB in cancer: from innocent bystander to major culprit.* Nat Rev Cancer, 2002. **2**(4): p. 301-10.

39. Gordan, J.D., C.B. Thompson, and M.C. Simon, *HIF and c-Myc: sibling rivals for control of cancer cell metabolism and proliferation.* Cancer Cell, 2007. **12**(2): p. 108-13.

40. Kim, J.W., et al., *HIF-1-mediated expression of pyruvate dehydrogenase kinase: a metabolic switch required for cellular adaptation to hypoxia.* Cell Metab, 2006. **3**(3): p. 177-85.

41. Papandreou, I., et al., *HIF-1 mediates adaptation to hypoxia by actively downregulating mitochondrial oxygen consumption.* Cell Metab, 2006. **3**(3): p. 187-97.

42. Huang, L.E., et al., *Activation of hypoxia-inducible transcription factor depends primarily upon redox-sensitive stabilization of its alpha subunit.* J Biol Chem, 1996. **271**(50): p. 32253-9.

43. Lando, D., et al., *A redox mechanism controls differential DNA binding activities of hypoxia-inducible factor (HIF) 1alpha and the HIF-like factor.* J Biol Chem, 2000. **275**(7): p. 4618-27.

44. Welsh, S.J., et al., *The redox protein thioredoxin-1 (Trx-1) increases hypoxia-inducible factor 1alpha protein expression: Trx-1 overexpression results in increased vascular endothelial growth factor production and enhanced tumor angiogenesis.* Cancer Res, 2002. **62**(17): p. 5089-95.

45. Welsh, S.J., et al., *The thioredoxin redox inhibitors 1-methylpropyl 2-imidazolyl disulfide and pleurotin inhibit hypoxia-induced factor 1alpha and vascular endothelial growth factor formation.* Mol Cancer Ther, 2003. **2**(3): p. 235-43.

46. Chuang, J.Y., et al., *Overexpression of Sp1 leads to p53-dependent apoptosis in cancer cells.* Int J Cancer, 2009.

47. Lu, S. and M.C. Archer, *Sp1 coordinately regulates de novo lipogenesis and proliferation in cancer cells.* Int J Cancer, 2009.

48. Zuckerman, V., et al., *Tumour suppression by p53: the importance of apoptosis and cellular senescence.* J Pathol, 2009.

49. Billiet, L., et al., *Enhanced VDUP-1 gene expression by PPARgamma agonist induces apoptosis in human macrophage.* J Cell Physiol, 2008. **214**(1): p. 183-91.

50. Chen, J., et al., *Thioredoxin-interacting protein: a critical link between glucose toxicity and beta-cell apoptosis.* Diabetes, 2008. **57**(4): p. 938-44.

51. Jeon, J.H., et al., *Tumor suppressor VDUP1 increases p27(kip1) stability by inhibiting JAB1.* Cancer Res, 2005. **65**(11): p. 4485-9.

52. Kim, S.Y., et al., *Diverse functions of VDUP1 in cell proliferation, differentiation, and diseases.* Cell Mol Immunol, 2007. **4**(5): p. 345-51.

53. Yoshioka, J., et al., *Thioredoxin-interacting protein controls cardiac hypertrophy through regulation of thioredoxin activity.* Circulation, 2004. **109**(21): p. 2581-6.

54. Lee, K.N., et al., *VDUP1 is required for the development of natural killer cells.* Immunity, 2005. **22**(2): p. 195-208.

55. Miyazaki, K., et al., *Elevated serum level of thioredoxin in patients with hepatocellular carcinoma.* Biotherapy, 1998. **11**(4): p. 277-88.

56. Nakamura, H., et al., *Expression and growth-promoting effect of adult T-cell leukemia-derived factor. A human thioredoxin homologue in hepatocellular carcinoma.* Cancer, 1992. **69**(8): p. 2091-7.

57. Tagaya, Y., et al., *ATL-derived factor (ADF), an IL-2 receptor/Tac inducer homologous to thioredoxin; possible involvement of dithiol-reduction in the IL-2 receptor induction.* Embo J, 1989. **8**(3): p. 757-64.

58. Han, H., et al., *Identification of differentially expressed genes in pancreatic cancer cells using cDNA microarray.* Cancer Res, 2002. **62**(10): p. 2890-6.

59. Nakamura, H., et al., *Expression of thioredoxin and glutaredoxin, redox-regulating proteins, in pancreatic cancer.* Cancer Detect Prev, 2000. **24**(1): p. 53-60.

60. Gasdaska, P.Y., et al., *The predicted amino acid sequence of human thioredoxin is identical to that of the autocrine growth factor human adult T-cell derived factor (ADF): thioredoxin mRNA is elevated in some human tumors.* Biochim Biophys Acta, 1994. **1218**(3): p. 292-6.

61. Kakolyris, S., et al., *Thioredoxin expression is associated with lymph node status and prognosis in early operable non-small cell lung cancer.* Clin Cancer Res, 2001. **7**(10): p. 3087-91.

62. Raffel, J., et al., *Increased expression of thioredoxin-1 in human colorectal cancer is associated with decreased patient survival.* J Lab Clin Med, 2003. **142**(1): p. 46-51.

63. Sheth, S.S., et al., *Hepatocellular carcinoma in Txnip-deficient mice.* Oncogene, 2006. **25**(25): p. 3528-36.

64. Ikarashi, M., et al., *Vitamin D3 up-regulated protein 1 (VDUP1) expression in gastrointestinal cancer and its relation to stage of disease.* Anticancer Res, 2002. **22**(6C): p. 4045-8.

65. de Vos, S., et al., *Gene expression profile of serial samples of transformed B-cell lymphomas.* Lab Invest, 2003. **83**(2): p. 271-85.

66. Butler, L.M., et al., *The histone deacetylase inhibitor SAHA arrests cancer cell growth, up-regulates thioredoxin-binding protein-2, and down-regulates thioredoxin.* Proc Natl Acad Sci U S A, 2002. **99**(18): p. 11700-5.

67. Yang, X., L.H. Young, and J.M. Voigt, *Expression of a vitamin D-regulated gene (VDUP-1) in untreated- and MNU-treated rat mammary tissue.* Breast Cancer Res Treat, 1998. **48**(1): p. 33-44.

68. Goldberg, S.F., et al., *Melanoma metastasis suppression by chromosome 6: evidence for a pathway regulated by CRSP3 and TXNIP.* Cancer Res, 2003. **63**(2): p. 432-40.

69. Park, S.H. and M. Silva, *Effect of intermittent pneumatic soft-tissue compression on fracture-healing in an animal model.* J Bone Joint Surg Am, 2003. **85-A**(8): p. 1446-53.

70. Tao, L., et al., *Cardioprotective effects of thioredoxin in myocardial ischemia and reperfusion: role of S-nitrosation [corrected].* Proc Natl Acad Sci U S A, 2004. **101**(31): p. 11471-6.

71. Das, S., et al., *The effect of Euryale ferox (Makhana), an herb of aquatic origin, on myocardial ischemic reperfusion injury.* Mol Cell Biochem, 2006. **289**(1-2): p. 55-63.

72. Xiang, G., et al., *Catalytic degradation of vitamin D up-regulated protein 1 mRNA enhances cardiomyocyte survival and prevents left ventricular remodeling after myocardial ischemia.* J Biol Chem, 2005. **280**(47): p. 39394-402.

73. Abdiu, A., et al., *Thioredoxin blood level increases after severe burn injury.* Antioxid Redox Signal, 2000. **2**(4): p. 707-16.

74. Maurice, M.M., et al., *Expression of the thioredoxin-thioredoxin reductase system in the inflamed joints of patients with rheumatoid arthritis.* Arthritis Rheum, 1999. **42**(11): p. 2430-9.

75. Sumida, Y., et al., *Serum thioredoxin levels as an indicator of oxidative stress in patients with hepatitis C virus infection.* J Hepatol, 2000. **33**(4): p. 616-22.

76. Gasdaska, J.R., M. Berggren, and G. Powis, *Cell growth stimulation by the redox protein thioredoxin occurs by a novel helper mechanism.* Cell Growth Differ, 1995. **6**(12): p. 1643-50.

77. Bertini, R., et al., *Thioredoxin, a redox enzyme released in infection and inflammation, is a unique chemoattractant for neutrophils, monocytes, and T cells.* J Exp Med, 1999. **189**(11): p. 1783-9.

78. Miyamoto, S., et al., *Increased plasma levels of thioredoxin in patients with coronary spastic angina.* Antioxid Redox Signal, 2004. **6**(1): p. 75-80.

79. Miyamoto, S., et al., *Plasma thioredoxin levels and platelet aggregability in patients with acute myocardial infarction.* Am Heart J, 2003. **146**(3): p. 465-71.

80. Soejima, H., et al., *Increased plasma thioredoxin in patients with acute myocardial infarction.* Clin Cardiol, 2003. **26**(12): p. 583-7.

81. Yamamoto, M., et al., *Inhibition of endogenous thioredoxin in the heart increases oxidative stress and cardiac hypertrophy.* J Clin Invest, 2003. **112**(9): p. 1395-406.

82. Ebrahimian, T., et al., *Cardiac hypertrophy is associated with altered thioredoxin and ASK-1 signaling in a mouse model of menopause.* Am J Physiol Heart Circ Physiol, 2008. **295**(4): p. H1481-8.

83. Nishida, K. and K. Otsu, *The role of apoptosis signal-regulating kinase 1 in cardiomyocyte apoptosis.* Antioxid Redox Signal, 2006. **8**(9-10): p. 1729-36.

84. Satoh, M., et al., *Inhibition of apoptosis-regulated signaling kinase-1 and prevention of congestive heart failure by estrogen.* Circulation, 2007. **115**(25): p. 3197-204.

85. Ago, T., et al., *Thioredoxin1 upregulates mitochondrial proteins related to oxidative phosphorylation and TCA cycle in the heart.* Antioxid Redox Signal, 2006. **8**(9-10): p. 1635-50.

86. Li, X., et al., *Redox regulation of Ito remodeling in diabetic rat heart.* Am J Physiol Heart Circ Physiol, 2005. **288**(3): p. H1417-24.

87. Minn, A.H., C. Hafele, and A. Shalev, *Thioredoxin-interacting protein is stimulated by glucose through a carbohydrate response element and induces beta-cell apoptosis.* Endocrinology, 2005. **146**(5): p. 2397-405.

88. Pang, S.T., et al., *Thioredoxin-interacting protein: an oxidative stress-related gene is upregulated by glucose in human prostate carcinoma cells.* J Mol Endocrinol, 2009. **42**(3): p. 205-14.

89. Shalev, A., et al., *Oligonucleotide microarray analysis of intact human pancreatic islets: identification of glucose-responsive genes and a highly regulated TGFbeta signaling pathway.* Endocrinology, 2002. **143**(9): p. 3695-8.

90. Turturro, F., E. Friday, and T. Welbourne, *Hyperglycemia regulates thioredoxin-ROS activity through induction of thioredoxin-interacting protein (TXNIP) in metastatic breast cancer-derived cells MDA-MB-231.* BMC Cancer, 2007. **7**: p. 96.

91. Hui, S.T., et al., *Txnip balances metabolic and growth signaling via PTEN disulfide reduction.* Proc Natl Acad Sci U S A, 2008. **105**(10): p. 3921-6.

92. Parikh, H., et al., *TXNIP regulates peripheral glucose metabolism in humans.* PLoS Med, 2007. **4**(5): p. e158.

93. Shaked, M., et al., *Insulin counteracts glucotoxic effects by suppressing thioredoxin-interacting protein production in INS-1E beta cells and in Psammomys obesus pancreatic islets.* Diabetologia, 2009. **52**(4): p. 636-44.

94. Suh, Y.A., et al., *Cell transformation by the superoxide-generating oxidase Mox1.* Nature, 1999. **401**(6748): p. 79-82.

95. Kajimoto, Y. and H. Kaneto, *Role of oxidative stress in pancreatic beta-cell dysfunction.* Ann N Y Acad Sci, 2004. **1011**: p. 168-76.

96. Kaneto, H., et al., *Beneficial effects of antioxidants in diabetes: possible protection of pancreatic beta-cells against glucose toxicity.* Diabetes, 1999. **48**(12): p. 2398-406.

97. Khoo, S., et al., *MAP kinases and their roles in pancreatic beta-cells.* Cell Biochem Biophys, 2004. **40**(3 Suppl): p. 191-200.

98. Lawrence, M.C., et al., *ERK1/2-dependent activation of transcription factors required for acute and chronic effects of glucose on the insulin gene promoter.* J Biol Chem, 2005. **280**(29): p. 26751-9.

99. Rhodes, C.J., *Type 2 diabetes-a matter of beta-cell life and death?* Science, 2005. **307**(5708): p. 380-4.

100. Wang, X., et al., *Gene and protein kinase expression profiling of reactive oxygen species-associated lipotoxicity in the pancreatic beta-cell line MIN6.* Diabetes, 2004. **53**(1): p. 129-40.

101. World, C.J., H. Yamawaki, and B.C. Berk, *Thioredoxin in the cardiovascular system.* J Mol Med, 2006. **84**(12): p. 997-1003.

102. Chen, J., et al., *Exenatide inhibits beta-cell apoptosis by decreasing thioredoxin-interacting protein.* Biochem Biophys Res Commun, 2006. **346**(3): p. 1067-74.

103. Chen, J., et al., *Thioredoxin-interacting protein deficiency induces Akt/Bcl-xL signaling and pancreatic beta-cell mass and protects against diabetes.* Faseb J, 2008. **22**(10): p. 3581-94.

104. Dandona, P., et al., *A novel view of metabolic syndrome.* Metab Syndr Relat Disord, 2004. **2**(1): p. 2-8.

105. Festa, A., et al., *Chronic subclinical inflammation as part of the insulin resistance syndrome: the Insulin Resistance Atherosclerosis Study (IRAS).* Circulation, 2000. **102**(1): p. 42-7.

106. Klein, B.E., R. Klein, and K.E. Lee, *Components of the metabolic syndrome and risk of cardiovascular disease and diabetes in Beaver Dam.* Diabetes Care, 2002. **25**(10): p. 1790-4.

107. Brownlee, M., *Biochemistry and molecular cell biology of diabetic complications.* Nature, 2001. **414**(6865): p. 813-20.

108. Park, L., et al., *Suppression of accelerated diabetic atherosclerosis by the soluble receptor for advanced glycation endproducts.* Nat Med, 1998. **4**(9): p. 1025-31.

109. Rosen, P., et al., *The role of oxidative stress in the onset and progression of diabetes and its complications: a summary of a Congress Series sponsored by UNESCO-MCBN, the American Diabetes Association and the German Diabetes Society.* Diabetes Metab Res Rev, 2001. **17**(3): p. 189-212.

110. Hui, T.Y., et al., *Mice lacking thioredoxin-interacting protein provide evidence linking cellular redox state to appropriate response to nutritional signals.* J Biol Chem, 2004. **279**(23): p. 24387-93.

111. Sheth, S.S., et al., *Thioredoxin-interacting protein deficiency disrupts the fasting-feeding metabolic transition.* J Lipid Res, 2005. **46**(1): p. 123-34.

112. Bodnar, J.S., et al., *Positional cloning of the combined hyperlipidemia gene Hyplip1.* Nat Genet, 2002. **30**(1): p. 110-6.

113. Gu, H., et al., *Deletion of a DNA polymerase beta gene segment in T cells using cell type-specific gene targeting.* Science, 1994. **265**(5168): p. 103-6.

114. Lewandoski, M., K.M. Wassarman, and G.R. Martin, *Zp3-cre, a transgenic mouse line for the activation or inactivation of loxP-flanked target genes specifically in the female germ line.* Curr Biol, 1997. **7**(2): p. 148-51.

115. Huang, S. and M.P. Czech, *The GLUT4 glucose transporter.* Cell Metab, 2007. **5**(4): p. 237-52.

116. Sakamoto, K. and G.D. Holman, *Emerging role for AS160/TBC1D4 and TBC1D1 in the regulation of GLUT4 traffic.* Am J Physiol Endocrinol Metab, 2008. **295**(1): p. E29-37.

117. Taniguchi, C.M., B. Emanuelli, and C.R. Kahn, *Critical nodes in signalling pathways: insights into insulin action.* Nat Rev Mol Cell Biol, 2006. **7**(2): p. 85-96.

118. Thong, F.S., C.B. Dugani, and A. Klip, *Turning signals on and off: GLUT4 traffic in the insulin-signaling highway.* Physiology (Bethesda), 2005. **20**: p. 271-84.

119. Ali, S. and D.J. Drucker, *Benefits and limitations of reducing glucagon action for the treatment of type 2 diabetes.* Am J Physiol Endocrinol Metab, 2009. **296**(3): p. E415-21.

120. Jiang, G. and B.B. Zhang, *Glucagon and regulation of glucose metabolism.* Am J Physiol Endocrinol Metab, 2003. **284**(4): p. E671-8.

121. Sloop, K.W., M.D. Michael, and J.S. Moyers, *Glucagon as a target for the treatment of Type 2 diabetes.* Expert Opin Ther Targets, 2005. **9**(3): p. 593-600.

122. Kumar, A., et al., *Muscle-specific deletion of rictor impairs insulin-stimulated glucose transport and enhances Basal glycogen synthase activity.* Mol Cell Biol, 2008. **28**(1): p. 61-70.

123. Mora, A., et al., *PDK1, the master regulator of AGC kinase signal transduction.* Semin Cell Dev Biol, 2004. **15**(2): p. 161-70.

124. Sarbassov, D.D., et al., *Phosphorylation and regulation of Akt/PKB by the rictor-mTOR complex.* Science, 2005. **307**(5712): p. 1098-101.

125. Bates, M.W., H.A. Krebs, and D.H. Williamson, *Turnover rates of ketone bodies in normal, starved and alloxan-diabetic rats.* Biochem J, 1968. **110**(4): p. 655-61.

126. Fukao, T., G.D. Lopaschuk, and G.A. Mitchell, *Pathways and control of ketone body metabolism: on the fringe of lipid biochemistry.* Prostaglandins Leukot Essent Fatty Acids, 2004. **70**(3): p. 243-51.

127. Hansen, W. and P. Bottermann, *Glycolysis and its interaction with a gluconeogenic precursor in perfused rat liver.* Diabetologia, 1975. **11**(5): p. 445-9.

128. Cantley, L.C. and B.G. Neel, *New insights into tumor suppression: PTEN suppresses tumor formation by restraining the phosphoinositide 3-kinase/AKT pathway.* Proc Natl Acad Sci U S A, 1999. **96**(8): p. 4240-5.

129. Maehama, T., G.S. Taylor, and J.E. Dixon, *PTEN and myotubularin: novel phosphoinositide phosphatases.* Annu Rev Biochem, 2001. **70**: p. 247-79.

130. Lee, S.R., et al., *Reversible inactivation of the tumor suppressor PTEN by H2O2.* J Biol Chem, 2002. **277**(23): p. 20336-42.

131. Leslie, N.R., et al., *Redox regulation of PI 3-kinase signalling via inactivation of PTEN.* Embo J, 2003. **22**(20): p. 5501-10.

132. Horton, J.D., J.L. Goldstein, and M.S. Brown, *SREBPs: activators of the complete program of cholesterol and fatty acid synthesis in the liver.* J Clin Invest, 2002. **109**(9): p. 1125-31.

133. Seo, J.H., et al., *The major target of the endogenously generated reactive oxygen species in response to insulin stimulation is phosphatase and tensin homolog and not phosphoinositide-3 kinase (PI-3 kinase) in the PI-3 kinase/Akt pathway.* Mol Biol Cell, 2005. **16**(1): p. 348-57.

134. Pelicano, H., et al., *Mitochondrial respiration defects in cancer cells cause activation of Akt survival pathway through a redox-mediated mechanism.* J Cell Biol, 2006. **175**(6): p. 913-23.

135. McGarry, J.D. and D.W. Foster, *Regulation of hepatic fatty acid oxidation and ketone body production.* Annu Rev Biochem, 1980. **49**: p. 395-420.

136. Castellani, L.W., et al., *Mapping a gene for combined hyperlipidaemia in a mutant mouse strain.* Nat Genet, 1998. **18**(4): p. 374-7.

137. Ikegami, T., et al., *Model mice for tissue-specific deletion of the manganese superoxide dismutase (MnSOD) gene.* Biochem Biophys Res Commun, 2002. **296**(3): p. 729-36.

138. Davidson, M.B., *Role of glucose transport and GLUT4 transporter protein in type 2 diabetes mellitus.* J Clin Endocrinol Metab, 1993. **77**(1): p. 25-6.

139. Kraegen, E.W., et al., *Dose-response curves for in vivo insulin sensitivity in individual tissues in rats.* Am J Physiol, 1985. **248**(3 Pt 1): p. E353-62.

140. Yki-Jarvinen, H., et al., *Kinetics of glucose disposal in whole body and across the forearm in man.* J Clin Invest, 1987. **79**(6): p. 1713-9.

141. Zierath, J.R. and Y. Kawano, *The effect of hyperglycaemia on glucose disposal and insulin signal transduction in skeletal muscle.* Best Pract Res Clin Endocrinol Metab, 2003. **17**(3): p. 385-98.

142. Hue, L. and H. Taegtmeyer, *The Randle Cycle Revisited: A New Head for an Old Hat.* Am J Physiol Endocrinol Metab, 2009.

143. Randle, P.J., *Regulatory interactions between lipids and carbohydrates: the glucose fatty acid cycle after 35 years.* Diabetes Metab Rev, 1998. **14**(4): p. 263-83.

144. Randle, P.J., et al., *The glucose fatty-acid cycle. Its role in insulin sensitivity and the metabolic disturbances of diabetes mellitus.* Lancet, 1963. **1**(7285): p. 785-9.

145. Randle, P.J., E.A. Newsholme, and P.B. Garland, *Regulation of glucose uptake by muscle. 8. Effects of fatty acids, ketone bodies and pyruvate, and of alloxan-diabetes and starvation, on the uptake and metabolic fate of glucose in rat heart and diaphragm muscles.* Biochem J, 1964. **93**(3): p. 652-65.

146. Zisman, A., et al., *Targeted disruption of the glucose transporter 4 selectively in muscle causes insulin resistance and glucose intolerance.* Nat Med, 2000. **6**(8): p. 924-8.

147. Kim, H.J., et al., *Differential effects of interleukin-6 and -10 on skeletal muscle and liver insulin action in vivo.* Diabetes, 2004. **53**(4): p. 1060-7.

148. Schirra, F., et al., *Androgen regulation of lipogenic pathways in the mouse meibomian gland.* Exp Eye Res, 2006. **83**(2): p. 291-6.

149. Millward, C.A., et al., *Mice with a deletion in the gene for CCAAT/enhancer-binding protein beta are protected against diet-induced obesity.* Diabetes, 2007. **56**(1): p. 161-7.

150. Hansen, P.A., E.A. Gulve, and J.O. Holloszy, *Suitability of 2-deoxyglucose for in vitro measurement of glucose transport activity in skeletal muscle.* J Appl Physiol, 1994. **76**(2): p. 979-85.

151. Kahn, B.B., et al., *AMP-activated protein kinase: ancient energy gauge provides clues to modern understanding of metabolism.* Cell Metab, 2005. **1**(1): p. 15-25.

152. Scott, J.W., J.S. Oakhill, and B.J. van Denderen, *AMPK/SNF1 structure: a menage a trois of energy-sensing.* Front Biosci, 2009. **14**: p. 596-610.

153. Carling, D., M.J. Sanders, and A. Woods, *The regulation of AMP-activated protein kinase by upstream kinases.* Int J Obes (Lond), 2008. **32 Suppl 4**: p. S55-9.

154. Shaw, R.J., et al., *The tumor suppressor LKB1 kinase directly activates AMP-activated kinase and regulates apoptosis in response to energy stress.* Proc Natl Acad Sci U S A, 2004. **101**(10): p. 3329-35.

155. Witczak, C.A., C.G. Sharoff, and L.J. Goodyear, *AMP-activated protein kinase in skeletal muscle: from structure and localization to its role as a master regulator of cellular metabolism.* Cell Mol Life Sci, 2008. **65**(23): p. 3737-55.

156. Sakamoto, K., et al., *Deficiency of LKB1 in skeletal muscle prevents AMPK activation and glucose uptake during contraction.* Embo J, 2005. **24**(10): p. 1810-20.

157. Hardie, D.G., *AMP-activated/SNF1 protein kinases: conserved guardians of cellular energy.* Nat Rev Mol Cell Biol, 2007. **8**(10): p. 774-85.

158. Hue, L. and M.H. Rider, *The AMP-activated protein kinase: more than an energy sensor.* Essays Biochem, 2007. **43**: p. 121-37.

159. McGarry, J.D., G.P. Mannaerts, and D.W. Foster, *A possible role for malonyl-CoA in the regulation of hepatic fatty acid oxidation and ketogenesis.* J Clin Invest, 1977. **60**(1): p. 265-70.

160. Taegtmeyer, H., R. Hems, and H.A. Krebs, *Utilization of energy-providing substrates in the isolated working rat heart.* Biochem J, 1980. **186**(3): p. 701-11.

161. Baas, A.F., et al., *Activation of the tumour suppressor kinase LKB1 by the STE20-like pseudokinase STRAD.* Embo J, 2003. **22**(12): p. 3062-72.

162. Boudeau, J., et al., *MO25alpha/beta interact with STRADalpha/beta enhancing their ability to bind, activate and localize LKB1 in the cytoplasm.* Embo J, 2003. **22**(19): p. 5102-14.

163. Brajenovic, M., et al., *Comprehensive proteomic analysis of human Par protein complexes reveals an interconnected protein network.* J Biol Chem, 2004. **279**(13): p. 12804-11.

164. Hardie, D.G., *New roles for the LKB1-->AMPK pathway.* Curr Opin Cell Biol, 2005. **17**(2): p. 167-73.

165. Scott, J.W., et al., *CBS domains form energy-sensing modules whose binding of adenosine ligands is disrupted by disease mutations.* J Clin Invest, 2004. **113**(2): p. 274-84.

166. Hardie, D.G., D. Carling, and M. Carlson, *The AMP-activated/SNF1 protein kinase subfamily: metabolic sensors of the eukaryotic cell?* Annu Rev Biochem, 1998. **67**: p. 821-55.

167. Marette, A., et al., *Abundance, localization, and insulin-induced translocation of glucose transporters in red and white muscle.* Am J Physiol, 1992. **263**(2 Pt 1): p. C443-52.

168. Bell, G.I., et al., *Molecular biology of mammalian glucose transporters.* Diabetes Care, 1990. **13**(3): p. 198-208.

169. Ren, J.M., et al., *Evidence from transgenic mice that glucose transport is rate-limiting for glycogen deposition and glycolysis in skeletal muscle.* J Biol Chem, 1993. **268**(22): p. 16113-5.

170. Castello, A., et al., *Perinatal hypothyroidism impairs the normal transition of GLUT4 and GLUT1 glucose transporters from fetal to neonatal levels in heart and brown adipose tissue. Evidence for tissue-specific regulation of GLUT4 expression by thyroid hormone.* J Biol Chem, 1994. **269**(8): p. 5905-12.

171. Megeney, L.A., et al., *Regulation of muscle glucose transport and GLUT-4 by nerve-derived factors and activity-related processes.* Am J Physiol, 1995. **269**(5 Pt 2): p. R1148-53.

172. Cushman, S.W. and L.J. Wardzala, *Potential mechanism of insulin action on glucose transport in the isolated rat adipose cell. Apparent translocation of intracellular transport systems to the plasma membrane.* J Biol Chem, 1980. **255**(10): p. 4758-62.

173. Hayashi, T., et al., *Evidence for 5' AMP-activated protein kinase mediation of the effect of muscle contraction on glucose transport.* Diabetes, 1998. **47**(8): p. 1369-73.

174. Kurth-Kraczek, E.J., et al., *5' AMP-activated protein kinase activation causes GLUT4 translocation in skeletal muscle.* Diabetes, 1999. **48**(8): p. 1667-71.

175. Merrill, G.F., et al., *AICA riboside increases AMP-activated protein kinase, fatty acid oxidation, and glucose uptake in rat muscle.* Am J Physiol, 1997. **273**(6 Pt 1): p. E1107-12.

176. Sugden, M.C. and M.J. Holness, *Mechanisms underlying regulation of the expression and activities of the mammalian pyruvate dehydrogenase kinases.* Arch Physiol Biochem, 2006. **112**(3): p. 139-49.

177. McBride, A., et al., *The glycogen-binding domain on the AMPK beta subunit allows the kinase to act as a glycogen sensor.* Cell Metab, 2009. **9**(1): p. 23-34.

178. McBride, A. and D.G. Hardie, *AMP-activated protein kinase--a sensor of glycogen as well as AMP and ATP?* Acta Physiol (Oxf), 2009. **196**(1): p. 99-113.

179. Luptak, I., et al., *Aberrant activation of AMP-activated protein kinase remodels metabolic network in favor of cardiac glycogen storage.* J Clin Invest, 2007. **117**(5): p. 1432-9.

180. Milan, D., et al., *A mutation in PRKAG3 associated with excess glycogen content in pig skeletal muscle.* Science, 2000. **288**(5469): p. 1248-51.

181. Cross, D.A., et al., *Inhibition of glycogen synthase kinase-3 by insulin mediated by protein kinase B.* Nature, 1995. **378**(6559): p. 785-9.

182. Srivastava, A.K. and S.K. Pandey, *Potential mechanism(s) involved in the regulation of glycogen synthesis by insulin.* Mol Cell Biochem, 1998. **182**(1-2): p. 135-41.

183. Cohen, P., et al., *Separation and characterisation of glycogen synthase kinase 3, glycogen synthase kinase 4 and glycogen synthase kinase 5 from rabbit skeletal muscle.* Eur J Biochem, 1982. **124**(1): p. 21-35.

184. Huang, K.P., et al., *Phosphorylation and inactivation of rabbit skeletal muscle glycogen synthase: distinction between kinase Fa-, phosphorylase kinase-, and glycogen synthase (casein) kinase-1-catalyzed reactions.* Arch Biochem Biophys, 1984. **232**(1): p. 111-7.

185. Wang, Y. and P.J. Roach, *Inactivation of rabbit muscle glycogen synthase by glycogen synthase kinase-3. Dominant role of the phosphorylation of Ser-640 (site-3a).* J Biol Chem, 1993. **268**(32): p. 23876-80.

186. Roach, P.J., *Control of glycogen synthase by hierarchal protein phosphorylation.* Faseb J, 1990. **4**(12): p. 2961-8.

187. Skurat, A.V., A.D. Dietrich, and P.J. Roach, *Glycogen synthase sensitivity to insulin and glucose-6-phosphate is mediated by both NH2- and COOH-terminal phosphorylation sites.* Diabetes, 2000. **49**(7): p. 1096-100.

188. Johnson, L.N., *Glycogen phosphorylase: control by phosphorylation and allosteric effectors.* Faseb J, 1992. **6**(6): p. 2274-82.

189. Zhou, M., et al., *Insulin-dependent protein trafficking in skeletal muscle cells.* Am J Physiol, 1998. **275**(2 Pt 1): p. E187-96.

190. Randle, P.J., *Metabolic fuel selection: general integration at the whole-body level.* Proc Nutr Soc, 1995. **54**(1): p. 317-27.

191. Randle, P.J., A.L. Kerbey, and J. Espinal, *Mechanisms decreasing glucose oxidation in diabetes and starvation: role of lipid fuels and hormones.* Diabetes Metab Rev, 1988. **4**(7): p. 623-38.

192. Hall, R.K. and D.K. Granner, *Insulin regulates expression of metabolic genes through divergent signaling pathways.* J Basic Clin Physiol Pharmacol, 1999. **10**(2): p. 119-33.

193. Hanson, R.W. and L. Reshef, *Regulation of phosphoenolpyruvate carboxykinase (GTP) gene expression.* Annu Rev Biochem, 1997. **66**: p. 581-611.

194. Burgering, B.M. and P.J. Coffer, *Protein kinase B (c-Akt) in phosphatidylinositol-3-OH kinase signal transduction.* Nature, 1995. **376**(6541): p. 599-602.

195. Franke, T.F., D.R. Kaplan, and L.C. Cantley, *PI3K: downstream AKTion blocks apoptosis.* Cell, 1997. **88**(4): p. 435-7.

196. Klip, A., *The many ways to regulate glucose transporter 4.* Appl Physiol Nutr Metab, 2009. **34**(3): p. 481-7.

197. Wan, X. and L.J. Helman, *Levels of PTEN protein modulate Akt phosphorylation on serine 473, but not on threonine 308, in IGF-II-overexpressing rhabdomyosarcomas cells.* Oncogene, 2003. **22**(50): p. 8205-11.

198. Wu, X., et al., *The PTEN/MMAC1 tumor suppressor phosphatase functions as a negative regulator of the phosphoinositide 3-kinase/Akt pathway.* Proc Natl Acad Sci U S A, 1998. **95**(26): p. 15587-91.

199. Meuillet, E.J., et al., *Thioredoxin-1 binds to the C2 domain of PTEN inhibiting PTEN's lipid phosphatase activity and membrane binding: a mechanism for the functional loss of PTEN's tumor suppressor activity.* Arch Biochem Biophys, 2004. **429**(2): p. 123-33.

200. Cho, S.H., et al., *Redox regulation of PTEN and protein tyrosine phosphatases in H(2)O(2) mediated cell signaling.* FEBS Lett, 2004. **560**(1-3): p. 7-13.

201. Kwon, J., et al., *Reversible oxidation and inactivation of the tumor suppressor PTEN in cells stimulated with peptide growth factors.* Proc Natl Acad Sci U S A, 2004. **101**(47): p. 16419-24.

202. Meng, T.C., T. Fukada, and N.K. Tonks, *Reversible oxidation and inactivation of protein tyrosine phosphatases in vivo.* Mol Cell, 2002. **9**(2): p. 387-99.

203. Horman, S., et al., *Insulin antagonizes ischemia-induced Thr172 phosphorylation of AMP-activated protein kinase alpha-subunits in heart via hierarchical phosphorylation of Ser485/491.* J Biol Chem, 2006. **281**(9): p. 5335-40.

204. Kovacic, S., et al., *Akt activity negatively regulates phosphorylation of AMP-activated protein kinase in the heart.* J Biol Chem, 2003. **278**(41): p. 39422-7.

205. Buller, C.L., et al., *A GSK-3/TSC2/mTOR pathway regulates glucose uptake and GLUT1 glucose transporter expression.* Am J Physiol Cell Physiol, 2008. **295**(3): p. C836-43.

206. Pore, N., et al., *Akt1 activation can augment hypoxia-inducible factor-1alpha expression by increasing protein translation through a mammalian target of rapamycin-independent pathway.* Mol Cancer Res, 2006. **4**(7): p. 471-9.

207. Zhou, Q.L., et al., *Akt substrate TBC1D1 regulates GLUT1 expression through the mTOR pathway in 3T3-L1 adipocytes.* Biochem J, 2008. **411**(3): p. 647-55.

208. Feron, O., *Pyruvate into lactate and back: From the Warburg effect to symbiotic energy fuel exchange in cancer cells.* Radiother Oncol, 2009.

209. Kim, J.W. and C.V. Dang, *Cancer's molecular sweet tooth and the Warburg effect.* Cancer Res, 2006. **66**(18): p. 8927-30.

210. Vander Heiden, M.G., L.C. Cantley, and C.B. Thompson, *Understanding the Warburg effect: the metabolic requirements of cell proliferation.* Science, 2009. **324**(5930): p. 1029-33.

211. Warburg, O., *On the origin of cancer cells.* Science, 1956. **123**(3191): p. 309-14.

212. Warburg, O., *On respiratory impairment in cancer cells.* Science, 1956. **124**(3215): p. 269-70.

213. Findlay, M., et al., *Noninvasive monitoring of tumor metabolism using fluorodeoxyglucose and positron emission tomography in colorectal cancer liver metastases: correlation with tumor response to fluorouracil.* J Clin Oncol, 1996. **14**(3): p. 700-8.

214. Gatenby, R.A. and R.J. Gillies, *Glycolysis in cancer: a potential target for therapy.* Int J Biochem Cell Biol, 2007. **39**(7-8): p. 1358-66.

215. Jansson, T., et al., *Positron emission tomography studies in patients with locally advanced and/or metastatic breast cancer: a method for early therapy evaluation?* J Clin Oncol, 1995. **13**(6): p. 1470-7.

216. van Baardwijk, A., et al., *The maximum uptake of (18)F-deoxyglucose on positron emission tomography scan correlates with survival, hypoxia inducible factor-1alpha and GLUT-1 in non-small cell lung cancer.* Eur J Cancer, 2007. **43**(9): p. 1392-8.

217. Patel, M.S. and L.G. Korotchkina, *Regulation of the pyruvate dehydrogenase complex.* Biochem Soc Trans, 2006. **34**(Pt 2): p. 217-22.

218. Lawson, J.E., et al., *Molecular cloning and expression of the catalytic subunit of bovine pyruvate dehydrogenase phosphatase and sequence similarity with protein phosphatase 2C.* Biochemistry, 1993. **32**(35): p. 8987-93.

219. Cooper, R.H., P.J. Randle, and R.M. Denton, *Stimulation of phosphorylation and inactivation of pyruvate dehydrogenase by physiological inhibitors of the pyruvate dehydrogenase reaction.* Nature, 1975. **257**(5529): p. 808-9.

220. Pettit, F.H., J.W. Pelley, and L.J. Reed, *Regulation of pyruvate dehydrogenase kinase and phosphatase by acetyl-CoA/CoA and NADH/NAD ratios.* Biochem Biophys Res Commun, 1975. **65**(2): p. 575-82.

221. Sugden, M.C. and M.J. Holness, *Interactive regulation of the pyruvate dehydrogenase complex and the carnitine palmitoyltransferase system.* Faseb J, 1994. **8**(1): p. 54-61.

222. Wieland, O.H., *The mammalian pyruvate dehydrogenase complex: structure and regulation.* Rev Physiol Biochem Pharmacol, 1983. **96**: p. 123-70.

223. Brunengraber, H. and C.R. Roe, *Anaplerotic molecules: current and future.* J Inherit Metab Dis, 2006. **29**(2-3): p. 327-31.

224. Comte, B., et al., *A 13C mass isotopomer study of anaplerotic pyruvate carboxylation in perfused rat hearts.* J Biol Chem, 1997. **272**(42): p. 26125-31.

225. Gibala, M.J., M.E. Young, and H. Taegtmeyer, *Anaplerosis of the citric acid cycle: role in energy metabolism of heart and skeletal muscle.* Acta Physiol Scand, 2000. **168**(4): p. 657-65.

226. Freminet, A. and C. Poyart, *Lactate-glucose interrelations, glucose recycling and the Cori cycle in normal fed rats.* Pflugers Arch, 1975. **361**(1): p. 25-31.

227. Shearer, J.D., et al., *Alteration in pyruvate metabolism in the liver of tumor-bearing rats.* Cancer Res, 1984. **44**(10): p. 4443-6.

228. Bergeron, R., et al., *Effect of 5-aminoimidazole-4-carboxamide-1-beta-D-ribofuranoside infusion on in vivo glucose and lipid metabolism in lean and obese Zucker rats.* Diabetes, 2001. **50**(5): p. 1076-82.

229. Hayashi, T., et al., *Metabolic stress and altered glucose transport: activation of AMP-activated protein kinase as a unifying coupling mechanism.* Diabetes, 2000. **49**(4): p. 527-31.

230. Ihlemann, J., et al., *Effect of tension on contraction-induced glucose transport in rat skeletal muscle.* Am J Physiol, 1999. **277**(2 Pt 1): p. E208-14.

231. Atkinson, L.L., M.A. Fischer, and G.D. Lopaschuk, *Leptin activates cardiac fatty acid oxidation independent of changes in the AMP-activated protein kinase-acetyl-CoA carboxylase-malonyl-CoA axis.* J Biol Chem, 2002. **277**(33): p. 29424-30.

232. Kudo, N., et al., *High rates of fatty acid oxidation during reperfusion of ischemic hearts are associated with a decrease in malonyl-CoA levels due to an increase in 5'-AMP-activated protein kinase inhibition of acetyl-CoA carboxylase.* J Biol Chem, 1995. **270**(29): p. 17513-20.

233. McGarry, J.D. and N.F. Brown, *The mitochondrial carnitine palmitoyltransferase system. From concept to molecular analysis.* Eur J Biochem, 1997. **244**(1): p. 1-14.

234. McGarry, J.D., Y. Takabayashi, and D.W. Foster, *The role of malonyl-coa in the coordination of fatty acid synthesis and oxidation in isolated rat hepatocytes.* J Biol Chem, 1978. **253**(22): p. 8294-300.

235. Bergeron, R., et al., *Chronic activation of AMP kinase results in NRF-1 activation and mitochondrial biogenesis.* Am J Physiol Endocrinol Metab, 2001. **281**(6): p. E1340-6.

236. Jager, S., et al., *AMP-activated protein kinase (AMPK) action in skeletal muscle via direct phosphorylation of PGC-1alpha.* Proc Natl Acad Sci U S A, 2007. **104**(29): p. 12017-22.

237. Winder, W.W., et al., *Activation of AMP-activated protein kinase increases mitochondrial enzymes in skeletal muscle.* J Appl Physiol, 2000. **88**(6): p. 2219-26.

238. Zong, H., et al., *AMP kinase is required for mitochondrial biogenesis in skeletal muscle in response to chronic energy deprivation.* Proc Natl Acad Sci U S A, 2002. **99**(25): p. 15983-7.

239. Patwari, P., et al., *Thioredoxin-independent regulation of metabolism by the alpha-arrestin proteins.* J Biol Chem, 2009.

240. Lefkowitz, R.J., K. Rajagopal, and E.J. Whalen, *New roles for beta-arrestins in cell signaling: not just for seven-transmembrane receptors.* Mol Cell, 2006. **24**(5): p. 643-52.